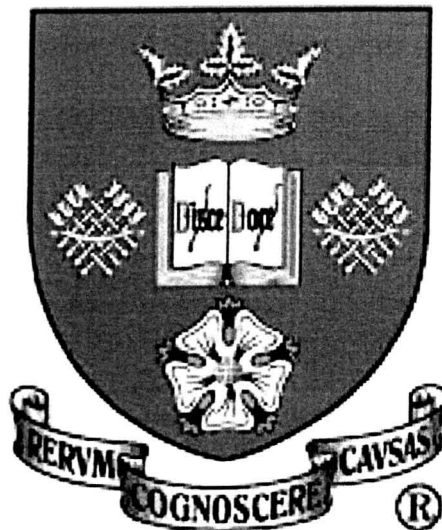


**An investigation of the influence of Interleukin-1
on the arterial response to experimental injury**



Allison C Morton MBChB, BMedSci, MRCP (UK)

Division of Clinical Sciences North

The University of Sheffield

Thesis submitted for the degree of Doctor of Philosophy

September 2004

ACKNOWLEDGEMENTS

I would like to thank the following for their help and contribution in the preparation of this thesis:

The British Heart Foundation for funding this work as part of a Program Grant awarded to Professor David Crossman, Dr Sheila Francis and Professor Steven Dower.

Professor David Crossman, Dr Sheila Francis, Dr Julian Gunn and Professor Steven Dower for their supervision of this work and their continued encouragement and support.

Nadine Arnold without whose assistance this work would not have been possible as she taught me all I needed to know about pigs and was a good friend through out difficult times.

Richard Varcoe, who performed the Real-time PCR for this work and Chris Toombs from Amgen who provided the IL-1ra for the study and also analysed the IL-1ra ELISA and initial pharmacokinetic data.

Abbott Vascular (formerly Biocompatibles) who provided all the intracoronary stents for this work. A special mention must be made for David Kirkham who worked for Abbott Vascular and went out of his way to locate the correct size

of stent for my work and had them sent to me in Sheffield at regular intervals over the 2 years this work took to do.

Finally, a special thank goes to my parents and close friends, whose constant love, support and belief in me despite difficult times was unfaltering.

TABLE OF CONTENTS

	Page
ACKNOWLEDGEMENTS	1
CONTENTS	3
LIST OF FIGURES	16
LIST OF TABLES	20
ABBREVIATIONS	21
SUMMARY	25
CHAPTER 1: INTRODUCTION	
1.1 ATHEROSCLEROSIS	
1.1.1 Definition	27
1.1.2 Pathophysiology of atherosclerosis and the role of inflammation	27
1.1.3 Factors responsible for endothelial cell dysfunction	29
1.1.4 Plaque rupture	29
1.2 INTERLEUKIN-1 AND ATHEROSCLEROSIS	
1.2.1 Cytokines	30
1.2.2 The Interleukin-1 (IL-1) family	31
1.2.3 Interleukin-1 alpha (IL-1 α)	31
1.2.4 Interleukin-1 beta (IL-1 β)	32
1.2.5 Interleukin-1 receptor antagonist (IL-1ra)	33
1.2.6 The Interleukin-1 receptors	33

1.2.7	The role of interleukin-1 in atherosclerosis	34
1.2.8	Interleukin-1 administered to humans	35
1.2.9	The role of Interleukin-1 in atherosclerosis	35
1.2.10	Interleukin-1 receptor antagonist and amelioration of disease	36
1.3	CARDIAC MANIFESTATIONS OF ATHEROSCLEROSIS – CORONARY HEART DISEASE	
1.3.1	Incidence of coronary heart disease	37
1.3.2	<i>Angina pectoris</i>	38
1.3.3	Patho-physiologic mechanisms in stable and unstable angina	38
1.3.4	Clinical presentation of stable and unstable angina	39
1.3.5	Treatment of stable angina	40
1.3.6	Indications for PCI and CABG	41
1.3.7	Anti-inflammatory treatment strategies	41
1.4	PERCUTANEOUS CORONARY INTERVENTION (PCI)	
1.4.1	Percutaneous Coronary Intervention: an historical perspective	42
1.4.2	Proposed patho-physiologic mechanisms of PTCA	43
1.4.3	Limitations of PTCA	44
1.4.4	Intracoronary stenting	44

1.5	RESTENOSIS AFTER PCI	
1.5.1	Clinical and angiographic restenosis	45
1.5.2	Time-course of restenosis	48
1.5.3	Pathogenesis of restenosis	48
1.5.4	The importance of inflammation in restenosis	49
1.5.5	Anti-inflammatory approaches to restenosis	50
1.5.6	Current approaches to restenosis	51
1.5.7	In-stent restenosis, current treatment options	52
1.5.8	Drug-eluting stents	52
1.6	TREATMENT DELIVERY	
1.6.1	Systemic versus local therapy	54
1.7	CONCLUSIONS AND FUTURE DIRECTIONS	
1.7.1	The future of anti-restenotic treatment	56
1.8	AIMS OF THIS THESIS	56
CHAPTER 2: HUMAN IL-1 TYPE II INTERLEUKIN-1 RECEPTOR AS AN INHIBITOR OF PORCINE IL-1		
2.1	INTRODUCTION	
2.1.1	Possible inhibitors of Interleukin-1 signalling	58
2.1.2	Surface plasmon resonance	60
2.1.3	Aims of this study	63

2.2 MATERIALS AND METHODS

2.2.1 Receptor immobilisation to the BIAcore chip surface 65

2.2.2 Ligand binding to sIL-1RII on the chip surface 65

2.3 RESULTS

2.3.1 Immobilisation of the type II receptor 67

2.3.2 Ligand binding 70

2.4 DISCUSSION

2.4.1 Summary of findings 74

2.4.2 Why does porcine IL-1 not bind to sIL-1RII? 74

2.5 CONCLUSIONS AND FUTURE DIRECTIONS 75

CHAPTER 3: DELIVERY AND PHARMACOKINETICS OF HUMAN IL-1RA IN PIGS

3.1 INTRODUCTION

3.1.1 IL-1ra as an inhibitor of IL-1 77

3.1.2 Human IL-1ra and its inhibition of porcine IL-1 78

3.1.3 Dosing regimen for IL-1ra 78

3.1.4 Mode of delivery of IL-1ra 78

3.1.5 Aims of this study 80

3.2 MATERIALS AND METHODS

3.2.1	Yorkshire white pigs	81
3.2.2	Animal husbandry	81
3.2.3	Legal considerations	81
3.2.4	Cytokines	82
3.2.5	Subcutaneous osmotic pumps	82
3.2.6	Filling and priming of the osmotic pumps	83
3.2.7	Implantation of subcutaneous mini osmotic pumps	83
3.2.8	Pharmacokinetics of IL-1ra	84
3.2.9	Pharmacokinetics of subcutaneous IL-1ra release from Miniosmotic pumps	84
3.2.10	Pharmacokinetics of intravenous bolus administration	85
3.2.11	Determination of serum levels of IL-1ra after administration	85

3.3 RESULTS

3.3.1	Pharmacokinetics of inhibitor release from mini osmotic pumps - subcutaneous infusion	86
3.3.2	Intravenous bolus administration	86
3.3.2	Pharmacokinetics of inhibitor release from iv bolus and mini osmotic pumps	89

3.4 DISCUSSION

3.4.1	Summary of findings	91
-------	---------------------	----

3.4.2	Delivery strategy	91
3.4.2	Steady state levels	92
3.4.3	The importance of an intravenous bolus	92
3.4.4	How much IL-1ra is enough?	93

3.5 CONCLUSIONS AND FUTURE DIRECTIONS 93

CHAPTER 4: DOSE-RESPONSE ANALYSIS – INHIBITION OF IL-1 INDUCED INFLAMMATION IN A PORCINE SKIN MODEL

4.1 INTRODUCTION

4.1.1	Skin as a surrogate for the coronary artery	95
4.1.2	Bioassay for IL-1ra effects on inflammation in pig skin.	96
4.1.3	Myeloperoxidase	97
4.1.4	Aims of this study	97

4.2 MATERIALS AND METHODS

4.2.1	Intradermal injection of Interleukin-1 with and without intravenous bolus and continuous subcutaneous infusion of IL-1ra – dose response analysis	98
4.2.2	Measurement of myeloperoxidase in skin samples	100
4.2.3	Preparation of pig neutrophils by Percoll density gradient centrifugation	101
4.2.4	Preparation of porcine skin samples for myeloperoxidase assay	102

4.2.5	Preparation of standards for myeloperoxidase assay	103
4.2.6	Assay to detect the levels of myeloperoxidase in the skin samples	103
4.2.7	Immunostaining of wax embedded skin sections	104
4.2.8	Myeloperoxidase staining of wax embedded sections of pig skin	104
4.2.9	Assessment of neutrophil recruitment to the skin	106
4.2.10	Neutrophil extraction	106
4.3	RESULTS	
4.3.1	Neutrophil accumulation in response to intradermal injection of porcine IL-1 β	107
4.3.2	Neutrophil accumulation in porcine skin after intradermal injection of porcine IL-1 β , with and without implantation of subcutaneous mini pumps and iv bolus of IL-1ra	107
4.3.3	Histological analysis of wax embedded sections – Haematoxylin and eosin staining	113
4.3.4	Histological analysis of wax embedded sections - Myeloperoxidase Immunostaining	114
4.4	DISCUSSION	
4.4.1	Summary of findings	115
4.4.2	Myeloperoxidase as a surrogate marker for neutrophils	116

**CHAPTER 5: MODULATION OF THE PORCINE CORONARY ARTERY
RESPONSE TO OVERSIZED BALLOON ANGIOPLASTY AND STENTING.****5.1 INTRODUCTION**

5.1.1	Animal models of experimental injury and restenosis	118
5.1.2	Porcine coronary experimental injury model	119
5.1.3	Porcine coronary stent model	119
5.1.4	Aims of this study	120

5.2 MATERIALS AND METHODS

5.2.1	Experimental injury	121
5.2.2	Porcine coronary balloon angioplasty	121
5.2.3	Porcine intracoronary stent placement	124
5.2.4	Artery extraction and tissue processing	125
5.2.5	Histology	126
5.2.6	Histomorphometric analysis	126
5.2.7	Arterial injury score and corrections	127

5.3 RESULTS – PTCA SECTION ANALYSIS

5.3.1	Histomorphometric analysis of PTCA sections	130
5.3.2	PTCA section analysis	130
5.3.3	Total vessel cross-sectional area	131

5.3.4	Injury score	131
5.3.5	Neointimal area of the PTCA sections	133
5.3.6	Lumen area of the PTCA sections	133
5.3.7	Intima: media ratio of the PTCA treated arteries	133
5.4	RESULTS – INTRACORONARY STENTING	
5.4.1	Histomorphometric analysis of stented sections	138
5.4.2	Analysis: 14-day infusion, 28-day time-point	140
5.4.2.1	Total vessel cross-sectional area	140
5.4.2.2	Injury Score	140
5.4.2.3	Neointima area	140
5.4.2.4	Cross-sectional lumen area	143
5.4.3	Analysis: 14-day infusion, 14-day time-point	147
5.4.3.1	Total vessel cross-sectional area	147
5.4.3.2	Injury Score	147
5.4.3.3	Neointima area	150
5.4.3.4	Cross-sectional lumen area	150
5.4.4	Analysis: 28-day infusion, 28-day time-point	154
5.4.4.1	Total vessel cross-sectional area	154
5.4.4.2	Injury Score	154
5.4.4.3	Neointima area	157
5.4.4.4	Cross-sectional lumen area	157
5.4.5	Analysis: 28-day infusion, 90-day time-point	161
5.4.5.1	Total vessel cross-sectional area	161
5.4.5.2	Injury Score	161

5.4.5.3	Neointima area	164
5.4.5.4	Cross-sectional lumen area	164
5.5	DISCUSSION	
5.5.1	Summary of findings	168
5.5.2	The effect of IL-1ra on the vessel response to balloon angioplasty	168
5.5.3	The effect of IL-1ra on the vessel response to intracoronary stenting	169
5.5.4	Implications of findings	171
5.6	CONCLUSIONS AND FUTURE DIRECTIONS	172
 CHAPTER 6: MECHANISM OF ACTION OF IL-1RA IN THE VESSEL WALL AFTER STENTING		
6.1	INTRODUCTION	
6.1.1	Regulation of production of IL-1	173
6.1.2	Quantification of tissue levels of IL-1	174
6.1.3	Aims of this study	174
6.2	MATERIALS AND METHODS	
6.2.1	Quantification of protein and mRNA levels from porcine coronary arteries	175
6.2.2	Sample collection	175

6.2.3	Protein extraction from porcine coronary arteries	176
6.2.4	Pierce MicroBCA™ protein assay	176
6.2.5	Sodium Dodecyl Sulphate Polyacrylamide Gel Electrophoresis: SDS PAGE	177
6.2.6	Acrylamide gel preparation	177
6.2.7	Sample loading and electrophoresis	178
6.2.8	Semi-Dry Electro Blotting	179
6.2.9	Staining proteins	179
6.2.10	Immunological Detection of Bound Proteins – Blocking Non-Specific Binding Sites	180
6.2.11	Immunological Detection of Bound Proteins – Primary Antibody Detection	180
6.2.12	Immunological Detection of Bound Proteins – Secondary Antibody Detection	180
6.2.13	Immunological Detection of Bound Proteins – Visualisation of Bound Proteins	181
6.2.14	Extraction of RNA from arterial tissue	181
6.2.14	Extraction of RNA from porcine vascular smooth muscle cells	181
6.2.16	Reverse transcription polymerase chain reaction	
6.2.16.1	Reverse transcription	184
6.2.16.2	Polymerase Chain Reaction (PCR)	184
6.2.17	PCR primer design	185
6.2.18	Agarose Gel Electrophoresis	187
6.2.19	TA cloning into Plasmid Vectors	187

6.2.20	Transformation of DNA into bacteria	188
6.2.21	Cloning PCR products	189
6.2.22	Plasmid DNA Miniprep	190
6.2.22.1	The QIAprep Spin Miniprep Kit	190
6.2.22.2	Restriction Digest of Plasmid	191
6.2.23	Plasmid DNA Maxiprep	191
6.2.23.1	EndoFree Plasmid Maxi Protocol	192
6.2.24	Analysis of mRNA content of tissue using the Real-Time Quantitative reverse transcription polymerase chain reaction (RT-PCR)	193
6.2.25	Quantitative Real time polymerase chain reaction	197
6.2	RESULTS	
6.3.1	Protein assay	199
6.3.2	Detection of protein levels – Western blots	199
6.3.3	RT-PCR, cDNA amplification and TA cloning of porcine IL-1alpha and IL-1ra	203
6.3.4	Extraction of RNA from porcine coronary arteries	206
6.3.5	Real-time PCR	206
6.4	DISCUSSION	
6.4.1	Summary of findings	209
6.4.2	Detection of protein levels – Western Blotting	209
6.4.3	Detection of mRNA	210
6.4.4	REST© software analysis	210

6.5	CONCLUSIONS AND FUTURE DIRECTIONS	211
	CHAPTER 7: CONCLUSIONS AND FUTURE WORK	212
	REFERENCES	221
	TECHNICAL APPENDIX	237
	A. REAGENTS AND STOCK SOLUTIONS	
A.1	BIAcore Reagents and Stock Solutions	237
A.2	RNA Reagents and Stock Solutions	237
A.3	Protein Stock Reagents and Buffers	238
A.4	Plasmid Reagents and Stock Solutions	239
	B. DNA / RNA CONCENTRATION CALCULATIONS	
B.1	RNA Concentration Calculation	241
B.2	Oligonucleotide Concentration Calculation	241
B.3	Molar Concentration Calculation	241
B.4	DNA Concentration Calculation	241
	C. PROTEIN ELECTROPHORESIS	
C.1	Resolving Gel Preparation	242
C.2	Stacking Gel Preparation	242
D	MEETING ABSTRACTS	243

LIST OF FIGURES

Figure		Page Number
1	The angiographic appearance of restenosis	47
2	SPR optical unit and a sensor chip	62
3	Immobilisation of sIL-1RII to (a) flow cell 2 and (b) flow cell 4 of the sensor chip	68
4	Preparation of control flow cell (a) 2 and (b) 3	69
5	Binding of human IL-1 β to immobilised sIL-1RII and a control flow cell	71
6	Binding of porcine IL-1 α to immobilised sIL-1RII	72
7	Binding of porcine IL-1 β to immobilised sIL-1RII	73
8	Serum concentration of IL-1ra following implantation of subcutaneous pumps that release IL-1ra	87
9	Serum concentration of IL-1ra after administration of an intravenous bolus	88
10	Serum concentration of IL-1ra after iv bolus and subcutaneous mini osmotic pump insertion	90
11	Grid markings for intradermal injection sites	99
12	Neutrophil accumulation in response to increasing doses of porcine IL-1 β	108
13	Neutrophil accumulation in response to increasing doses of intradermal injections of porcine IL-1 α	109

14	Neutrophil accumulation in response to intradermal IL-1 β (1000 Units)	110
15	MPO Immunostaining of skin sections taken from pigs without IL-1ra and with IL-1ra after id injection of IL-1 β 6h before harvest	112
16	Porcine percutaneous coronary intervention – technique	123
17	Measurements taken for histomorphometric analysis of PTCA sections	128
18	Modulation of PTCA Injury by IL-1ra: (a) Total Vessel Cross-sectional area (mm ²) and (b) % IEL breach (injury score)	132
19	Modulation of PTCA Injury by IL-1ra: Neointimal cross-sectional area (mm ²)	134
20	Modulation of PTCA Injury by IL-1ra: Cross-sectional area of the lumen (mm ²)	135
21	Modulation of PTCA Injury by IL-1ra corrected for vessel size and injury	136
22	Tissue response to PTCA in porcine coronary arteries	137
23	Measurements taken for histomorphometric analysis of stented sections	139
24	Modulation of intracoronary stenting by IL-1ra (14 day infusion; 28 day analysis): Cross sectional vessel area	141
25	Modulation of intracoronary stenting by IL-1ra (14 day infusion; 28 day analysis): Injury score correction	142
26	Modulation of intracoronary stenting by IL-1ra (14 day	

	infusion; 28 day analysis): Neointima Area	144
27	Tissue response to intracoronary stenting (14 day infusion; 28 day analysis)	145
28	Modulation of intracoronary stenting by IL-1ra (14 day infusion; 28 day analysis): Lumen Area	146
29	Modulation of intracoronary stenting by IL-1ra (14 day infusion; 14 day analysis): Total vessel area	148
30	Modulation of intracoronary stenting by IL-1ra (14 day infusion; 14 day analysis): Injury score correction	149
31	Modulation of intracoronary stenting by IL-1ra (14 day infusion; 14 day analysis): Neointima Area	151
32	Tissue response to intracoronary stenting (14 day infusion; 14 day analysis)	152
33	Modulation of intracoronary stenting by IL-1ra (14 day infusion; 14 day analysis): Lumen Area	153
34	Modulation of porcine coronary artery response to stenting by IL-1ra (28 day infusion; 28 day analysis): Total vessel cross-sectional area (mm ²).	155
35	Modulation of porcine coronary artery response to stenting by IL-1ra (28 day infusion; 28 day analysis): Injury Score correction	156
36	Modulation of porcine coronary artery response to stenting by IL-1ra (28 day infusion; 28 day analysis): Neointima Area	158
37	Tissue response to intracoronary stenting (28 day	

	infusion; 28 day analysis)	159
38	Modulation of porcine coronary artery response to stenting by IL-1ra (28 day infusion; 28 day analysis): Lumen area	160
39	Modulation of porcine coronary artery response to stenting by IL-1ra (28 day infusion; 90 day analysis): Vessel area	162
40	Modulation of porcine coronary artery response to stenting by IL-1ra (28 day infusion; 90 day analysis): Injury score	163
41	Modulation of porcine coronary artery response to stenting by IL-1ra (28 day infusion; 90 day analysis): Neointima area	165
42	Tissue response to intracoronary stenting (28 day infusion; 90 day analysis)	166
43	Modulation of porcine coronary artery response to stenting by IL-1ra (28 day infusion; 90 day analysis): Lumen area	167
44	An example of a standard curve obtained using the Pierce MicroBCA™ protein assay	200
45	Independent Western blots for (a) IL-1 β , 17kDa and (b) loading control α -tubulin, 55kDa	201
46	Amplification of porcine IL-1 α from porcine vascular smooth muscle cells (VSMC)	204
47	Minipreps of IL-1 α cDNA from porcine VSMCs	205

48	Melt curves generated during qRTPCR	207
49	Box and whisker plots showing the effect of IL-1ra therapy on vessel wall (a) IL-1 α mRNA and (b) IL-1 β mRNA levels	208

LIST OF TABLES

Table Number		Page Number
1	Primers constructed for PCR	186
2	Primers constructed for Real-Time PCR	195

ABBREVIATIONS

AMV-RT	<i>avian myeloblastosis virus</i> reverse transcriptase
APS	ammonium persulphate
ATP	Adenosine Triphosphate
BARI	Bypass Angioplasty Revascularisation Investigation
CABG	Coronary Artery Bypass Graft
CAD	coronary artery disease
CHD	Coronary heart disease
CRP	C Reactive Protein
d	days
DAB	diaminobenzidine tetrahydrochloride
DNA	Deoxyribonucleic Acid
EAST	Emory Angioplasty or Surgery Trial
ECL	enhanced chemiluminescence
EDC	ethylcarbodiimide
EDTA	ethylenediaminetetra acetic acid
h	hours
H&E	Haematoxylin and eosin
HEPES	N-2-hydroxyethylpiperazine-N-2-ethanesulphonic acid
HRP	Horse radish peroxidase
HTAB	hexa-decyl-trimethyl-ammonium bromide
ICE	Interleukin-1 converting enzyme
IL	Interleukin
IL-1 α	Interleukin-1 alpha

IL-1 β	Interleukin-1 beta
IL-1ra	Interleukin-1 receptor antagonist
IL-1R1	Type 1 Interleukin-1 receptor
IL-1R2	Type 2 Interleukin-1 receptor
IL-1RAcP	Interleukin-1 accessory protein
id	intra-dermal
im	intra-muscular
iv	intra-venous
IVUS	Intra-vascular Ultrasound
kg	kilo-grams
LAD	Left anterior descending
LDL	Low Density Lipoprotein
LPS	lipopolysaccharide
mM	milliMoles
M	Moles
min	minutes
MLD	Mid lumen diameter
mg	milli-grams
mmHg	milli-metres of mercury
MOPS	3-(N-Morpholino) propanesulfonic acid
MPO	Myeloperoxidase
ng	nano-grams
NGS	Normal goat serum
NHS	N-hydroxysuccinimide
PAGE	polyacrylamide gel electrophoresis

PBS	Phosphate buffered saline
PC	Phosphylcholine
PCI	Percutaneous Coronary Intervention
PDGF	Platelet derived growth factor
PMSF	phenylmethylsulfonyl fluoride
PPP	Platelet poor plasma
PRESTO	Prevention of REStenosis with Tranilast and its Outcomes
PRP	Platelet rich plasma
PSGL	P-selectin glycoprotein ligand
PTCA	Percutaneous transluminal coronary angioplasty
RAVEL	randomised study with the sirolimus coated BX velocity™ balloon expandable stent in the treatment of patients with <i>de novo</i> native coronary artery lesions
RCA	Right coronary artery
RITA	Randomised Intervention Treatment of Angina (trial)
rpm	revolutions per minute
RT-PCR	reverse transcription polymerase chain reaction
RU	Response Units
sec	seconds
sc	subcutaneous
SDS	sodium dodecyl sulphate
SPR	surface plasmon resonance
SPW	surface plasmon waves
Taq	<i>thermus aquaticus</i>

TEMED	N,N,N,N'-tetramethylethylenediamine
TLR	Target lesion revascularisation
TNF	tumour necrosis factor
U	Units
UV	ultraviolet
µg	micrograms
µl	microlitres
VSMC	Vascular smooth muscle cell
X-gal	5-bromo-4-chloro-3-indolyl-β-galactopyranoside

SUMMARY

Interleukin-1 (IL-1) is involved in the pathogenesis of coronary artery disease (CAD) and restenosis. IL-1 receptor antagonist (IL-1ra) blocks IL-1 signalling by competitive binding to the Type 1 IL-1 receptor. IL-1ra has been used successfully to modulate inflammatory diseases but its effect on coronary artery injury or restenosis is unknown. An alternative therapeutic target for inhibition of IL-1 is the human soluble type II IL-1 receptor. However, assessment of its binding capacity for porcine IL-1 using surface plasmon resonance technology determined that the human type II IL-1R could not bind porcine IL-1, thereby preventing its use in this work. This work therefore aimed to examine the effect of IL-1ra on the porcine coronary response to injury.

Initial pharmacokinetic studies in pig skin determined the inhibitory plasma level of IL-1ra; an intravenous bolus of 0.5mg/kg followed by a 14-day continuous subcutaneous infusion of 2mg/kg/24h. Five groups of animals were studied, all being randomised to either IL-1ra or vehicle according to the above protocol. Group 1: 12 pigs underwent oversized (1.25:1) angioplasty of 2 coronary vessels. Analysis was at 28 days. Groups 2, 3,4 and 5 underwent coronary stenting (1.25:1). Group 3 was analysed at 14 days, Groups 2 and 4 at 28 days and Group 5 at 90 days. Histomorphometric measurements were made. A further group of animals were studied in which the IL-1ra was infused for 14 days and analysis was at 17 days in order to determine vessel wall levels of IL-1 by real time PCR.

After an initial early peak, plasma levels of IL-1ra ranged from 150 - 250ng/ml for the 14-day infusion. In Group 1, IL-1ra resulted in a 23% decrease in intima:media ratio normalised to internal elastic lamina fracture length (0.044 ± 0.005 vs. 0.057 ± 0.004 ; $p = 0.01$). Group 2 showed a 34% increase in neointimal area (0.38 ± 0.04 vs. $0.25 \pm 0.02\text{mm}^2$; $p = 0.001$) in the IL-1ra treated animals. Contrastingly, in Groups 3, 4 and 5, there was a 33%, 38% and 41% decrease in neointimal area (0.16 ± 0.1 vs. $0.26 \pm 0.16 \text{mm}^2$; $p < 0.0001$; 0.19 ± 0.07 vs. $0.29 \pm 0.19 \text{mm}^2$; $p < 0.0004$; 0.13 ± 0.01 vs. $0.22 \pm 0.01 \text{mm}^2$; $p < 0.000001$ respectively). No differences in IL-1 levels in the vessel wall were detected 3 days after cessation of IL-1ra therapy.

In porcine coronary arteries, IL-1ra was associated with a significant reduction in neointima formation when vessels underwent oversized balloon angioplasty and following stenting for the duration of the infusion and when the infusion was continued for 28-days. However, in the stent model there was an increase in neointima formation after discontinuation of the infusion, which is not explained by an increase in vessel wall IL-1. Thus, IL-1ra shows excellent promise as a new therapy for inhibition of neointima formation. This work has shown that at least 28 days of therapy is needed.

CHAPTER ONE

INTRODUCTION

1.1 Atherosclerosis

1.1.1 Definition

Complications of atherosclerosis are the most common causes of death in the western world. The term atherosclerosis originates from the Greek, *athere* (meaning 'gruel'), which describes the soft, lipid rich core of the plaque and *skleros* (meaning 'hard') that describes the hard fibrous capsule that surrounds the core. Gresham defined atherosclerosis in 1986 as '*a disease of the arteries in which fatty plaques develop on their inner walls, with eventual obstruction of blood flow*' [1]. The term atherosclerosis is now synonymous with coronary heart disease (CHD) [2].

1.1.2 Pathophysiology of atherosclerosis and the role of inflammation

Research over the last two decades has provided convincing evidence that inflammation plays a key role in the initiation and progression of coronary heart disease [3] and that atheromatous plaque disruption is directly related to the development of acute coronary syndromes.

Both Ross [3] and Glass [4] have described the vessel wall response to injury in detail. The earliest events in the pathogenesis of atherosclerosis are

thought to be injury to the arterial intima and oxidation of low density lipoprotein (LDL) in the subintimal space [5]. This results in an inflammatory reaction that leads to the release of cytokines and chemoattractant molecules. These molecules are responsible for the recruitment of neutrophils and monocytes from the circulation and their adhesion to the vascular wall.

There are different stages in the development of an atherosclerotic plaque, the starting point of which is now thought to be endothelial cell dysfunction [3] which leads to compensatory mechanisms that change the normal homeostatic properties of the endothelium. Permeability of the endothelium and its "stickiness" with respect to platelets and leukocytes is altered. The endothelium loses its anticoagulant effect, becoming procoagulant, forming and releasing cytokines (e.g. Interleukin-1) and vasoactive molecules. An intermediate plaque forms secondary to smooth muscle cell migration and proliferation within this area. This results in the artery wall becoming thickened. An atherosclerotic plaque in its immature form starts as a fatty streak that is a purely inflammatory lesion. This process continues with time, resulting in the formation of an atherosclerotic plaque. The artery compensates by gradually dilating (remodelling) which allows the artery lumen diameter to remain essentially unchanged despite a relatively large amount of disease [6]. Continued inflammation results in increased numbers of macrophages and lymphocytes from the blood entering the lesion. Again, activation of these leads to further cytokine release, which in turn cause further cell accumulation and may even result in necrosis. The cycle repeats itself with migration and proliferation of smooth muscle cells and consequent

formation of fibrous tissue. The lesion (now termed advanced or complicated) enlarges, eventually becoming covered with a fibrous cap. The compensatory dilatation of the artery at some point fails to keep up and the plaque then encroaches into the lumen and alters the flow of blood causing ischaemia. Inflammatory processes within the plaque continue and may result in a 'stable' plaque becoming 'unstable'. In an unstable plaque, lymphocytes activate macrophages resulting in increased expression of matrix metalloproteinases that cause collagen degradation and thinning of the fibrous cap. Thinning and rupture of this cap is the most common cause of intracoronary thrombus.

1.1.3 Factors responsible for endothelial cell dysfunction

Possible causes of endothelial cell dysfunction which lead to atherosclerosis include elevated blood lipids (especially LDL) [7], genetic predisposition [3], smoking [8] and diabetes [9] which lead to the formation of free radicals. In addition, more recent studies have implicated infectious microorganisms such as *Chlamydia pneumoniae* [10].

1.1.4 Plaque rupture

Advanced atherosclerotic lesions lead to ischaemic symptoms due to progressive lumen narrowing. It is plaque rupture however that results in clinically significant acute coronary syndromes or acute myocardial infarction. Plaque rupture exposes plaque lipids to blood components. This results in the initiation of the coagulation cascade and consequent platelet aggregation

and thrombosis. *Post mortem* analyses of atherosclerotic plaques suggest that small ruptures occur recurrently with evolution of the plaque but not all are clinically significant. Clinically significant ruptures usually involve the part of the plaque with a thin fibrous cap and large necrotic core. The risk of plaque rupture seems to depend upon plaque morphology rather than size or degree of stenosis [11]. Fibrosis with VSMC proliferation and collagen synthesis leads to hardening of the plaque whereas inflammation leads to fibrous cap degradation, which predisposes to plaque rupture.

1.2 Interleukin-1 and atherosclerosis

1.2.1 Cytokines

'Cytokines are regulatory proteins secreted by white blood cells and a variety of other blood cells in the body; the pleiotropic actions of cytokines include numerous effects on cells of the immune system and modulation of inflammatory responses' [12]. Interleukin 1 (IL-1) is a member of the cytokine family. The term interleukin was proposed by Aarden et al in 1979 in order to develop *'a system of nomenclature... based on (the proteins') ability to act as communication signals between different populations of leukocytes'* [13].

Although the name 'interleukin' implies that these agents act as communication signals between leukocytes, the term is not solely reserved for factors that can only act upon leukocytes.

1.2.2 The Interleukin-1 (IL-1) family

The majority of nucleated cell types secrete interleukin-1. It has a wide range of effects and exerts these on most cell types, often in combination with other cytokines. The IL-1 family is made up of 3 different members: IL-1alpha (IL-1 α), IL-1beta (IL-1 β) and IL-1receptor antagonist (IL-1ra). A separate gene encodes each member of the family. Cells that secrete IL-1 express the genes for all types but which one is secreted depends upon the level of expression of each gene. The IL-1 agonists, IL-1 α and IL-1 β , are structurally distinct. In most studies, the effect of their biological activity is indistinguishable. Both are 17-kD proteins coded by separate genes on chromosome 2. The IL-1 α and β proteins are synthesized by a variety of cell types including activated macrophages, stimulated lymphocytes and fibroblasts and are both potent mediators of inflammation and immunity. Both IL-1 α and β are synthesized as precursors with a molecular weight of 31kDa. Splicing of these into mature active forms requires specific cellular proteases. There are 2 receptors for IL-1. The type I receptor (IL1R1) is a signalling receptor (affinity IL-1ra>IL-1 α >IL-1 β), whereas the type II receptor (IL1R2) is a decoy receptor (affinity IL-1 β >IL-1 α >IL-1ra) [14].

1.2.3 Interleukin-1 alpha (IL-1 α)

The IL-1 α precursor (ProIL-1 α) is biologically active and is synthesized in association with microtubules and translated in the endoplasmic reticulum [15]. Because it lacks a leader peptide, there is no appreciable accumulation

of IL-1 α in any organelle and it remains in the cytosol. Immunohistochemical studies of IL-1 α in endotoxin-stimulated human blood monocytes reveal a diffuse staining pattern that is localised to the Golgi apparatus. IL-1 α , unlike IL-1 β is not usually found in the circulation or in body fluids (presumably because of its cell associated nature), except during severe disease in which case it is most likely released from dying cells.

1.2.4 Interleukin-1 beta (IL-1 β)

The IL-1 β precursor (ProIL-1 β) is not biologically active but is secreted as a result of cleavage of IL-1 β by Interleukin -1 β converting enzyme (ICE) [16]. Depending on the stimulus, 15 minutes after activation, IL-1 β mRNA levels rise rapidly and continue to do so up to 4 hours after which time levels begin to fall. Stimulants such as hypoxia [17] or complement (component C5a) [18] induce the synthesis of large amounts of IL-1 β mRNA in monocytes, although most of the mRNA produced gets degraded and is never translated into the IL-1 β protein. It appears that the IL-1 β mRNA needs to be stabilized before translation happens. There are many different mechanisms by which this occurs, and auto stabilization or stabilization by microbial products are 2 possibilities. The release of IL-1 from activated immune cells requires a secondary stimulus such as extracellular ATP acting on P2X7 receptors. Activation of these receptors leads to the shedding of microvesicles that contain bioactive IL-1 β [19].

1.2.5 Interleukin -1 receptor antagonist (IL-1ra)

IL-1ra is a specific receptor antagonist of IL-1 and is the only known naturally occurring cytokine antagonist. IL-1ra is secreted in 2 forms, the first (a secreted form of IL-1ra (sIL-1ra)), has a signal peptide and the profile of an acute phase reactant [20]; the second (the intracellular form (icIL-1ra)), has a number of subtypes, none of which have a signal peptide. IL-1ra is the molecule responsible for the blockade of the type 1 IL-1 receptor (IL-1R1). ProIL-1ra possesses a leader sequence and is synthesised, processed and secreted from the cell. Data from our laboratory suggests that this may be via a P2X7 receptor system [21]. In pharmacological studies, IL-1ra is required in 100 fold excess proportions to IL-1 β to block its effects [14]. There is evidence that disease outcome may be regulated by the balance between IL-1 β and IL-1ra. IL-1ra has been shown to block the inflammatory responses induced by IL-1 both *in vivo* and *in vitro*.

1.2.6 The Interleukin-1 Receptors

There are two primary Interleukin-1 receptors (Type-1 (IL-1RI) and Type-II (IL-1RII)), and one accessory protein (IL-1R-AcP). The two receptors are distinct gene products with both genes situated on the long arm of chromosome 2 [22]. IL-1RI is an 80kDa transmembrane protein and is the primary signal transducing receptor [23]. IL-1R-AcP is essential for IL-1 signalling via the IL-1RI [24]. IL-1 initially binds to the type-1 receptor with low affinity. Once bound, it is thought a structural change takes place that allows binding of the

IL-1R-AcP. Any subsequent binding of IL-1 then occurs with high affinity [25]. Although IL-1ra binds to the IL-1RI, no complex forms and therefore no signalling (agonist activity) occurs. The IL-1RII is a 68kDa membrane protein that lacks a cytosolic signal transducing domain and therefore remains functionally negative, acting as a decoy receptor. It preferentially binds IL-1 β , preventing its binding and therefore signalling via the IL-1RI [26]. It is worth noting that in primary cells, there are less than 100 IL-1RI per cell and a biological response occurs when as few as 2-3% of them are occupied [27].

1.2.7 The role of Interleukin-1 in atherosclerosis

There are multiple potential sources of IL-1 at the time of arterial injury. Adherent platelets may produce IL-1, as well as the recruited inflammatory cells. In addition endothelial cells, which re-grow and cover the site of injury may also produce IL-1. IL-1 has many inflammatory effects upon endothelial cells and vascular smooth muscle cells, plausibly associated with neointima formation and notable amongst these is the autocrine induction of PDGF by vascular smooth muscle cells [3]. A role for IL-1 in atherosclerosis was confirmed when IL-1 β mRNA was detected in human atherosclerotic plaques [28]. Subsequent work showed that treatment of porcine arteries with IL-1 β induced intimal lesions [29]. IL-1 β mRNA and protein have also been detected in coronary arteries of patients with ischaemic heart disease [30]. After experimental injury, IL-1 β mRNA is present in porcine coronary arteries within 1h of injury and persists up to 18h. IL-1 β protein, detected by immunohistochemistry is localised to the luminal endothelium and has peak

expression between 3 and 14 days post-PTCA [31]. Recktenwald *et al* have shown that mice deficient in the type 1 IL-1 receptor gene develop less neointima than wild-type mice [32]. These studies lead to the hypothesis that locally generated IL-1 β may contribute to atherosclerosis and the vascular response to balloon injury.

1.2.8 Interleukin-1 administered to humans

IL-1 α and IL-1 β have both been administered to humans. Subcutaneous injection was associated with significant local pain, erythema and swelling [33] and patients given a continuous intravenous infusion experienced a febrile response that increased in magnitude with increasing dose of IL-1. Nearly all patients receiving intravenous IL-1 at a dose of 100 ng/kg or greater experienced significant hypotension [34]. These studies confirmed the pyogenic and hypotension inducing properties of the molecule.

1.2.9 The role of IL-1ra in atherosclerosis

Several studies on IL-1ra have provided further evidence for the IL-1 family and its role in atherosclerosis. For example, IL-1ra inhibits the formation of intimal fatty streaks in apolipoprotein E-deficient mice [35] and IL-1ra knockout mice have been shown to spontaneously develop arterial inflammation [36]. A recent study by Isoda *et al* used knockout mice to test the hypothesis that IL-1ra was directly involved in neointima formation. They showed that the absence of IL-1ra promotes neointima formation in the

mouse model and provides more evidence for the role of IL-1 and IL-1ra in the vessel wall response to injury. In patient studies, plasma concentrations of IL-1ra are elevated in patients with atherosclerosis and levels correlate well with disease occurrence [37]. In addition, circulating levels of IL-1ra following acute myocardial infarction are elevated [38]. Interestingly, those patients with in-patient complications had a higher serum IL-1ra levels on admission.

1.2.10 Interleukin-1 receptor antagonist and amelioration of disease

Several clinical trials have used IL-1 receptor antagonist, the natural inhibitor of IL-1, in the treatment of disease with clinical success [39, 40]. However, none of these have studied its effect on coronary heart disease. A consistent observation in these trials is a reduction in the number of infiltrating neutrophils associated with local inflammation [41]. IL-1ra has been given to patients, with amongst other things, graft *versus* host disease and rheumatoid arthritis. A large double blind vehicle-controlled trial of IL-1ra in 472 patients with rheumatoid arthritis resulted in a dose-dependent reduction in the number of swollen joints and overall assessment of patient scores ($p=0.048$) [39]. Doses used ranged from 30 - 150mg/24h for 24 weeks, with no demonstrable side effects from the IL-1ra. A study looking at steroid resistant graft *versus* host disease used doses as high as 3400mg/24hr for 7 days with improvement in 16 out of 17 patients and no side effect profile [42]. Studies have shown IL-1ra to be safe when given to humans at high concentration (10mg/kg over 3 hours) [43].

1.3 Cardiac manifestations of atherosclerosis – coronary heart disease

1.3.1 Incidence of coronary heart disease

Cardiovascular disease is the most frequent cause of death amongst adults in developed countries. Coronary heart disease, the most common cause of death in the UK accounted for around 125,000 deaths in the UK in 2000, approximately 1 in 4 deaths in men and 1 in 6 deaths in women. It accounts for 26% of premature deaths in men and 16% in women. Approximately 1.5 million people suffer from angina in the UK (British Heart Foundation data, 2000). Using 1999 CHD mortality data from the Office for National Statistics, it has been estimated that 149,000 men and 125,000 women per year in the UK will have a myocardial infarction. In the USA, the Framingham study has shown the incidence of CHD is 5 per 1000 men per year aged 35 – 44 years, increasing to 59 per 1000 men per year aged 85 – 94 years. Women lag behind men by approximately a decade until after the menopause when the difference reduces. Heart disease in the UK is a significant problem, costing an estimated £10 billion per annum, including loss of earnings, disability benefit and the costs of caring, of which £1.6 billion is spent directly on health care (British Heart Foundation figures, 1998).

1.3.2 'Angina Pectoris' (angina)

The clinical manifestation of coronary heart disease is *angina pectoris*. Heberden first used this term in 1768 to describe '*a painful and most disagreeable sensation in the breast, which seems as if it would extinguish life, if it were to increase or continue*'. It was not until 1786 after participating in post-mortems of people who had died from angina that Jenner proposed it was due to '*a kind of firm fleshy tube, formed within the vessel, with a considerable quantity of ossific matter dispersed irregularly through it*', what we now understand to be atherosclerosis (the reader is again referred to the review of the history of CHD by Fye) [44]. There are four clinically recognised syndromes of angina; stable, unstable, Prinzmetals and Syndrome X. The first two are by far the commonest. Unstable angina is defined as unprovoked angina (at rest). Prinzmetals angina is a rare syndrome in which vasospasm occurs, usually at a site of minimal disease causing ST segment elevation on the ECG. Syndrome X encompasses angina, a positive test of provoked ischaemia (for example an exercise test) and angiographically normal coronary arteries. The cause is unclear but thought to be secondary to disease of small coronary vessels [45].

1.3.3 Patho-physiologic mechanisms in stable and unstable angina

Stable angina is most commonly related to an increase in myocardial oxygen demand triggered by physical activity. During exercise, when the demand by the myocardium for oxygen is greater, homeostatic mechanisms are activated

that lead to vasodilatation resulting in increased coronary artery diameter and consequent oxygen supply. Invariably, in patients with angina, a fixed coronary artery obstruction is present (i.e. an atherosclerotic plaque) which limits oxygen delivery during times of increased metabolic demand. Non-occlusive coronary thrombi (caused by unstable or 'ruptured' coronary plaques) are usually present in patients with unstable angina and cause an acute impairment in oxygen delivery. The neural pathways involved in angina have not been established, although sympathetic afferent nerves are thought to be involved.

1.3.4 Clinical presentation of stable and unstable angina

It is well established that many people have stable atherosclerotic plaques within their vasculature that remain so for years. These only cause symptoms of angina when they grow large enough to narrow the arterial lumen and impede blood flow. At necropsy, patients who have had chronic stable angina for years usually have one or more coronary arteries reduced by 50% in diameter [46]. The definition of angina is largely based on the clinical presentation. Stable angina pectoris is characterised by chest or arm discomfort associated with physical exertion, emotional stress or cold weather that is relieved by a short period of rest or sublingual nitroglycerin. Unstable angina is a poorly defined syndrome and describes a very heterogeneous population of patients with single or multi-vessel disease, with or without prior myocardial infarction. It includes patients with one of the following: (1) chest pain that occurs at rest (or with minimal exertion) lasting more than 20

minutes (2) a severe and frank pain of new onset (i.e., within one month) and (3) a pain that occurs with a crescendo pattern [47]. Unstable angina results from plaque that becomes unstable and prone to rupture due to episodic inflammatory events (see 1.1.2), resulting in the development of intracoronary thrombus and an acute coronary syndrome (an episode of chest pain that represents either unstable angina or myocardial infarction).

1.3.5 Treatment of stable angina

Pharmacological therapy with aspirin, nitrates and β -blockers provides the mainstay of treatment. Initial attempts at the surgical treatment of CHD were unsuccessful and it wasn't until the 1960s that Favoloro's procedure of aorto-coronary bypass grafting (CABG) under cardio-pulmonary bypass provided a successful, safe method of angina treatment. Initial operations were performed using the internal mammary artery and, as the technique developed, autologous saphenous veins were used. More recently, gastro-epiploic and radial arteries have been used. These developments have made the operation even more safe and successful. Other surgical approaches include sympathectomy and, in extreme cases, cardiac transplantation [48]. Since the 1980s, percutaneous revascularisation (percutaneous coronary intervention (PCI)) has also become a treatment option providing an alternative to surgery.

1.3.6 Indications for PCI and CABG

The clinical indication for revascularisation is poor symptom control by medical therapy. Over the last few years, due to advancements in the equipment available and increased operator experience, the indications for PCI have changed, encompassing a wider remit. A number of randomised trials have directly compared the efficacy of PCI and CABG in single and double vessel disease, with discrete stenoses (RITA 1993, BARI 1996, EAST 1994 to name a few). For a review of medical therapy vs. PCI vs. CABG see Kurbaan *et al.* [49]. In general, these studies revealed similar mortality figures (2 – 3% at one year), except in diabetic patients, who experience a higher mortality after PCI than CABG, within the limitations of the inclusion criteria. The difference was seen in the excess of re-interventions in the PCI group, reflecting both clinical and angiographic restenosis. There are no data on long-term follow-up but these will be important, because the mortality of re-do CABG is greater than first time operation; and PCI is easily repeatable at relatively low risk. With the advent of drug-eluting stents, the balance has now firmly tipped towards PCI.

1.3.7 Anti-inflammatory treatment strategies

The effects of anti-inflammatory treatment in unstable angina are unknown. It is well established that aspirin-like drugs are good anti-inflammatory agents, related to their action on cyclo-oxygenase. A potential beneficial effect of aspirin on the prevention of acute coronary syndrome was suggested by

Ridker *et al* [50]. They found that when apparently healthy men received aspirin, they had significantly fewer episodes of myocardial infarction during follow-up. This reduction was significantly associated with CRP levels. The greatest decrease in risk of future events was in those men with a high baseline C- reactive protein who received aspirin.

Numerous trials have shown that treatment with a statin (a cholesterol lowering agent) reduces the rate of major coronary events [51]. One beneficial effect of statins is their lowering of LDL-cholesterol, although pravastatin and cerivastatin have both been shown to reduce macrophage accumulation and matrix metalloproteinase expression in atherosclerotic plaques [52, 53]. These observations have led many to believe that there are non-lipid related mechanisms of statin action that include an anti-inflammatory effect. Many believe that anti-inflammatory strategies may help to reduce the incidence of coronary heart disease although, to date, none have been tested.

1.4 Percutaneous coronary intervention (PCI)

1.4.1 Percutaneous coronary intervention – an historical perspective

Percutaneous coronary intervention (PCI) comprises percutaneous transluminal coronary angioplasty (PTCA) and coronary stent implantation. Andreas Gruntzig, published his initial PTCA results in 1978 and pioneered the technique. Stent implantation has become commonplace since the mid-

1990s and technology in this area continues to grow. Although catheter based techniques of revascularisation have an initial success rate that exceeds 95%, the immediate benefit is still attenuated by restenosis (the return of clinical symptoms following an apparently successful intervention) that occurs over the following 6 months.

1.4.2 Proposed patho-physiologic mechanisms of PTCA

The original explanation given by Gruntzig for enlargement of a vessel lumen by PTCA was compression of plaque [54] but this is now thought to be a minor effect. Other contributing factors are the extrusion of liquid components of the soft plaque and cracking of the intimal plaque with resultant stretching of the media and adventitia (layers of the arterial wall) and expansion of the outer diameter of the vessel. Waller studied *post mortem* specimens derived from 76 PTCA sites in 66 patients who died following PTCA and found evidence of superficial intimal cracks in 16%, deeper cracks with medial dissection in 73%, extensive medial dissection in 7% and adventitial perforation in 3% [55]. He went on to state that five basic mechanisms are involved in PTCA: plaque compression; focal plaque tear; stretching of the contralateral normal segment of arterial wall; stretching of the whole artery with little plaque compression; and dissection. These mechanisms have been confirmed by intravascular ultrasound (IVUS) imaging [56].

1.4.3 Limitation of PTCA

The major drawback of PTCA is that up to 40% of patients return with symptomatic restenosis. Restenosis is a multifactorial process, and features an excessive neointimal (smooth muscle cell) response to injury, recoil of the artery and negative remodelling (in which the restenosing artery gets smaller rather than bigger to accommodate the intraluminal tissue). It therefore follows that forming and maintaining a large arterial lumen will reduce the impact of restenotic tissue on blood flow. One method of doing this is to implant a coronary stent, which scaffolds the artery thereby eliminating recoil.

1.4.4 Intracoronary stenting

Over 90% of PCI performed in the UK today involves the implantation of an intraluminal stent. Traditional coronary stents are bare-metal (stainless-steel) cages that scaffold the artery, stabilise the plaque and help to prevent arterial recoil and therefore restenosis. BENESTENT 1 and STRESS, two early but significant clinical trials, clearly showed that stenting in native vessels reduced the incidence of restenosis compared with PTCA alone [57, 58]. Stents eliminate acute recoil of the vessel but, unfortunately, neointima formation still occurs. It is worth noting that stenting actually results in more neointima formation than PTCA, but has an overall lower restenosis rate because of the prevention of unfavourable remodelling. In-stent restenosis using conventional bare metal stents occurs in 20 – 30% of patients (depending upon lesion and

patient type). A cure has proved elusive and, until a few years ago, remained one of the big outstanding challenges for investigators.

1.5 Restenosis after PCI

1.5.1 Clinical and angiographic Restenosis

Restenosis, an iatrogenic phenomenon, is commonly referred to 'as *the process where a stenotic coronary artery, which regained significant patency following mechanical intervention, reverts to its former state of insufficient lumen diameter (practically $\geq 50\%$ loss of the gain by PTCA or stent)* ' [59]. Of the 169 patients who underwent PTCA by Gruntzig, 31% required re-PTCA because of restenosis [60]. Since that time, for patients who undergo PTCA without placement of a stent, the number experiencing restenosis has not dramatically altered [61]. In studies that examine rates of restenosis following PCI, a distinction is made between clinical and angiographic restenosis, the former being those patients who require re-intervention because of re-presentation secondary to symptom recurrence, and the latter those in which restenosis is noted at follow-up angiography but is not clinically apparent to the patient. There are problems with these definitions: clinical restenosis is subjective and angiographic restenosis has been described in many different ways, resulting in differing rates that depend on the definition used. An example of angiographic restenosis following PTCA is shown in Figure 1. In studies, angiographic definitions are usually required and usually comprise a

categoric definition such as diameter stenosis $\geq 50\%$ at follow-up and also a continuous one such as late loss [62].

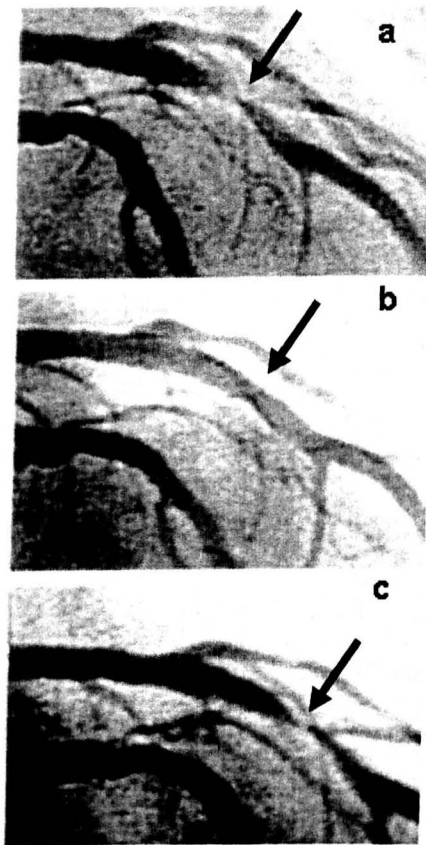


Figure 1 The angiographic appearance of restenosis

- (a) A tight localised stenosis in the left anterior descending artery is shown.
- (b) The appearance of the lesion following insertion of a stent.
- (c) Restenosis in the same lesion six months after initial stent deployment.

1.5.2 Time-course of restenosis

Two landmark studies in 1988 defined the time-course of restenosis. Both performed serial quantitative angiography after PTCA. The study by Nobuyoshi *et al* [63] followed patients to 4 months post-procedure, and that by Serruys *et al* [64] to 12 months. In both studies, over three to four months, the mean minimum lumen diameter (MLD) decreased by 20% and the reference diameter by 10%. There was no further reduction after that time. Future studies showed that restenosis is complete by six months [65].

1.5.3 Pathogenesis of restenosis

Information about restenosis at a cellular level has come from examination of tissue sections following atherectomy and at post mortem. Coronary angiography immediately following PTCA has shown plaque fissures and tears with mural thrombus in 70 – 80% of arteries despite the use of anticoagulant therapies [66]. Arterial tissue from atherectomy confirms that mural thrombus, intimal vascular smooth muscle cell (VSMC) and fibroblast proliferation occur within the first month of PTCA. Following these initial events, collagen and extracellular matrix (most likely synthesised by the VSMCs and fibroblasts) are more abundant. Thus, restenosis is a multi-factorial process.

In summary, the following events contribute to restenosis. Angioplasty causes vascular injury. This results in the exposure of the internal elastic lamina of the vessel, which is a thrombogenic surface. This promotes platelet

aggregation and adhesion that release cytokines and growth factors and attract circulating inflammatory cells, which adhere to and migrate into the already formed thrombus [67]. The initial events are therefore thrombosis and inflammation. Following this, granulation occurs where recruited VSMCs proliferate. Finally, a fibrous matrix forms, consisting of collagen and proteoglycans. Restenosis is localised to the site of balloon injury and its adjacent segment [55].

1.5.4 The importance of inflammation in restenosis

Inflammation occurs early on following angioplasty or stent insertion. Neutrophils, lymphocytes and monocytes have been detected within the mural thrombus seen following angioplasty in a rabbit model [68]. Both traumatic arterial injury following PTCA, or stent placement and subsequent inflammation, therefore contribute to neointima formation. Farb *et al* looked at the time-course of the histopathological response to stenting and showed that following stent insertion, there was fibrin, platelets and an acute inflammatory infiltrate around the stent struts. Over time, a chronic inflammatory infiltrate is evident [69]. Kornowski *et al* found a direct correlation between the inflammatory score (a score they devised to describe the extent and severity of an inflammatory cell infiltrate around metallic stent struts) and the degree of subsequent arterial injury and neointimal thickness [70]. At a cellular level, a single nucleotide polymorphism of the MAC-1 (CD11b/CD18) leukocyte integrin receptor has been shown to have a strong association with the incidence of restenosis [71].

The inflammatory process following PCI seems to be both specific to the site of injury and systemic. The local inflammatory response has already been described (see section 1.5.4). Evidence for a systemic response has been provided by several studies. Danenberg *et al.* demonstrated that administration of systemic bacterial lipopolysaccharide to a rabbit undergoing balloon angioplasty, resulted in increased neointima formation [72]. This effect was probably due to systemic activation of circulating leukocytes. A correlation of neointimal growth and systemic inflammation by the measurement of blood IL-1 β levels and the measurement of intimal growth was performed. In support of the role of inflammation, Schillinger *et al.* demonstrated that baseline and 48-hour post-procedure CRP levels were independent predictors of restenosis at 6-months following PCI [73].

1.5.4 Anti-inflammatory approaches to restenosis

Several anti-inflammatory strategies have been successful in inhibiting restenosis in animal models. IL-10 has been shown to inhibit neointima formation following both PTCA and stenting in hypercholesterolaemic rabbits and, by using an antibody directed against the β 2-integrin Mac 1 (CD11b/CD18) in the rabbit model, neointima formation has also been reduced [74]. In a pig model, Wang *et al.* showed that pre-treatment of animals with an antibody to P-selectin glycoprotein ligand (PSGL – the ligand for P-selectin on leukocytes) prior to balloon angioplasty significantly reduced neointima formation at 28-days [75].

The importance of an anti-inflammatory approach to atherosclerosis has already been discussed (see 1.3.8). From those data presented above, there is also significant evidence that inflammation plays an important role in the induction and continued formation of neointima. It follows therefore, that an anti-inflammatory approach to restenosis would be an attractive target for its prevention.

1.5.5 Current approaches to restenosis

Therapeutic approaches to restenosis may be preventative or therapeutic (i.e. treating the restenosis once it has occurred). The former approach is preferable as disease is always harder to treat once established. In order to help prevent restenosis, the angiographic result obtained during the procedure should be as good as possible with accurate stent sizing and as little damage to adjacent tissue as possible should occur. Despite all precautions, restenosis will still occur in a significant number of patients. Pharmacological approaches to inhibit restenosis have been developed and have focused on four main strategies; anti-proliferative; anti-inflammatory; anti-migratory and pro-endothelial. Systemic and local delivery approaches have been studied and are described further in 1.6. The work in this thesis has concentrated on an anti-inflammatory strategy to prevent restenosis.

1.5.6 In-stent restenosis – current treatment options

There are now two major treatments for in-stent restenosis. The first, called vascular brachytherapy is a secondary measure that is used once restenosis has developed. This technique reduces restenosis within an artery by about 60%, irrespective of whether β -emitting or γ -emitting radiation is used. However, radiation has safety issues and is limited by geographical miss (an area of restenosis that does not receive radiation therapy), edge of stent restenosis and late stent thrombosis. Primary preventative strategies have concentrated on eliminating restenosis at a cellular level. Different approaches have been tried, including anti-proliferative, anti-migratory, anti-inflammatory and pro-endothelial (healing) strategies. Agents that seemed promising following *in vitro* and *in vivo* animal studies often failed to translate into clinical efficacy in man. The reasons for these failures were unclear. It was not until a stent-based, local delivery system using a biologically inert polymer to release the drug (called a drug-eluting stent) was employed that results dramatically improved and clinical benefits were seen.

1.5.8 Drug-eluting stents

The first drug-eluting stent (CypherTM, Cordis) was recently made commercially available in the UK. Data from the RAVEL study and the 'First-in-man' study show that this device, which elutes the drug Sirolimus (Rapamycin), continues to produce a zero restenosis rate up to, and beyond, one year in selected lesions [76, 77]. Rapamycin is a naturally occurring

macrolide antibiotic, with immunosuppressant, anti-proliferative, anti-migratory and anti-vascular smooth muscle cell properties. It is produced by the actinomycete *Streptomyces hygroscopicus*, found on Eastern Island, and is a cell cycle inhibitor that arrests the cell at the end of the G1 cell cycle. The Sirolimus eluting stent has been followed by the Paclitaxel-eluting stent, Paclitaxel being another anti-proliferative agent. Paclitaxel was originally isolated from the bark of the Pacific Yew and exerts its anti-proliferative effects through microtubule stabilisation – shifting the balance of microtubule equilibrium towards assembly, leading to reduced proliferation, migration and signal transduction. The recently published TAXUS IV trial confirmed that Paclitaxel leads to equally impressive clinical results as Sirolimus [78]. These results have seen drug-eluting stents proclaimed by many as a great breakthrough for PCI with restenosis now solved, but others heed caution. One potential problem with drug eluting stents is that the biological effect is only seen where the drug is in contact with the arterial wall. Both of the available agents thus far have anti-proliferative actions, and their use in unstable patients with acute coronary syndromes is still unclear. It may be that these 'inflammatory' patients require a different approach. In view of this, a role for anti-inflammatory agents has been postulated. Dexamethasone is a glucocorticoid with predominantly anti-inflammatory effects. Clinical trials with the dexamethasone eluting stent seem promising with a 3.3% target lesion revascularisation (TLR), which is comparable to that seen with Sirolimus and Paclitaxel, although patient numbers are small and further studies are ongoing [79].

The initial results with drug eluting stents are impressive, but longer term follow-up is needed and may reveal effects that are less permanent than anticipated. No one single process is responsible for restenosis and, therefore, it may be that different approaches, including both local and systemic delivery of different agents, are necessary for different lesions or patient subtypes.

Advantages of drug-eluting stents are that they provide locally delivered drug with no systemic side effects. Drugs can be delivered over a defined period of time and the kinetics accurately determined to augment vascular healing.

Disadvantages are that the drugs can only be delivered for a defined period of time and due to physical limitations of the stent, only a finite amount of drug can be delivered. Economic concerns include their high price. If a systemic agent can be developed that inhibits restenosis, the use of oral agents in combination with bare metal stents may offer a cheaper and more effective means of dealing with restenosis.

1.6 Treatment delivery

1.6.1 Systemic versus local therapy

Since PTCA became widespread in the 1970s, attempts have been made to combat restenosis. Initial strategies concentrated on systemic drug therapy using numerous antiplatelet and anticoagulant drugs, with disappointing results. Following this, the role of calcium antagonists, omega 3 fatty acids,

steroids and various antiproliferative agents were studied [80]. Small initial studies showed promise. However, results were not corroborated in larger clinical trials. An example of this is the Prevention of REStenosis with Tranilast and its Outcomes (PRESTO) trial [81]. Tranilast is an antiallergy drug that has inhibitory effects on cytokines, TGF β and PDGF. In PRESTO, 11,500 patients were randomised to receive either systemic Tranilast or placebo. Despite promising earlier small-scale studies, the results were negative. The main reason cited for the negative results seen with systemic therapy was the failure to achieve high drug levels at the angioplasty site. This was supported by animal studies where efficacy was only seen when high drug dosages were used. It was these disappointing results that led to the development of local drug delivery systems. However, not all of these have been successful. Early experience with the antiproliferative agent Actinomycin D was disappointing because of a high restenosis rate and poor long-term outcome. It therefore seems that both the mode of delivery and the drug delivered are of equal importance. It is worth noting that the majority of clinical trials investigating the use of systemic therapies were conducted in the pre-stent era. There have been positive trials using systemic agents in the stent era such as oral Everolimus [82] and oral prednisolone [83].

1.7 Conclusions and future directions

1.7.1 The future of anti-restenosis therapy

Atherosclerosis is a chronic inflammatory condition and the majority of the clinical manifestations of the disease are the direct result of acute on chronic inflammatory states. Restenosis following PCI is similar to this in that the procedures performed induce local and systemic inflammation, resulting in leukocyte infiltration, cellular proliferation and ultimately neointima formation. Drug-eluting stents have reduced the incidence of restenosis following PCI, and the number of patients requiring re-intervention is now comparable to that of CABG [76]. Despite this, there is still uncertainty as to whether the two agents in current clinical use, sirolimus and paclitaxel, are sufficient to treat the wide variety of lesions found in every day practice. It is also worth considering that by concentrating on a different strategy, for example, an anti-inflammatory rather than an anti-proliferative one, the rate of restenosis may be reduced even further.

1.8 Aims of this thesis

The hypothesis behind this work was that inflammation plays a crucial role in the vessel wall response to injury and stenting and that Interleukin-1 is central to this inflammatory response. Since IL-1 signalling via the IL-1R1 receptor is a crucial determinant of the arterial response to injury, blocking this with either

IL-1ra or the type II receptor, could modify the response to injury. The aims of this thesis, therefore, was to:

Determine whether the human type II IL-1 receptor could be used as an inhibitor of porcine IL-1 using SPR; Establish that IL-1 signalling through the type 1 IL-1 receptor was a determinant of the vessel wall response to injury; Determine the effect of inhibiting IL-1 signalling in a model of oversized balloon angioplasty and coronary stenting in the pig; Quantify differences in IL-1 mRNAs in the vessel wall following injury.

CHAPTER 2

HUMAN IL-1 TYPE II INTERLEUKIN-1 RECEPTOR AS AN INHIBITOR OF PORCINE IL-1

2.1 INTRODUCTION

2.1.1 Possible inhibitors of Interleukin-1 signalling

In order to determine whether inhibition of IL-1 action prevents restenosis, initial experiments concentrated on finding a molecule or compound that could be used in the porcine model of experimental injury. The aim of any anti IL-1 strategy would be to prevent IL-1 binding to its surface signalling receptor. Possible naturally occurring inhibitors of IL-1 include Interleukin-1 receptor antagonist (IL-1ra) and the soluble forms of the IL-1 receptors. The IL-1 receptors as potential inhibitors were considered first.

The IL-1 Type 1 receptor (IL-1RI) has been used as an inhibitor of IL-1 in several studies. In a rat model of arthritis, local instillation of IL-1RI reduced joint swelling and tissue destruction [84]. In a model of experimental encephalitis, sIL-1RI reduced the severity of the disease [85]. However, there is some evidence that sIL-1RI may be ineffective in human disease. A phase-1 trial of sIL-1RI was conducted in patients with acute myeloid leukaemia. The drug was well tolerated but there was no clinical response to treatment and serum levels of IL-1 β remained unchanged [86]. The same was true

when sIL-1RI was given to patients with rheumatoid arthritis. There was no improvement in clinical outcome [87]. The reason for the lack of effect of sIL-1RI is thought to be because the sIL-1RI binds IL-1ra with the greatest affinity (i.e. greater affinity than with which it binds IL-1 α or IL-1 β) therefore, sIL-1RI binds endogenous IL-1ra in preference to IL-1 causing a reduction in its biological function [88].

IL-1RII can also be considered as a potential agent for IL-1 inhibition. There are three different mechanisms through which IL-1RII acts as an inhibitor of IL-1 that all involve reduction in ligand binding to the membrane bound type-1 receptor. The first is based on cell-surface bound IL-1II, which fails to trigger IL-1 signalling following ligand binding. This therefore acts as an inhibitor of IL-1 by competing with the IL-1RI for binding of the IL-1 agonists. The second mechanism is based on the soluble extracellular form of IL-1RII (sIL-1RII), which is released from the cell surface (due to protease activity) and binds IL-1 (thereby preventing it from binding to the type-1 receptor). Again, this receptor form produces no signal and therefore elicits no biological response. The binding of IL- β to sIL-1RII is effectively irreversible because of its long dissociation rate (>2h) [89]. The third mechanism involves the accessory protein (IL-1RAcP). Following binding of IL-1, the IL-1RII recruits the IL-1RAcP into its non-functioning complex thereby preventing it from binding to and forming a signalling complex with IL-1RI [90]. Using sIL-1RII as an inhibitor of IL-1 is thus analogous to using soluble antibodies against IL-1. Unlike IL-1RI, IL-1RII binds IL-1 with greater affinity than it binds IL-1ra. The efficacy of IL-1RII as an inhibitor of IL-1 has been confirmed using gene

transfer experiments. These have shown that in chondrocytes, both the sIL-1RII and IL-1ra are better inhibitors of IL-1 than sIL-1RI and are both of approximately equal potency.

An obvious target for IL-1 inhibition therefore was sIL-1RII and initial work concentrated on its use. To determine whether human sIL-1RII could be used as an inhibitor of porcine IL-1 in an experimental injury model, it was necessary to determine whether the human receptor would bind porcine IL-1. This was done using BIAcore methods where the optical phenomenon of surface plasmon resonance was used to detect refractive index changes (caused by ligand binding) in a surface layer of a gold foil-coated slide, illuminated by monochromatic light ($\lambda = 760\text{nm}$).

2.1.2 Surface plasmon resonance

All molecules react with each other, through specific interactions and bindings. In order to determine whether a particular inhibitor will be of use in any given system, it is first necessary to determine whether the inhibitor will interact with its target molecule (protein). One *in vitro* technique that can be used to investigate bimolecular interactions between proteins is surface plasmon resonance (SPR) [91]. It has been known for some time that electrons can move freely through metal. At a metal-medium interface however, dipole excitations cause the propagation of electron waves called surface plasmon waves (SPW). The BIAcore instrument is based on this optical phenomenon. The SPR optical unit consists of a source of light that

passes through a prism and strikes the surface of a flow cell such that the angle of the beam is totally reflected (Figure 2). When this occurs, the electromagnetic component of the beam propagates into the aqueous layer and interacts with mobile electrons in the gold film at the surface of the glass. At a particular wavelength and incident angle, a SPW of excited electrons (the plasmon resonance) is produced at the gold layer and is detected by the optical unit as reduced intensity of the reflected light beam (Figure 2). The SPR angle is sensitive to the composition of the layer at the gold surface. A baseline SPR angle is first calculated following binding of the ligand to the dextran matrix within the BIAcore chip. When protein flows across the chip, ligand binding causes an increase in the refractive index at the surface of the chip, thereby changing the SPR angle and the detection on the optical unit. The BIAcore technology reports the change in SPR angle as resonance units (RU), where 1000 RU corresponds to a change of $\sim 0.1^\circ$. For most proteins, this equates to binding of $\sim 1 \text{ ng/mm}^2$ of protein.

SPR has already been used to study the binding of human IL-1 α , IL-1 β and IL-1ra to human soluble IL-1 receptors [89]. This work confirms that SPR is a good technique for determining cytokine-receptor ligand binding and has been shown to be effective for IL-1.

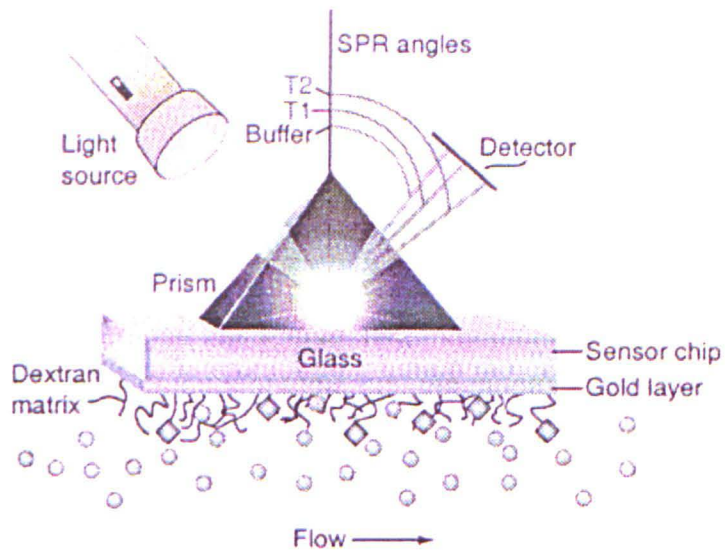


Figure 2 SPR optical unit and a sensor chip

The protein molecules (circles) bind to the immobilised ligand (diamonds) that is linked to the dextran matrix. The SPR angle (T1 before ligand binding and T2 after binding) defines the position of the reduced-intensity beam.

2.1.3 Aim of this study

The aim of this section of work was to determine whether human IL-1RII could bind porcine IL-1 and therefore be used as an inhibitor of IL-1 in a porcine model of experimental injury.

2.2 MATERIALS AND METHODS

All chemicals for were from Sigma (Poole, Dorset, UK), apart from the recombinant cytokines, which were from R&D Systems (Oxford, UK). All chemicals needed for the BIAcore system were obtained directly from BIAcore, UK.

The sensor chip (BIAcore, UK) consisted of Carboxymethyl-dextran linked to a layer of gold. This provided an interaction layer, which was approximately 100nm thick. One of the interacting molecules, in this case the human soluble type 2 IL-1 receptor (sIL-1RII), was bound to the gold-layer on the chip in order to create a biospecific recognition site. In order to achieve this binding, the chip was docked into the BIAcore machine with the gold-dextran layer forming one side of the flow cell through which the solutions run. The sIL-1II was covalently bound to the chip surface (via functional amine groups) to the dextran-carboxyl groups. This process is known as amine coupling. Once the ligand was bound, the excess NHS groups were blocked by a pulsed wave of ethanolamine (Biacore, UK). Any change in refractive index and therefore response units (RU) was due to binding of the ligand to the immobilised receptor. Further details of the type of BIAcore instrument (BIACORE 3000) used are given in the manufacturers handbook [92].

2.2.1 Receptor immobilisation to the BIAcore chip surface

All cytokines used for the BIAcore work were ordered 'carrier-free' to ensure that non-specific binding to the sensor chip by carrier proteins was avoided. The sIL-1RII was covalently immobilised to a hydrogel chip (BIAcore, UK), using N-hydroxysuccinimide (NHS)-based chemistry, i.e., via lysine ϵ -amino groups. Each chip had 4 flow cells to which ligand could be bound. The flow cells were paired up, with one used for ligand binding (the active cell), and the other as a control. Flow cells 2 and 4 were used for ligand binding and 1 and 3 as their respective controls. The chip surface was activated with a 7min pulse (35 μ L at 5 μ L/min) of a mixture of 50mM NHS and 200mM ethylcarbodiimide (EDC) premixed before injection. This was immediately followed by an injection of 100 μ L (at 5 μ L/min) of 10mM sodium acetate, pH 5.0 (BIAcore, UK), containing 40 μ g/ml sIL-1RII over flow cells 2 and 4. This step was omitted in the preparation of flow cells 1 and 3. Excess untreated NHS groups were then blocked with a pulse of 1.0M ethanolamine hydrochloride, pH 8.5 (35 μ L at 5 μ L/min). All reactions during the covalent coupling were performed with the standard BIAcore immobilisation buffer, 10mM sodium acetate, pH 5.0.

2.2.2 Ligand binding to sIL-1RII on the chip surface

These experiments were performed to determine whether human sIL1RII would bind porcine IL-1 ligands. Of all the human IL-1 ligands, human IL-1 β

binds to the human type II receptor with the greatest affinity [89]. The IL-1 β cytokine was therefore used as a positive control in the following experiments.

For measurement of direct ligand binding to immobilised sIL1RII, 50 μ L of each ligand was flowed over the chip at 5 μ L/min. Human IL-1 β (R&D Systems, Oxford, UK) was flowed over flow-cell 2 of the chip at a concentration of 2.94 μ M, (IL-1 β has previously been shown to bind to the type 2 receptor at a concentration of 3nM [89]). Porcine IL-1 β and IL-1 α were both used at 5.8 μ M and flowed over flow-cell 4 of the chip in the same way as the human ligand. All experiments were performed using the standard BIAcore running buffer, 0.15M HEPES-buffered saline, 3.4mM EDTA and 0.05% v/v Tween 20, pH 7.4.

2.3 RESULTS

2.3.1 Immobilisation of the type II receptor

Figure 3a and 3b show coupling of the sIL-1RII to flow cells 2 and 4 of the sensor chip. The horizontal lines on the chart represent the response units (RU) generated (as determined by the change in refractive index) by amine coupling of human sIL-1RII to the chip. Point A represents the initial injection of the NHS/EDC mixture over the chip. Point B indicates the start of injection of the sIL-1RII. There is a gradual increase in RU until point C when injection of the sIL-1RII stops and ethanolamine is flowed over the chip instead. This blocks excess untreated NHS groups and so the final change in RU due to binding of sIL-1RII receptor can be seen at point D. There is a change of 8786 response units (RU) after immobilization of the receptor to flow cell 2 and 8596 response units after its immobilization to flow cell 4. It is known that binding of 1ng/mm^2 of a protein results in a change in RU of approximately 1000 [92]. Therefore, approximately 8.79ng/mm^2 of sIL-1RII receptor is bound to flow cell 2 and 8.60ng/mm^2 to flow cell 4.

Figures 4a and 4b demonstrate the change in RU after amine coupling of flow cells 1 and 3, the control flow cells. The control flow cells are subjected to exactly the same conditions as the active cells (see Figures 3a and 3b) except that no sIL-1RII is flowed over the chip. There is a change of only 179 RU in flow cell 1 and 137RU in flow cell 3.

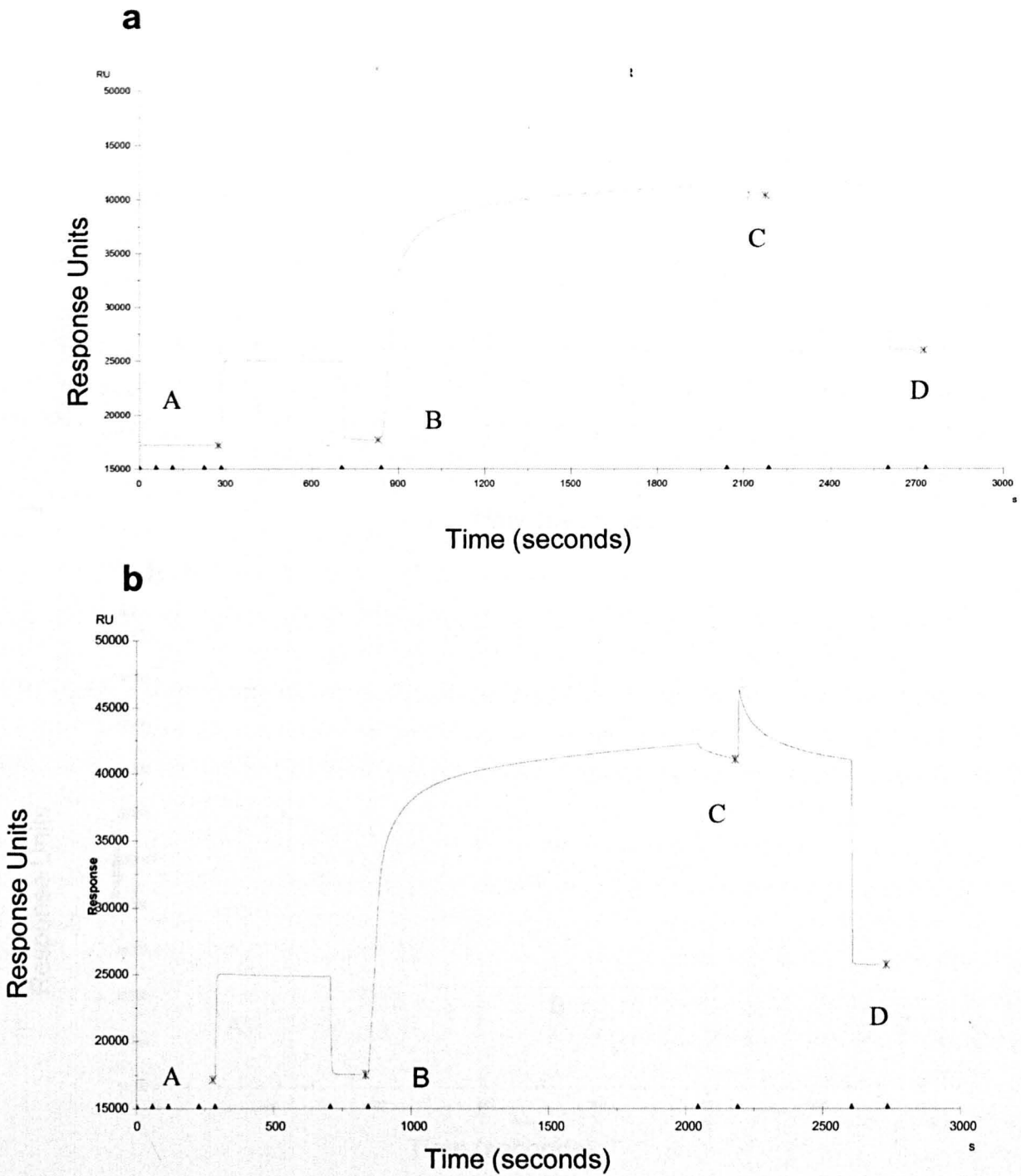


Figure 3 Immobilisation of sIL-1RII to (a) flow cell 2 and (b) flow cell

4 of the sensor chip

A: Injection 35 μ L of EDC/NHS coupling mixture

B: Injection of 100 μ L of human sIL-1RII

C: Injection of 35 μ L of ethanolamine

D: RU due to binding of sIL-1RII receptor

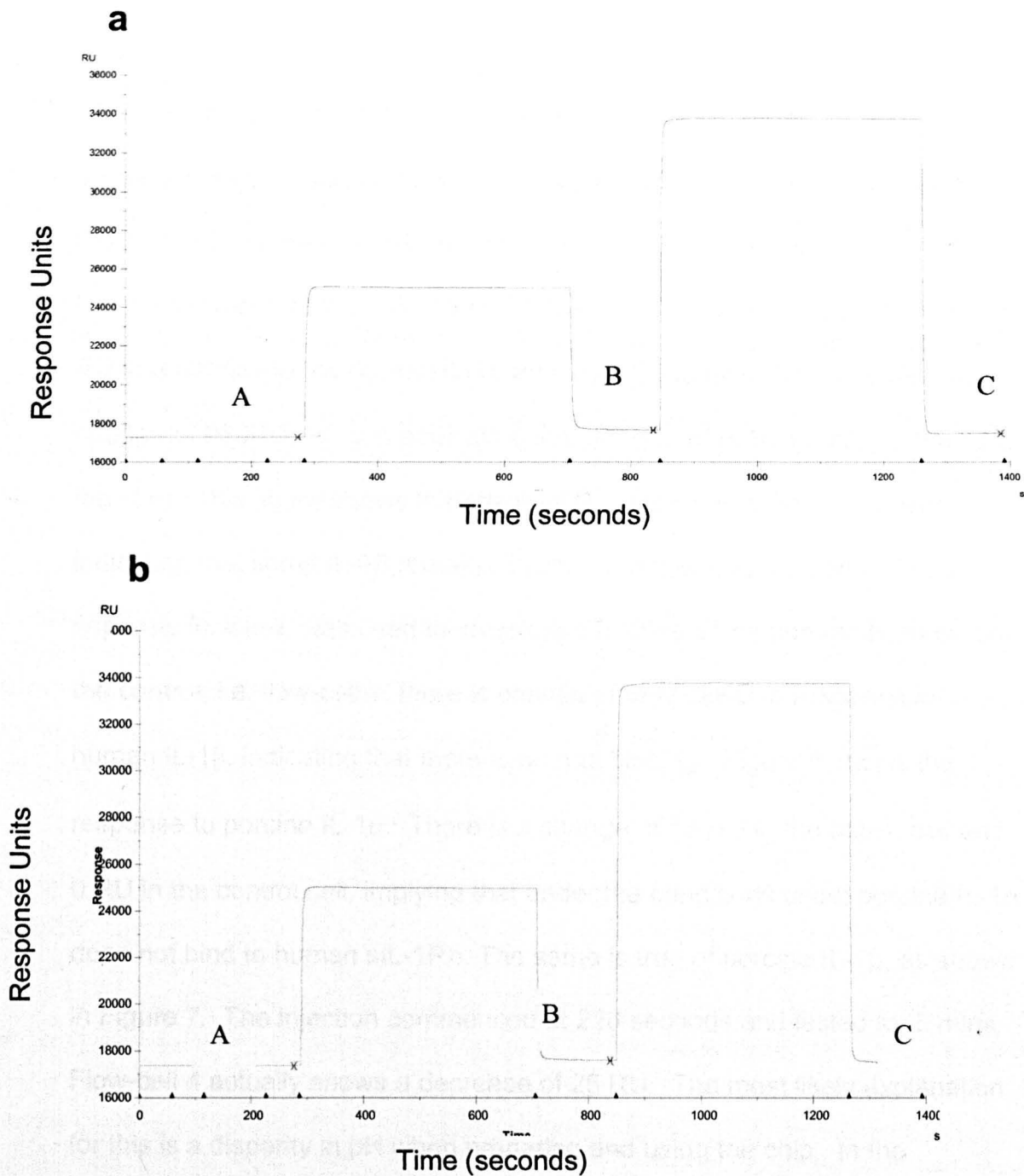


Figure 4 Preparation of control flow cell (a) 2 and (b) 3

A: Injection 35 μ L of EDC/NHS coupling mixture

B: Injection of 35 μ L of ethanolamine

C: RU due to amide coupling

2.3.2 Ligand binding

Ligand binding to sIL-1RII is shown in Figures 5 – 7 (pages 71 – 73). Figure 5 shows the response to human IL-1 β in flow cell 2. The pink line represents the flow cell that has sIL-1RII bound and the blue line the control cell. Human IL-1 β is flowed over the chip from 1500 seconds. There is a clear increase in RU in response to the human IL-1 β and after 5 minutes; there has been a change of 960RU. This is equivalent to 0.96ng/mm² of human IL-1 β bound to the chip. This figure shows that the total RU does not return to baseline, indicating that some IL-1 β remains bound. For this reason, flow-cell 4, a separate flow cell, was used to investigate binding of the porcine ligands. In the control, i.e. flow-cell 1, there is change of only 22RU in response to human IL-1 β , indicating that there is no real binding. Figure 6 shows the response to porcine IL-1 α . There is a change of 18 RU in the active cell and 0 RU in the control cell, implying that under the conditions used; porcine IL-1 α does not bind to human sIL-1RII. The same is true of porcine IL-1 β , as shown in Figure 7. The injection commenced at 220 seconds and lasted for 5 mins. Flow-cell 4 actually shows a decrease of 25 RU. The most likely explanation for this is a disparity in pH when preparing and using the chip. In the immobilisation step, the pH of the solutions used is 5.0. When attempting to bind the ligands, solutions of pH 7.4 are used. It is likely the decrease in RU is due to some elution of the sIL-1RII from the chip in response to change in pH.

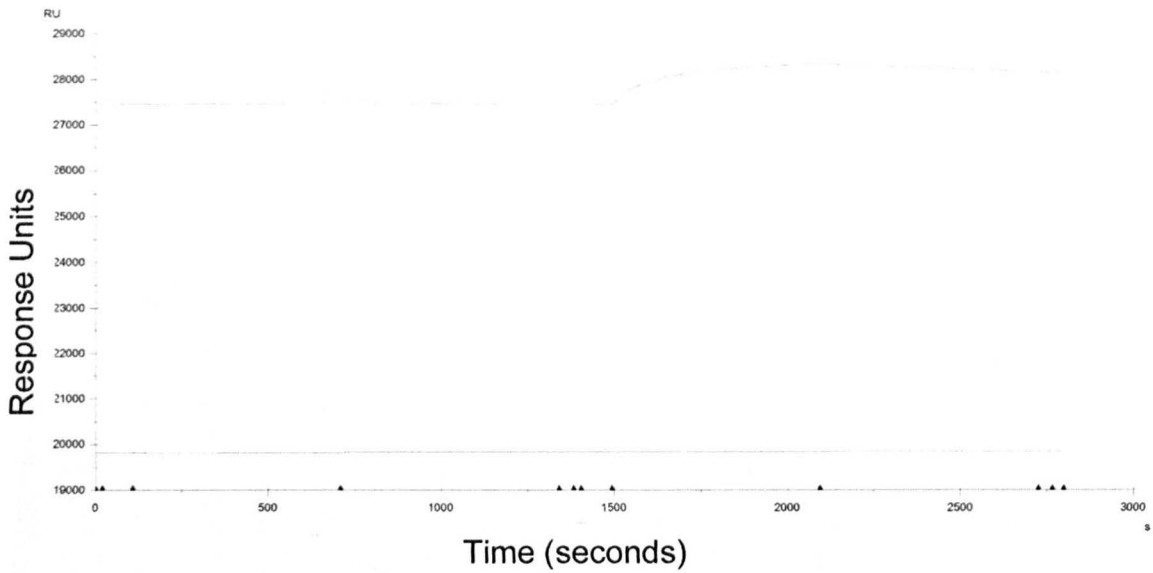


Figure 5 Binding of human IL-1 β to immobilised sIL-1RII and a control flow cell

The pink line shows the binding of human IL-1 β binds to the immobilised sIL-1RII receptor in flow cell 2 and the blue line the corresponding binding to the control cell. Note: The increase in RU 5 min after binding of human IL-1 β is 960RU. This is equivalent to 0.96ng/mm² of human IL-1 β bound to the chip.

was commenced at 110 seconds and lasted for 5 min. Note: The increase of 960 RU in the active cell and 0RU in the control cell is the binding of human IL-1 β to human sIL-1RII.

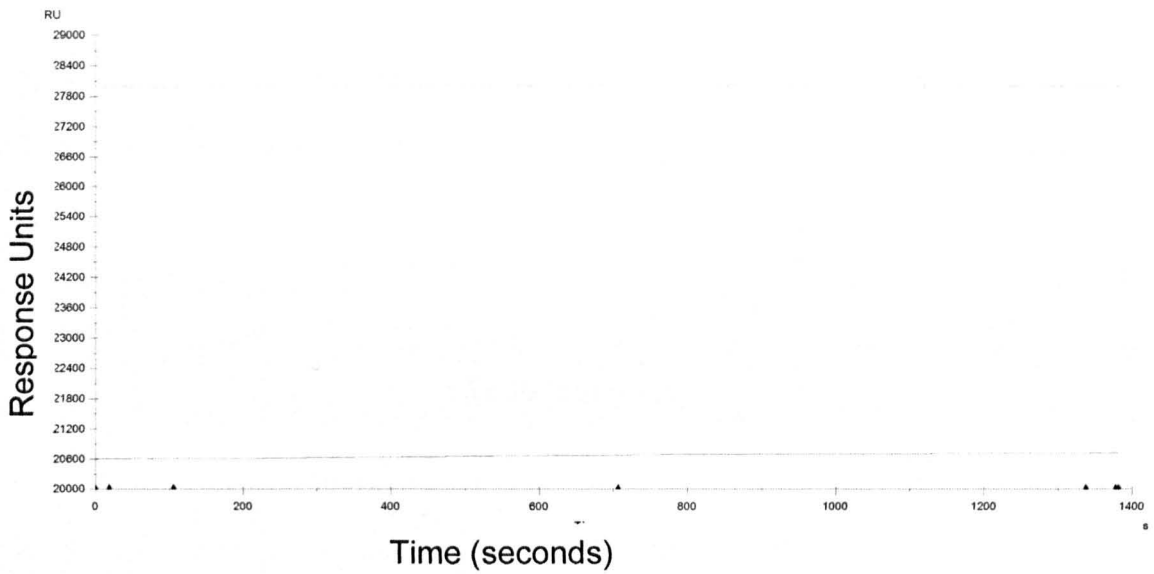


Figure 6 Binding of porcine IL-1 α to immobilised sIL-1RII

The green line shows the binding of porcine IL-1 α to flow cell 4 (with sIL-1RII attached) and the red line the binding to the control flow cell. The injection was commenced at 110 seconds and lasted for 5 mins. Note: A change of 18 RU in the active cell and 0 RU in the control cell, i.e. no binding of porcine IL-1 α to human sIL-1RII.

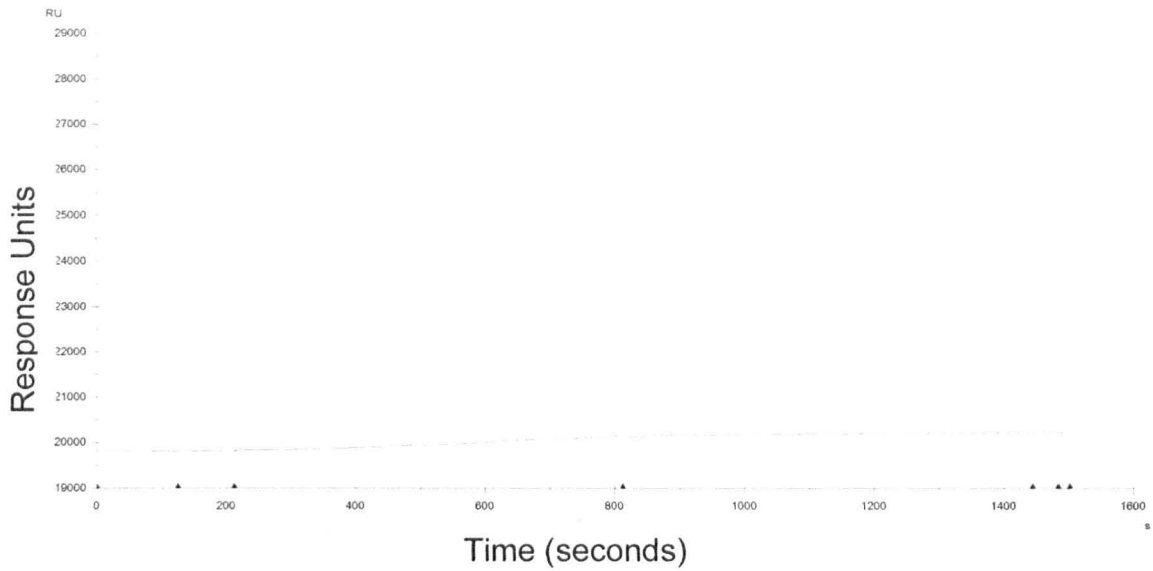


Figure 7 Binding of porcine IL-1 β to immobilised sIL-1RII

The green line shows the binding of porcine IL-1 β to flow cell 4 (with sIL-1RII attached) and the red line the binding to the control flow cell. The injection was commenced at 220 seconds and lasted for 5 mins. Note: A change of 0 RU in the active cell and 0 RU in the control cell, i.e. no binding of porcine IL-1 β to human sIL-1RII.

2.4 DISCUSSION

2.4.1 Summary of findings

These experiments were performed to determine whether the human sIL-1RII could be used to inhibit IL-1, in a porcine model of coronary artery experimental injury. The results presented here show that human sIL-1RII does not bind porcine IL-1 and therefore cannot be used as an inhibitor of IL-1 activity in this model.

2.4.2 Why does porcine IL-1 not bind to sIL-1RII?

Surface plasmon resonance was used to determine whether human sIL-1RII would bind porcine IL-1. Human sIL-1RII was captured on the surface of a sensor chip in a BIAcore instrument and the association kinetics of human IL-1 β , porcine IL-1 α and porcine IL-1 β ligands measured. The conditions were chosen to replicate those that had already been used to determine the binding kinetics of human IL-1 to human sIL-1RII and these were verified by the positive control, human IL-1 β , which bound to the immobilised sIL-1RII as expected [89]. It can be seen from the data presented (section 2.3.2) that under the conditions tested and the concentrations used, neither porcine IL-1 α nor porcine IL-1 β bound to the human sIL-1RII.

Several possible explanations for these results exist. Firstly, the homology between human IL-1 β and porcine IL-1 β is only 74% [93]. Ligand-receptor

interactions are highly specific and the differences in amino-acid sequence between the porcine and human ligands may prevent receptor-ligand complex formation. Secondly, direct binding may be limited by transport of the ligand to the chip surface. This seems unlikely as good binding was achieved between the human ligand and immobilised receptor implying the ligands were reaching the immobilised receptor and in contact with it long enough to bind. Thirdly, the carboxylated dextran matrix at neutral pH has a negative charge and may exert an effect on the binding affinity of the receptor. Fourthly, it is conceivable that binding of the ligands occurred but the off-rate of the ligand was so fast as to be undetectable by the BIAcore instrument. This seems highly unlikely due to the sensitivity of the machine and even if that were the case, it would still mean that the human IL-1RII could not be used as an efficient inhibitor in a porcine model.

2.5 Conclusions and future directions

Under the conditions tested in this thesis, human sIL-1RII does not bind porcine IL-1 α or porcine IL-1 β . In order to test the hypothesis that IL-1 is a crucial determinant in the coronary artery response to injury and intracoronary stenting, an inhibitor that can be tested in an animal model of experimental injury is required. There is another commercially available inhibitor of IL-1, IL-1ra, that has already been tested in an animal model and was found to be effective [94]. IL-1ra is commercially available (Anakinra; Amgen) and is already in clinical use for the treatment of rheumatoid arthritis [95].

Previous work had shown that human IL-1ra is inhibitory in the mouse [35] and preliminary work in our laboratory, using an *in vitro* radioligand binding assay had determined it was inhibitory to IL-1 signalling in the pig (data not shown).

In order to take this work forward, it was decided to concentrate on inhibition of porcine IL-1 using human IL-1ra to determine whether the coronary artery response to injury could be modified.

CHAPTER 3

DELIVERY AND PHARMACOKINETICS OF HUMAN IL-1RA IN PIGS

3.1 INTRODUCTION

3.1.1 IL-1ra as an inhibitor of IL-1

As discussed in 1.2.5, IL-1ra is a naturally occurring antagonist of IL-1. It has been used with good effect in the treatment of rheumatoid arthritis in humans [40] and is well tolerated at high doses with few side effects. It acts as a competitive inhibitor by binding preferentially to the type 1 IL-1 receptor thereby preventing the up-regulation of down-stream inflammatory cytokines such as IL-6 and IL-8. IL-1ra is an acute phase protein that is produced in a pattern that immediately follows IL-1 production. Mice that lack IL-1ra spontaneously develop arthritis [96]. This suggests that it is the balance between IL-1 and IL-1ra that is crucial in disease prevention. It follows that the ratio of IL-1 to IL-1ra is imbalanced either because of excess IL1 production or reduced IL-1ra production. The onset of inflammatory conditions leads to a rapid induction of sIL-1ra synthesis by the liver [97]. IL-1ra is needed in 100-fold excess over IL-1 in order to exert its effects [20]. Given the short half-life of IL-1ra, prolonged administration regimes are required.

3.1.2 Human IL-1ra and inhibition of porcine IL-1

The homology between human and porcine IL-1ra is 80%. Preliminary work in our laboratory using an *in vitro* bioassay determined that human IL-1ra was an effective inhibitor of porcine IL-1 and therefore had potential to be used in a porcine model of experimental injury. This was confirmed by *in vivo* data available from our collaborators at Amgen.

3.1.3 Dosing regimen for IL-1ra

Numerous studies have used different doses of IL-1ra to inhibit IL-1. Elhage *et al* used IL-1ra in a mouse model of fatty streak formation at a dose of 25mg/kg/24h [35]. In a study by Bendele *et al* on the efficacy of IL-1ra in a rat model of rheumatoid arthritis, the dose studied was 5mg/kg/24h [94]. In human studies, doses as high as 3400mg/24h have been used [42].

Interestingly, the doses used in individual studies span a wide range and each seems to be effective. It has been reported that IL-1ra needs to be circulating in 100-fold excess to IL-1 levels to exert its effects [20]. The work presented in this thesis used an initial dose of 2mg/kg/24h. This was based on a recommendation from Amgen who provided the drug.

3.1.4 Mode of delivery of IL-1ra

IL-1ra has a short half-life of 3 – 6 hours [98]. Whatever the dosage, in order for IL-1ra to have a sustained effect it must be given by a continuous infusion.

The operating paradigm is such that the IL-1ra is circulating at high levels at the time of injury. There are two possible methods of giving a continuous infusion, via an intravenous or subcutaneous route. The advantages of giving a continuous intravenous infusion are that the serum levels are often more predictable and high circulating levels can be rapidly achieved. Against this route, although continuous intravenous administration is technically feasible and possible, in large animals, it is fraught with difficulty. Any intravenous access will have to be central for a prolonged infusion. This means that an intravenous line will need to be placed into either the internal jugular or subclavian artery and then to administer the infusion, the line will have to be connected to an external syringe driver or similar device and placed on the animal. This necessitates the animal wearing a 'coat' with pockets to house the device, which is cumbersome, heavy and uncomfortable for the animal. Once the animals have fully recovered from their anaesthetic they are returned to their pen where they live with other pigs until death (in this case up to 28-days). Being naturally inquisitive animals, in the experience of our laboratory, they often chew anything out of the ordinary including intravenous lines and syringe drivers. Consequently, a central line could become displaced over night leaving the animal without its infusion for anything up to 24 hours at a weekend. As the half-life of IL-1ra is much shorter than this (3 – 6 hours), an animal could potentially be without drug for a critical amount of time thereby biasing the experiment and its results.

The advantages of subcutaneous administration are that mini-osmotic pumps are available that can deliver a fixed rate of drug for a fixed amount of time,

thereby allowing predictable infusion times (see 3.2.5). These pumps are placed in a subcutaneous pocket (in the case of a pig in the groin crease of the animal). Insertion therefore involves a single operation and the animal is left with a wound. If the pumps need replacing again, a simple quick operation is all that is needed. There is no need for an external driver to deliver the drug. Against subcutaneous administration, serum levels can be erratic and unpredictable and when osmotic pumps are used, there have been occasional reports of swelling around the pumps.

Given the above, it was decided to use subcutaneous mini-osmotic pumps to deliver a continuous infusion of drug, with an intravenous bolus at the time of injury if necessary to ensure initial high circulating levels.

3.1.5 Aims of this study

The aim of this section of the research was to determine the optimal delivery method and consequently, the pharmacokinetics of human IL-1ra delivery to a pig.

3.2 MATERIALS AND METHODS

3.2.1 Yorkshire White pigs

In vivo work was performed on normo-lipemic, domestic, crossbred Yorkshire White pigs. They were of either sex, obtained from a Home Office designated supplier and weighed approximately 20kg.

3.2.2 Animal husbandry

Animals were housed at the University of Sheffield in appropriately sized pens. They were fed unmodified pelleted chow and had free access to water. Animals were examined daily to ensure well-being. Diseased animals were not used for this study and any complications such as infection were dealt with using standard veterinary procedures.

3.2.3 Legal considerations

Animal experiments were performed under an appropriate UK Home Office Project Licence (Dr J Gunn, 50/01335) and Personal Licence (Dr A Morton, 40/6898). All experiments were performed in a Home Office designated establishment (Field Laboratory, University of Sheffield).

3.2.4 Cytokines

The human IL-1receptor antagonist (IL-1ra) used for the following work was a gift from Dr C. Toombs, Amgen, CA, USA. All other cytokines were purchased from R&D systems. The initial dose of IL-1ra used in this study (2mg/kg/24h) was that recommended by Dr C. Toombs. The dose used was based on both animal and clinical data Amgen had collected on the use of IL-1ra in rheumatoid arthritis.

3.2.5 Subcutaneous osmotic pumps

In order to give a continuous infusion of IL-1ra, subcutaneous osmotic minipumps were used. These are miniature, implantable pumps that continuously deliver the agent of choice at a controlled rate for a set time, without the need for external connectors or frequent animal handling. Alzet pumps work by osmotic displacement. The empty reservoir within the core of the pump is filled with IL-1ra solution, using a blunt ended filling tube. The chamber surrounding the reservoir (but isolated from it by an impermeable layer) contains a high concentration of salt solution. Due to this high concentration of salt, water enters the pumps through its outer surface, which is a semi-permeable layer. The entry of water increases the volume of salt in the chamber, causing compression of the flexible reservoir and delivery of the IL-1ra via the exit port. To ensure that mean rate of delivery; pump-to-pump consistency; and the accuracy of pumping over time is consistent, the supplier calibrates the pumps.

3.2.6 Filling and priming of the osmotic pumps

Osmotic pumps were purchased from Charles River UK Ltd. Kent, UK. Each 2ml2 pump held 2ml of solution and released for 14d at a flow rate of 5 μ l/hr. Three pumps were inserted into each animal in order to achieve the required dosage. The volume of solution loaded into the pumps was calculated according to a method supplied by Charles River Ltd. First, the empty pump together with its flow moderator was weighed. A blunt-tipped filling tube was then used to fill the pump with IL-1ra. A dose of 2mg/kg/24h was delivered to the animal (as advised by Amgen). Once full, the excess solution was wiped off and the flow moderator inserted until the cap was flush with the top of the pump. The pump was then re-weighed. The difference in weights gave the net weight of solution loaded. For aqueous solutions, the weight in milligrams (mg) is approximately the same as the volume in microlitres (μ l). The fill volume for all pumps was >90% of the reservoir volume specified on the specifications sticker attached to the information sheet sent with the pumps. This ensured that sufficient solution was loaded. Once full, the pumps were primed for use in a beaker of normal saline at 37°C overnight.

3.2.7 Implantation of subcutaneous mini osmotic pumps

Prior to pump implantation, pigs were sedated with an intramuscular injection of azaperone (12mg/kg, Janssen Animal Health). Anaesthesia was induced by intravenous propofol, (4mg/kg, Zeneca Pharmaceuticals) and maintained by inhaled isoflurane (4-6%) in oxygen (1L/min) via endotracheal tube.

Animals were positioned supine on the table with their legs secured, the groin crease was cleaned with iodine and sterile towels used to cover the cleaned area. An incision approximately 1.5 inches long was made in the groin crease. A pocket for the pumps was created subcutaneously by blunt dissection. The filled pumps were inserted into the pocket, delivery portal first (to minimise interaction between the compound delivered and the healing of the incision). The wound was closed with 2.0 Vicryl sutures and the animals allowed to recover.

3.2.8 Pharmacokinetics of IL-1ra

Initially the release profile of the IL-1ra from the osmotic pumps was determined. It was important to know the circulating levels of IL-1ra after pump implantation and how long levels were maintained for in order to ensure consistency for subsequent procedures.

3.2.9 Pharmacokinetics of subcutaneous IL-1ra release from Miniosmotic pumps

Subcutaneous mini osmotic pumps were inserted as 2.3.2. Blood (2ml) was collected into heparinised syringes at the following time points: pre-procedure; at implantation; 10min; 20min; 30min; 1h; 2h; 4h; 8h; 24h; 48h; 72h; 7d; 10d; 14d; 17d; 23d and 28d. The blood was immediately centrifuged at 2000rpm for 3min; serum was extracted, aliquoted (200 μ L per sample) and stored at –80°C until use.

3.2.10 Pharmacokinetics of intravenous bolus administration

This experiment was carried out as above (2.3.1) except that before the pumps were inserted, intravenous (iv) access was gained in either an ear vein or the femoral vein and at the time of pump implantation, an iv bolus of IL-1ra at a dose of 0.5mg/kg was given. Blood was sampled at the following time points: pre-procedure; at implantation; 15min; 30min; 45min; 1h; 1h15min; 1h30min; 1h45min; 2h; 3h; 4h; 5h; 6h; 7h; 8h; 9h; 10h; 24h and 48h.

3.2.11 Determination of serum levels of IL-1ra after administration

Serum samples were collected as 2.4.1, stored at -80°C and shipped on dry ice to Amgen Inc. for analysis.

3.3 RESULTS

3.3.1 Pharmacokinetics of inhibitor release from mini osmotic pumps - subcutaneous infusion

The pharmacokinetics of IL-1ra release from the mini osmotic pumps are shown in Figures 8a and 8b. Each time-point represents the mean value from serum samples taken from 3 separate pigs. There is a peak elution at 8 hours. After this a steady state of release is achieved with serum levels of 150 – 250ng/ml. This level is maintained for 18 days after which, the serum levels decrease. By 23 days, no more IL-1ra is eluted.

3.3.2 Intravenous bolus administration

To ensure that IL-1ra is circulating at the time of injury, an intravenous (iv) bolus of IL-1ra (0.5mg/kg) was given at the time of pump implantation. In Figure 9, each time-point represents the mean value from serum samples taken from 2 separate pigs. Peak levels occurs at time-point 0 i.e. immediately after injection. After this, a steady state of release is achieved with serum levels of 150 – 250 ng/ml.

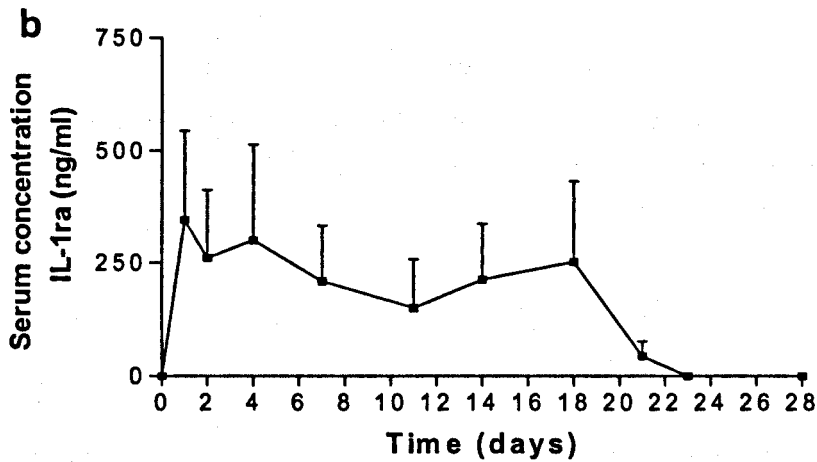
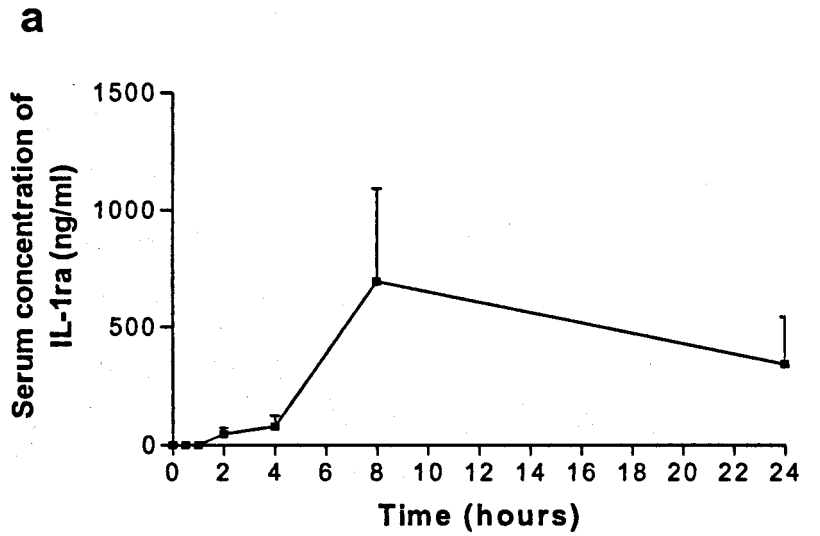


Figure 8 Serum concentration of IL-1ra following implantation of subcutaneous pumps that release IL-1ra at 2mg/kg/24h

(a) shows the first 24h of elution with a peak of 680ng/ml falling to steady state; (b) shows steady state levels up to 18 days with no elution after 23 days (n=3).

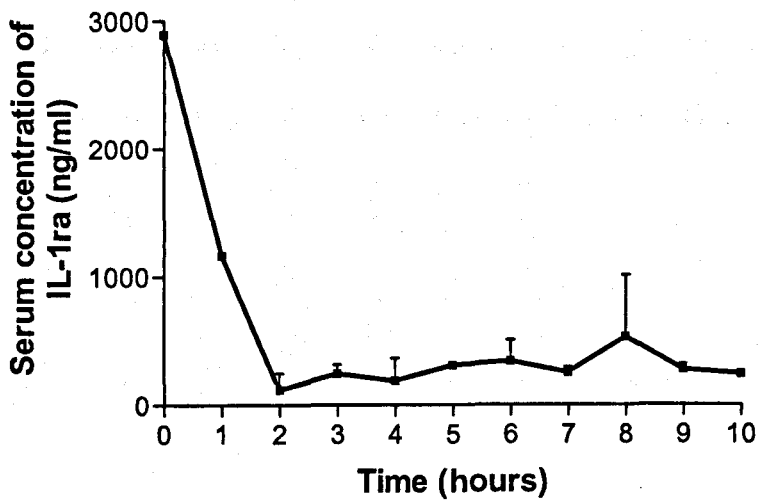


Figure 9 Serum concentration of IL-1ra after administration of an intravenous bolus (dose 0.5mg/kg) (n=2)

Note a rapid peak of elution of IL-1ra (2.9 μ g/ml) immediately post bolus.

Steady state levels are maintained over the subsequent 8h.

3.3.3 Pharmacokinetics of inhibitor release from iv bolus and mini osmotic pumps

The combined data from intravenous bolus and insertion of subcutaneous mini osmotic pumps are shown in figure 10. It can be seen, that peak elution of IL-1ra occurs immediately after the intravenous bolus has been given and, by 1 hour, the serum concentration has reached steady state with serum levels of 150 – 250 ng/ml. This level is maintained for 18 days after which time the level decreases to below 100ng/ml. By 23 days, there is no elution of IL-1ra from the miniosmotic pumps.

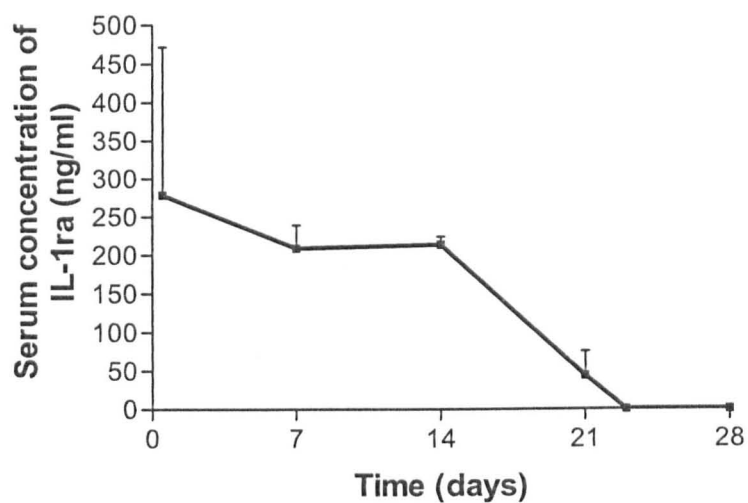


Figure 10 Serum concentration of IL-1ra after iv bolus and subcutaneous mini osmotic pump insertion

Note: an initial high peak (Fig 9) occurs followed by maintenance of steady state levels for 14-days. Levels fall below 100ng/ml at 18 days and to 0 by 23 days.

3.4 DISCUSSION

3.4.1 Summary of findings

The pharmacokinetic data for the administration of human Interleukin-1 receptor antagonist to the domestic pig show that both methods of administration (intravenous and subcutaneous mini pump) cause an initial peak of IL-1ra in the plasma, after which time levels rapidly decrease to a steady state level of 150 – 250ng/ml. This suggests that after administration, IL-1ra is compartmentalised within the body, leaving a steady level to circulate.

3.4.2 Delivery strategy

In chronic conditions, therapy needs to be sustained for an extended period and large doses may be necessary. In the case of IL-1ra, which has a short half-life, the route of administration of IL-1ra will be critical to its success as a commercially available drug. In the treatment of patients with rheumatoid arthritis, large amounts of recombinant protein are needed [40]. Various slow release formations are being investigated but a pump device still seems to be the most likely method of administration. Pumps have the advantage over subcutaneous injection that they provide a uniform release of drug. However, a question exists over protein lability under physiological conditions. The research reported here show that a steady state of drug elution can be

obtained using miniosmotic pumps. The efficacy of the delivered IL-1ra still needs to be established.

3.4.3 Steady state levels

According to the manufacturers instructions, the pumps elute for 14-days. It can be seen from the serum levels obtained that the pumps actually release drug for up to 18-days. After this time the levels of serum IL-1 fall to below 100ng/ml and by 23-days, levels are undetectable. The reasons for prolonged administration are unclear. As the half-life of IL-1ra is 3-6 hours, this continued release must be either from the pumps that are left *in situ* or from a slow release compartment. The level of detectable IL-1ra falls to below 100ng/ml after 21-days and it is likely that the effect of the inhibitor on IL-1 is negligible after this time (although this has not been formally tested).

3.4.4 The importance of an intravenous bolus

It is reported that high levels of IL-1ra circulating at the time of injury are required, since the initial events in the vessel wall response to injury occur early on and rapidly [3]. As already discussed (1.2.7), work from our group has shown that IL-1 β is up-regulated in the porcine vessel wall as early as 6 - hours following PTCA [31]. Given that a 100-fold excess of IL-1ra is required to inhibit IL-1, a subcutaneous infusion started at the same time as the experimental injury was performed may not provide sufficient amounts of IL-1ra for complete IL-1 inhibition. To ensure high circulating levels at the time

of injury, either the pumps would have to be implanted a day before the injury or an intravenous bolus delivered. To implant the pumps a day before vessel injury or stenting would necessitate the animal undergoing another procedure and therefore another anaesthetic. With this in mind, an intravenous bolus was chosen since it was easy to administer, involved no added anaesthetic or increase in procedure time.

3.4.5 How much IL-1ra is enough?

The amount of circulating IL-1ra needed to inhibit the inflammatory response induced by IL-1 is unknown. Previous work looking at the effect of IL-1ra on rheumatoid arthritis in a rat model found that administration of 5mg/kg/24hr of IL-1ra gave serum levels of 5.5µg/ml that was sufficient to cause complete (90%) suppression of established arthritis [94]. Interestingly, in this study, the response in an adjuvant-induced arthritis model was not as dramatic highlighting the variability in response seen by different models with identical serum levels. The role of antagonising IL-1 in fatty streak formation (the initial step in the atherosclerotic process) in apolipoprotein-E deficient mice (a standard animal model of atherosclerosis) has also been studied [35]. Here, specific antagonism of IL-1 with IL-1ra was effective in reducing fatty streak formation, suggesting a crucial role for IL-1 in the initial step of the atherosclerotic process. In this work, administration of 2mg/kg/24h of IL-1ra led to serum levels of 150 – 250 ng/ml for the duration of the infusion. Although the serum levels we obtained were lower than that seen in the study on rheumatoid arthritis, these levels were remarkably consistent and it would

seem that any excess IL-1ra circulating in the pig model is either compartmentalised or rapidly excreted by the kidneys, leaving a maximum of 250ng/ml available in the serum. It is uncertain whether this serum level is high enough to suppress IL-1 activity or if higher levels will be necessary after injury. These initial data however, confirm that human IL-1ra can be administered to pigs with no obvious side effects and that human IL-1ra can be detected in pig serum following administration i.e. there is no species cross-reactivity with the human IL-1ra.

3.5 Conclusions and Future Directions

Human IL-1ra administered to pigs as an intravenous bolus (0.5mg/kg) followed by a continuous subcutaneous infusion (2mg/kg/24h), gives an initial peak followed by a steady state serum concentration of 150 – 250ng/ml. This work has shown that human IL-1ra can be delivered successfully to a pig in the manner described above. Serum levels are consistent and reproducible between animals implying a working delivery system with predictable pharmacokinetics. The next step is to establish whether the serum levels obtained are high enough to inhibit porcine IL-1 and therefore inflammation. In order to do this, a skin bioassay as a surrogate for the porcine coronary artery will be used.

CHAPTER 4

DOSE-RESPONSE ANALYSIS – INHIBITION OF IL-1 INDUCED INFLAMMATION IN A PORCINE SKIN MODEL

4.1 INTRODUCTION

4.1.1 Skin as a surrogate for the coronary artery

In order to determine the efficacy of human IL-1ra as an inhibitor of porcine IL-1, it was necessary to use a bioassay that allowed a large number of samples to be taken from each animal. It was important to determine whether IL-1ra at the dose studied was inhibitory to IL-1 induced inflammation before moving onto the model of experimental injury to ensure that the serum level being delivered was adequate to abolish an inflammatory response. It follows therefore that if the dose of IL-1ra given were not anti-inflammatory then higher doses would be necessary to examine the efficacy of an anti-IL-1 approach to restenosis. A porcine coronary artery model does not allow either varying doses of IL-1 or different time-points to be tested in the same animal because each animal can receive only one infusion and in order to harvest the artery, the animal must be killed, thereby limiting the information obtained from each animal. Also, there is no established model of porcine coronary artery inflammation. As an alternative to the coronary artery, a model of inflammation in pigskin was used. Advantages of using pigskin include similarities between pig and human skin [99] and the ability to study

replicate skin-spots within the same animal for several treatments at several different time-points. A study by Binns *et al* [100] used a similar model to examine the importance of E-selectin antagonism on neutrophil infiltration. In this model, cytokines were injected intradermally into the ventral-abdominal and medial-thigh skin at 24h, 4h, 2h and 45 min before exsanguination. Neutrophil accumulation was maximal at 4h pre sacrifice. There was little accumulation in unstimulated skin [100]. This skin model would therefore be appropriate to establish whether IL-1ra at the dose studied could inhibit the inflammatory reaction induced by intradermal IL-1 injection, before moving on to study any IL-1ra effect on restenosis.

4.1.2 Bioassay for IL-1ra effects on inflammation in pig skin.

Changes in the vascular endothelium occur during an inflammatory response that allows access of neutrophils and lymphocytes to tissues. Neutrophil recruitment to intradermal (id) injections of porcine IL-1 α and IL-1 β was used as a bioassay of *in vivo* IL-1 antagonism by the selected dose of human IL-1ra [100]. Neutrophils constitute approximately half the circulating white cell population in most species, including pigs and are characterised by a multilobed nucleus and cytoplasmic granules. The primary function of the neutrophil is in host defence. Neutrophils therefore accumulate at sites of infection and inflammation. Accumulation is a controlled event such that the inflammatory responses usually resolve acutely with the efficient removal (within days) of the inciting stimulus. If control mechanisms fail and there is an over-exuberant response or non-resolving response to injury, then

neutrophil accumulation and activation can lead to tissue destruction. Of importance to any bioassay is the standard curve, which is used to accurately determine the response induced by a particular agent or change in conditions. In this case, the standard curve was created using neutrophils extracted from pig blood. A large number of peripheral neutrophils can be isolated from each animal, thereby providing a simple, reproducible standard for each assay.

4.1.3 Myeloperoxidase

Myeloperoxidase (MPO) is a cationic protease that is an abundant component of neutrophil azurophil granules. It constitutes 5% of the dry weight of the cell and is released when neutrophils are activated [101]. Myeloperoxidase (MPO) activity is a direct measure of neutrophil presence and a surrogate marker for their infiltration into tissue [102]. Many different assays are available that can detect MPO and these can be used to indicate neutrophil levels within tissue [102-104].

4.1.4 Aim of this study

The aim of this section of work was to determine whether the circulating serum dose of IL-1ra (150 – 250ng/ml) achieved by an intravenous bolus of 0.5mg/kg and a continuous subcutaneous infusion of 2mg/kg/24h was sufficient to inhibit neutrophilic inflammation induced by intradermal IL-1 injection.

4.2 MATERIALS AND METHODS

4.2.1 Intradermal injection of Interleukin-1 with and with out intravenous bolus and continuous subcutaneous infusion of IL-1ra – dose response analysis

The skin assay (discussed in 4.1.2) is a useful model for investigating the effects of interleukin-1 in a non-invasive manner. Multiple sites can be used and therefore multiple doses and time-points analysed in the same animal.

Stock solutions of IL-1 α and IL-1 β (both from R&D systems, Oxford, UK) at concentrations: 300U; 1000U; 3000U and 10,000U were prepared, using the vehicle as a diluent. Pumps were filled and primed with 2mg/kg/24h of IL-1ra as described in section 3.2.6. Pigs were anaesthetised as previously described section 3.2.7. If the pig was to receive IL-1ra, intravenous access was gained and a pocket created for pump implantation. The pumps were inserted and an intravenous bolus given immediately prior to the first intradermal (id) injection. A pre-prepared plan for id injection was made. A grid was drawn onto the abdomen of the animal (see Figure 11). Each grid had 60 individual points marked in a 12 X 5 formation and each point was labelled with a number and letter i.e. 5 rows horizontally labelled A - E and 12 rows vertically labelled 1 - 12. Each dose and time-point was documented on a paper copy of the grid and then at the appropriate time, the id injection given in the corresponding point on the abdomen of the animal. Each injection consisted of 0.1ml of porcine IL-1 α , porcine IL-1 β or saline (used as a

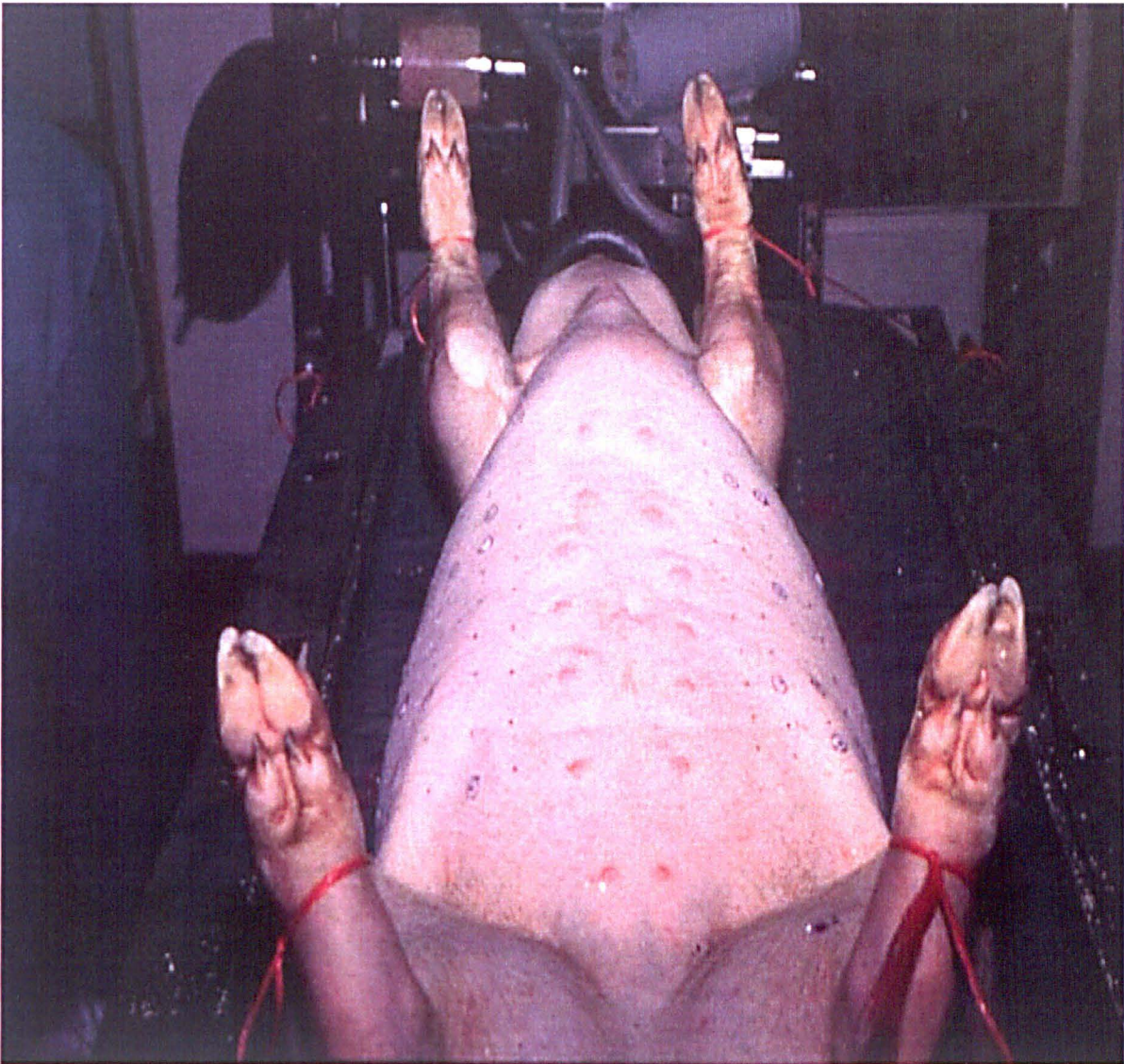


Figure 11 Grid markings for intradermal injection sites

Animals had a 12 X 5 grid drawn onto the ventral abdominal wall as shown. Intradermal injections were made over each separate 'dot' and then each injection site was circled to depict external limits for subsequent disk removal.

control). Intradermal injections were performed at the following time points: 24hr; 6hr; 4hr; 2hr; 1h and 0h pre-death [100]. 3 – 5 separate discs of skin were injected for each time-point. At time point 0, the pig was killed by lethal injection and the skin on the ventral surface of the pig harvested by superficially cutting through the skin around the grid and removing the skin using sharp and blunt dissection. Once removed, the skin was stretched out and nailed to a piece of wood. Each disk of skin was removed using a hammer and punch (Footprint Tools, Sheffield, UK) and the disks then either placed into formalin for 24h followed by PBS (for histology) or frozen and stored in liquid nitrogen for later use.

From previous experiments in our group after injury [31], IL-1 β is expressed in pig coronary arteries up to 14d but maximally at day 3. The half-life of IL-1ra in humans after subcutaneous infusion is 3 – 6 hours (data from Amgen). In order to determine whether the sc infusion alone would continue to inhibit neutrophil recruitment after the effect of the iv bolus had disappeared, in 1 pig, sc pumps were inserted and an iv bolus given 3 days prior to any id injections.

4.2.2 Measurement of myeloperoxidase in skin samples

The levels of MPO were measured in skin biopsies. The skin sections were made into homogenates by a process described in 4.2.4. The MPO concentration was determined by a previously described colorimetric-based method [103] using ultraviolet spectrophotometry and Labsystems Genesis v3.05 software.

4.2.3 Preparation of pig neutrophils by Percoll density gradient centrifugation

Pig neutrophils were isolated as a standard for the bioassay of inflammation in pigskin. 20ml of pig blood was added to 2.2ml of 3.8% (v/v) citrate in a 50ml falcon tube. This solution was then centrifuged at 300g for 20 min at 20°C to separate the plasma and platelets from the red and white blood cells. After centrifugation, the platelet rich plasma (PRP) was removed, leaving the red and white blood cells. To the falcon tube containing the PRP, 2 – 3 ml of 90% (v/v) Percoll was added beneath the PRP layer and this was centrifuged at 2000g for 20min (in order to remove the platelets from the plasma). Once the PRP had been centrifuged, the platelet poor plasma (PPP) was removed and kept for isolation of neutrophils on a Percoll gradient.

To the tube containing the red and white blood cells, 2.5ml of 6% (w/v) dextran was added and the volume made up to 20 ml with normal saline. This tube was mixed by gentle inversion and allowed to settle at room temperature for 30 min (a process known as dextran sedimentation).

The following solutions were prepared in order to create a percoll gradient:

42% percoll = 1050 μ l percoll + 1450 μ l PPP

51% percoll = 1275 μ l percoll + 1225 μ l PPP

After settling for 30min, the upper layer of leukocytes was removed from the tube that had undergone dextran sedimentation. This was then centrifuged at 300g for 8min. After this time, the supernatant was removed and re-

suspended with 2ml PPP. The percoll density gradient was then constructed in a falcon tube with 2mls of 51% percoll on the bottom and 2ml of 42% percoll on the top. The leukocyte suspension was then added to this gradient and centrifuged at 260g for 11 min 30sec. After centrifugation, the plasma and monocyte layer were removed and the neutrophil layer extracted. The remaining PPP was added to the neutrophils and the solution centrifuged at 170g for 8 min. The neutrophil pellet obtained was resuspended in 25ml of 0.2% NaCl and 25ml of 1.6% NaCl (v/v) was then added. This resulted in lysis of any remaining red blood cells. A haemocytometer was used to perform a cell count and a cytopspin at 100rpm for 5min was performed in preparation for a differential cell count. The slides were fixed and stained using Diff-quick (Dade Diagnostics, Aguada, PR) and a differential count performed manually under a light microscope using X400 objective. The remaining solution was centrifuged at 170g for 8 min and the neutrophil pellet obtained, re-suspended in 1ml PGB Ca/MG solution (PBS, 20mM glucose and 0.5%BSA and 100mM Ca/Mg) and stored in the fridge until required but no longer than 4 hours.

4.2.4 Preparation of porcine skin samples for myeloperoxidase assay

Tissue levels of MPO can be used as a surrogate marker for neutrophils.

Levels of MPO are reliably determined by assay, but tissue must first be homogenised in order to release any MPO present.

Tissue was homogenised using a small homogeniser (Footprint tools, Sheffield, UK) in 0.5% HTAB (hexa-decyl-trimethyl-ammonium bromide) using 10mM MOPS (3-(N-Morpholino) propanesulfonic acid) at pH7 as the diluent. Pigskin disks were removed from liquid nitrogen and thawed on ice. All excess fat was removed with a scalpel and the disk weighed and cut into small pieces. The pieces were placed into 5 ml tubes and 2 ml of homogenisation buffer added. The tissue and buffer was kept on ice and homogenised for 10 bursts of 10 sec using a small rotor (Footprint Tools, Sheffield, UK). The homogenate was transferred to 2 ml eppendorf microfuge tubes and centrifuged at 4000 g for 20 min at 4 °C. The supernatant was then stored at -20°C for later use.

4.2.5 Preparation of standards for myeloperoxidase assay

Porcine neutrophils, once extracted (see section 4.2.3), were used as a standard for each assay plate, using a maximum concentration of 0.35 – 0.45 x 10⁶/ml.

4.2.6 Assay to detect the levels of myeloperoxidase in the skin samples

The system used for this assay was an enzymatic reaction based on the peroxidase-catalyzed oxidation of 3,3', 5,5'-tetramethylbenzidine (TMB) that resulting in the formation of a blue colour which could then be read optically on a plate reader at 620nm.

The assay was performed in a 96-well plate and each plate read at 620nm at room temperature, using Labsystems Genesis V3.05 software. To each of the required wells on a 96-well plate, 20 μ l of sample or standard and 180 μ l of diluted substrate solution were added in order. Colour development was allowed to proceed for 5 minutes and the plate was then read. The unknowns were compared with a known concentration of neutrophils using a standard curve generated by the Labsystems software. The optical density of samples without colour substrate was subtracted from equivalent samples with colour substrate.

4.2.7 Immunostaining of wax embedded skin sections

The skin sections were fixed in formalin for 24 hours and then transferred into phosphate buffered saline (PBS). They were then processed, embedded into paraffin wax and cut (approximately 5 μ m thick) on a microtome by the Department of Histopathology, Northern General Hospital. They were then stained with haematoxylin and eosin (H&E) by the Department of Histopathology, Northern General Hospital. The morphology of the tissue was examined after staining under light microscopy. Semi-quantification of absolute numbers of neutrophils by manual counting was made.

4.2.8 Myeloperoxidase staining of wax embedded sections of pig skin

Myeloperoxidase staining was used to detect neutrophils. Sections were prepared as detailed in 4.2.7. In addition, in preparation for immunostaining,

slides to be stained were rehydrated (submerged in xylene for 10 min, then sequentially into 100% alcohol, 100% alcohol, 90% (v/v) alcohol and 70% (v/v) alcohol for 1 min). Slides were then incubated in 3% v/v hydrogen peroxide for 10 min in order to inhibit endogenous peroxidases and then washed in water. To block inappropriate activity of the secondary antibody, the slides were then incubated for 30 min at room temperature in a humidified chamber with 100 μ L per slide of 1 in 10 normal goat serum (NGS) + 1% (w/v) Marvel (the serum used corresponded to the species in which the secondary antibody was raised). The NGS was removed and 100 μ L of a primary myeloperoxidase monoclonal antibody (1:350) (Vector Limited, UK) was put onto each slide and incubated for 1h in the humidified chamber. Following incubation with the primary antibody, the slides were washed (3 x 5 min) and then further incubated in the humidified chamber at room temperature with 100 μ L of biotinylated goat anti-rabbit antibody (1:200, Vector Limited, UK) for 30 min. The ABC reagents (Elite ABC-HRP kit, Vector) were mixed and incubated at room temperature for 30 min to form an avidin DH biotinylated horseradish peroxidase H complex. The avidin binds to the biotinylated secondary antibody whilst the peroxidase reacts with the chromagen DAB (diaminobenzidine tetrahydrochloride) to produce a brown precipitate. The slides were washed in PBS (3 x 5 min) and then placed back into the humidified chamber for 30 min and incubated with 100 μ L of tertiary antibody (ABC-HRP kit as described above). After incubation, the slides were washed (3 x 5 min) and then incubated with 100 μ L DAB substrate for 5min. The slides were rinsed in running tap water for 1 min. Slides were counter stained with Carazzis Haemotoxylin for 1 min, rinsed in tap water and then

dehydrated through an ethanol series. The slides were then mounted in DPX mounting medium. Slides were viewed using light microscopy.

4.2.9 Assessment of neutrophil recruitment to the skin

Neutrophils are attracted to sites of inflammation by for example cytokine release. They therefore provide a good indicator of the extent and level of inflammation and were used as a surrogate marker of the inflammatory response in the experiments described in this chapter.

4.2.10 Neutrophil extraction

Neutrophils were extracted from pigs on the same day as the experiments for use as a standard in the MPO assay (sections 4.2.3 and 4.2.6). It was necessary to extract neutrophils each time the assay was performed as when frozen for use at a different time, the signal due to MPO activity deteriorated. The viability of the cells (as determined by trypan blue staining) also decreased after freezing (to <85% in all cases). In order to be certain that the concentration of neutrophils used for the standard was accurate, they were freshly prepared for each experiment. The viability (as determined by trypan blue staining) in all instances was >96% and each extraction consisted of >94% neutrophils as determined by Diff-quick (Dade diagnostics, Aguada, PR) staining.

4.3 RESULTS

4.3.1 Neutrophil accumulation in response to intradermal injection of porcine IL-1 β

Initial experiments were performed with no IL-1ra in order to determine the baseline response to the intradermal injections. Figures 12 and 13 show that at all doses, intradermal injection of IL-1 β resulted in greater neutrophil accumulation than IL-1 α . The maximal response for IL-1 β occurred in response to 1000Units IL-1 β and upward. Neutrophil recruitment was maximal when injections were performed at 4-6hours pre-death. These findings support the findings by Binns *et al.* who also found the maximum inflammatory response to be at 4h. For subsequent experiments, IL-1 β was used at a dose of 1000Units and injections were performed from 6 hours onwards (pre-death).

4.3.2 Neutrophil accumulation in porcine skin after intradermal injection of porcine IL-1 β , with and with out implantation of subcutaneous mini pumps and iv bolus of IL-1ra

Figures 14 and 15 show the myeloperoxidase tissue levels after intradermal injection of IL-1 β at 1000Units or normal saline with and with-out iv bolus and sc infusion of IL-1ra. As shown, after intradermal injection of IL-1 β 4 – 6 hours pre-death, neutrophil accumulation is greatest. In view of this, tissue levels of MPO were determined from intradermal injections given from 6hours



Figure 12 Neutrophil accumulation in response to increasing doses of porcine IL-1 β

Note: The maximum inflammatory response occurred following injection of 1000 Units of IL-1 β , 4 hours before sacrifice of the animal. Data are pooled from 3 different experiments, using 3 different animals and the injection sites are from different parts of the abdominal wall of the animal. Control tissue received saline only.

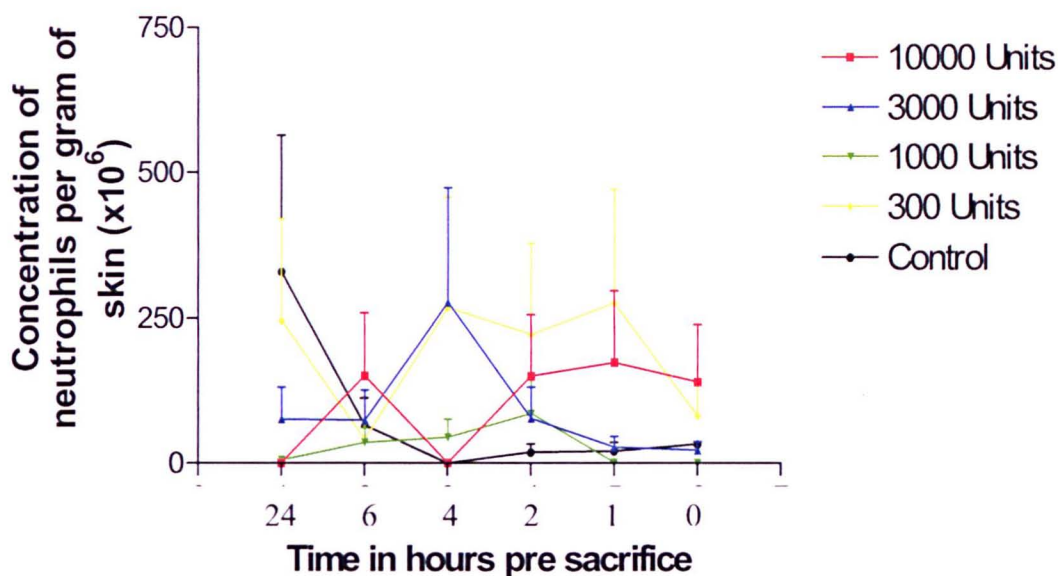


Figure 13 Neutrophil accumulation in response to increasing doses of intradermal injections of porcine IL-1 α

Note: The maximum response occurs after injection of 300 Units of IL-1 α 1 hour before sacrifice of the animal. At all time-points, IL-1 α induces less of an inflammatory response than IL-1 β . Data are pooled from 3 different experiments, using 3 different animals and the injection sites are from different parts of the abdominal wall of the animal. Control tissue received saline only.

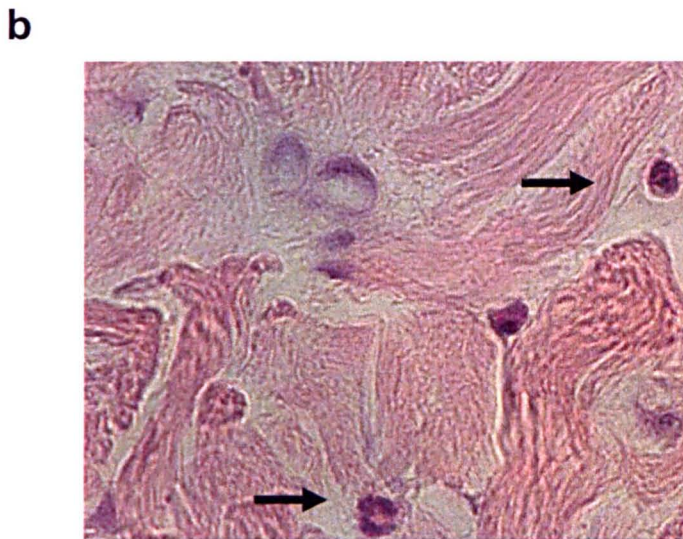
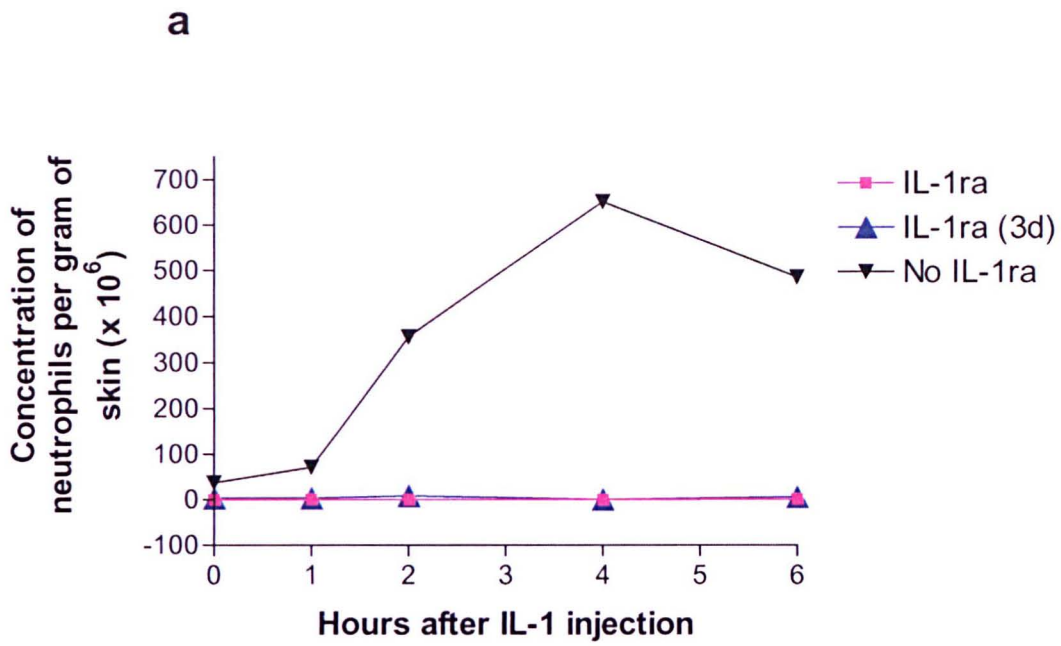


Figure 14 Neutrophil accumulation in response to intradermal IL-1 β (1000 Units)

(a) The black inverted triangles (- \blacktriangledown -) (n=1) represent values for pigs that received no IL-1ra. Pink squares (- \blacksquare -) (n=2) and triangles (- \blacktriangle -) (n=1)

demonstrate neutrophil accumulation in animals that received both an iv bolus and subcutaneous infusion of IL-1ra at day 0 and day 3 respectively.

Administration of IL-1ra leads to near complete abolition of the inflammatory response induced by id IL-1 injection. (b) H&E staining, magnification X1000 before reproduction, showing neutrophil infiltration after id injection of IL-1beta 1000Units, 6h before death. The arrows indicate the neutrophils.

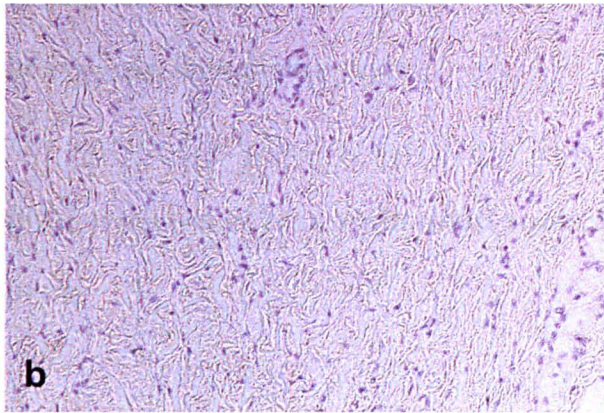
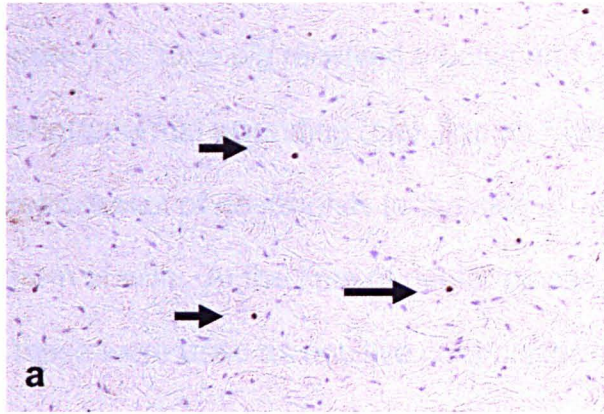


Figure 15 MPO Immunostaining of skin sections taken from pigs without IL-1ra and with IL-1ra after id injection of IL-1 β 6h before harvest

The arrows demonstrate positive MPO staining. (a) Positively stained neutrophils can be seen. (b) there are no positively stained cells.

Magnification x200 before reproduction

to death. Two pigs received an iv bolus of IL-1ra and had mini-osmotic pumps inserted immediately prior to the first intradermal injection of IL-1 β (blue line on Figure 13). One pig received a bolus and had pumps inserted 3 days prior to the intradermal wounding (pink line on Figure 14). In both instances, the recruitment of neutrophils to the skin is dramatically reduced to $<10 \times 10^6$ per gram of skin. At the time of death, pieces of spleen were harvested and these were used as positive controls for each assay. Each piece of spleen had 250 – 300 $\times 10^7$ neutrophils per gram of tissue. After death, some skin that had not been injected was removed and assayed. These discs had $<20 \times 10^6$ neutrophils per gram of tissue, as did skin that had been injected with normal saline after death.

4.3.3 Histological analysis of wax embedded sections - Haemotoxylin and eosin staining

Haemotoxylin and eosin (H&E) staining allowed neutrophils to be identified under light microscopy at x1000 magnification (Figure 14b). Although the intention had been to quantify the number of neutrophils present, this was not possible for the following reasons: (1) each section was only 5 μ thick and therefore a large number of sections would have to be analysed to get any meaningful results; (2) as the skin was only being used as a guide for dosing, it was felt to be more appropriate to determine the effects of IL-1ra in the coronary artery; (3) neutrophils could only be accurately identified at x1000 magnification making counting very time-consuming; (4) depending on the angle the section was cut at it was felt likely that some neutrophils would be

sectioned obliquely and therefore missed on counting as they would not be easily identifiable.

4.3.4 Histological analysis of wax embedded sections -

Myeloperoxidase Immunostaining

Clear myeloperoxidase staining worked is shown in Figure 15, which illustrates disc sections taken from animals with and without IL-1ra infusions. It can clearly be seen that in those animals that received IL-1ra, the number of positive cells is dramatically reduced compared with sections from animals that did not receive IL-1ra for the same time-point. This was not quantified because following assessment of multiple sections it became clear that this was an all or nothing response.

4.3 DISCUSSION

4.3.1 Summary of findings

Those data presented in this chapter provide evidence that after intradermal injection of IL-1 β and IL-1 α , there is neutrophil recruitment to pig skin, as demonstrated by the presence of myeloperoxidase (MPO). Numerous studies have used myeloperoxidase (a major constituent of neutrophil cytoplasmic granules) as a surrogate for neutrophil recruitment [102, 105]. Mullane *et al* used myeloperoxidase activity as a quantitative assessment of neutrophil infiltration into ischaemic myocardium; other groups have used this assay on skin samples [105]. In these studies, IL-1 β appears to induce a greater inflammatory response than IL-1 α . This is interesting as in most other cases their biological activity is indistinguishable [14].

Neutrophil recruitment is maximal when IL-1 is injected 4 – 6 hr pre-death. This is in keeping with results from Binns *et al* who used radiolabelled neutrophils to study inflammation after intradermal injection of IL-1 α into pigskin [100]. In these studies, the inflammatory response was maximal at 4h, tailing off at 24 h (there was no intermediate time point), which is consistent with those data presented in this thesis.

4.3.2 Myeloperoxidase as a surrogate marker for neutrophils

The experiments performed have provided a quantified measure of neutrophil recruitment (MPO assay) and these data have been supported with histological studies. The bioassay employed MPO as a surrogate marker and although this is well-established practice, actual neutrophil numbers were not quantified. Neutrophil recruitment to the inflammatory stimulus (in this case id IL-1 injection) could have been determined using radiolabelling techniques, but there would be uncertainty as to whether the radiolabelled cells were in the inflammatory lesion itself or the surrounding tissues. By employing a bioassay that allows the whole inflammatory lesion to be explanted and examined, this uncertainty is eliminated. Colorimetric assays are reproducible and comparisons between studies done on different days were easy with use of the standard curve. The dramatic response seen with IL-1ra use indicates with certainty that there is complete inhibition of IL-1.

4.4 Conclusions and future directions

These data convincingly show that in animals that receive IL-1ra, neutrophil recruitment to sites of IL-1 β intradermal injection is inhibited. Inhibition is maintained at 3 days when the effect of the intravenous bolus has worn off. Immunostaining of sections of pigskin for MPO provides added support for the data obtained by the assay. It is reported that IL-1ra is required in 100 fold excess to IL-1 β to block its effects [14]. The response to IL-1ra in this study is dramatic with all neutrophil recruitment being effectively inhibited in pigskin.

The dose of IL-1ra was 2mg/kg/24 hours, with a steady state of 150 – 250ng/ml and the dose of IL-1 β injected was 1000 Units (5ng), equivalent to a 1000 fold excess of IL-1ra. It may be that a dose of 2mg/kg/24 hr after an initial intravenous bolus of 0.5mg/kg is too high and the same effects could be seen with a lower dose of IL-1ra. There are no data in the literature to provide any guidance as to what dose of IL-1ra is enough. In terms of doses used in other trials, the dose we have used is consistent if not lower than doses currently undergoing clinical trial in humans [39, 40]. It is also important to note that the aim was to inhibit IL-1 activity in the coronary artery. IL-1 β is detected in porcine coronary arteries up to 14 days after injury [31]. The data presented here provide evidence that after delivery of IL-1ra as described, circulating levels will be maintained at 150 – 250 ng/ml for 18 days ensuring adequate availability after injury.

This initial work has demonstrated that IL-1ra (at the dose studied) is a potent inhibitor of neutrophil recruitment to pigskin after local intradermal injection of IL-1 β . It has further confirmed that human IL-1ra can be used to inhibit porcine IL-1 and indicates testing this strategy in a porcine model of balloon injury and coronary stenting.

CHAPTER 5

MODULATION OF THE PORCINE CORONARY ARTERY RESPONSE TO OVERSIZED BALLOON ANGIOPLASTY AND STENTING

5.1 INTRODUCTION

5.1.1 Animal models of experimental injury and restenosis

The ideal animal model for evaluation of restenosis is unclear. Generally, animal models serve to provide a mechanistic insight into biological processes rather than a means of predicting the human response to a treatment or intervention. Proof of concept studies can be performed and important information on issues such as toxicity of an agent can be examined. The coronary arteries of swine provide a good model for the study of restenosis (see section 5.1.2). The other animal model frequently used is the rabbit iliac artery [106, 107] but disadvantages of the rabbit model are that all studies are performed in peripheral arteries and therefore the effects on the heart such as arrhythmias are not identified.

5.1.2 Porcine coronary experimental injury model

The pig has become the model of choice for studying the effects of vascular injury on the neointimal response in coronary arteries gaining wide acceptance over the past decade. The domestic pig (*Sus scrofa*) is a readily available species whose cardiovascular anatomy and physiology is similar to that of man [108]. In a 20 - 30kg pig, the heart - to - body size ratio is very similar to that of man [109]. The local proliferative response induced by interventional techniques (e.g. PTCA) is very similar in appearance in both pig and human coronary vessels [110]. In the pig, neointimal thickness resulting from vascular injury is directly proportional to the depth of the arterial injury, similar to the relationship thought to exist in humans [111]. Vascular damage induced by oversized intraluminal balloon injury in the porcine coronary artery can therefore be used as a model of arterial disease.

5.1.3 Porcine coronary stent model

This model provides a method for examining the impact of therapeutic agents on in-stent restenosis. It consists of normal swine coronary arteries injured by the placement of an oversized stent. Different ratios of over-sizing are used to provide differing levels of injury. A ratio of 1.1:1 will provide a mild injury, 1.25:1 a moderate injury and 1.4:1 extensive injury. After 28 days, the animals are sacrificed and the hearts' perfusion fixed. The stented segments are removed, embedded and sectioned for histomorphometric analysis. The close histological resemblance between the lesions produced and human

restenosis, make it an excellent and widely used model [110]. Critics of the model point out that stents are placed into juvenile animals with normal hearts.

5.1.4 Aims of this study

The aim of this section of work was to determine the effect of IL-1ra on the porcine coronary artery response to oversized balloon angioplasty and stent placement.

5.3 MATERIALS AND METHODS

5.2.1 Experimental Injury

The effect of IL-1ra on experimental injury i.e. coronary balloon angioplasty (PTCA) was assessed in the first instance. 12 pigs, providing 24 arteries underwent insertion of subcutaneous mini pump, iv bolus and then PTCA. A time-point of 28 days was studied. This was followed by experiments to determine the effects of IL-1ra on restenosis following stent implantation. The BiodivYsio™ Phosphorylcholine (PC) coated intravascular stent was used in this study. All stents were either 3.0 mm or 3.5 mm in diameter and their lengths varied from 11 – 15 mm. The BiodivYsio™ stent is a flexible, balloon expandable, PC-coated stent composed of laser-cut 316L implant grade stainless steel metal tubing. The stent is mounted on a rapid exchange PTCA balloon delivery system, the PenChant™ delivery system. The PC coating has been shown previously to have no effect on neointimal formation in this model [112]

5.2.2 Porcine coronary balloon angioplasty

Each pig was sedated with an intramuscular injection of azaperone (12mg/kg, Janssen Animal Health). Anaesthesia was induced by intravenous propofol, (4mg/kg, Zeneca Pharmaceuticals) and maintained by inhaled enflurane (4-6%) in oxygen (1L/min) via endotracheal tube. Continuous electrocardiographic monitoring (Siemens) was performed through out the

experiment. In all animals, subcutaneous mini pumps were inserted into the groin immediately after anaesthesia at the start of the procedure. An incision was made along the groin crease between the ventral abdominal wall and the hind-leg, a pocket slightly larger than the size of 3 pumps created by blunt dissection, all 3 pumps inserted and then the skin was closed with a continuous running suture. The iv bolus of IL-1ra was given after the heparin bolus, before manipulation of the catheter.

A ventral midline neck incision was made to the right of the midline. The right carotid artery was exposed and an angiographic guide catheter manoeuvred under fluoroscopic guidance into the left or right coronary ostium (the surgical appearance is shown in Figure 16). Standard angiographic contrast medium (Hexabrix 320, Mallinkrodt) was used. A 6F right 1 Amplatz catheter was used to enter the left anterior descending artery (LAD) and a 7F right 2 Amplatz catheter was used to enter the right coronary artery (RCA). All animals received 2500 U sodium heparin after insertion of the carotid sheath. No assessment of coagulation was performed. The balloon catheter was positioned over a guidewire in the coronary artery. Quantified digitised angiography (the IDIS system) was used to determine the site of balloon inflation such that the balloon/artery ratio was 1.25:1 (a 3.5 mm balloon in a 2.8 mm section of the artery). The balloon was inflated 3 times at 8 atmospheres for 10 seconds. An angiogram was performed at the end of each procedure to document arterial patency. After PTCA, the catheters were removed and the carotid artery ligated with a 2.0 Vicryl suture. The animal

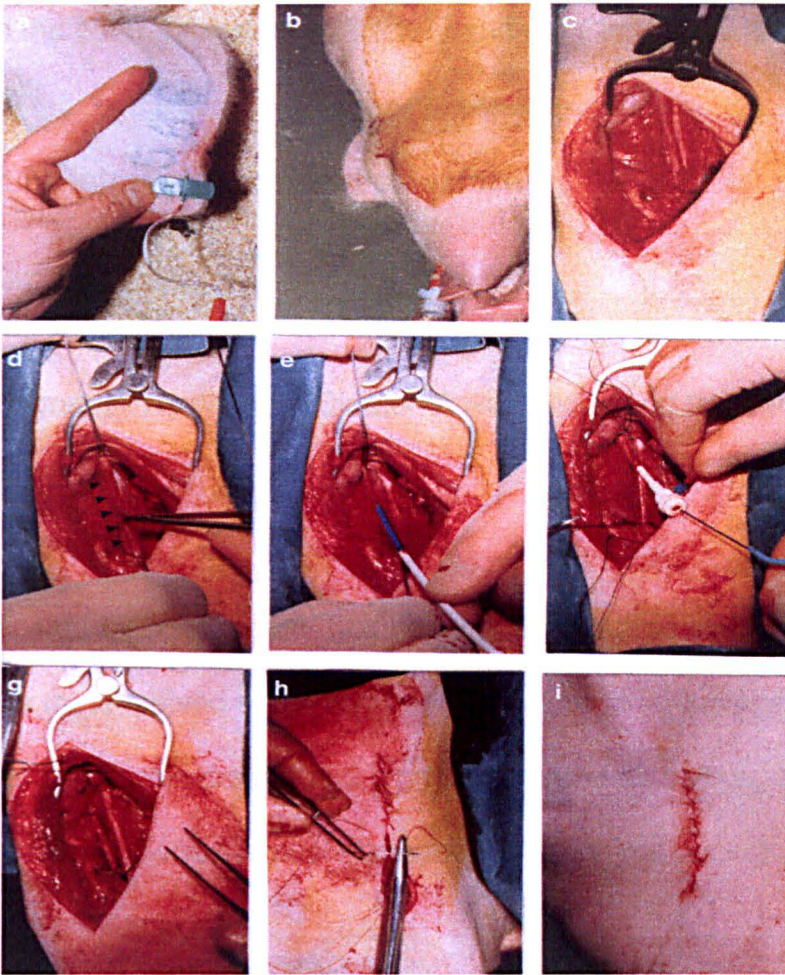


Figure 16 Porcine percutaneous coronary intervention – the technique

The carotid artery is exposed and a sheath inserted (a – e). Coronary artery guide catheters are inserted through the carotid sheath and manipulated into the ostia of the coronary arteries to perform angiography and PCI (f). At the end of the procedure, the carotid is ligated and the wound closed, allowing full recovery of the animal (g – i).

was allowed to recover. No neurological deficit occurred because of collateral supply from the contralateral carotid artery and the Circle of Willis.

5.2.3 Porcine intracoronary stent placement

Each pig was sedated and anaesthetised as in section 5.2.2. Continuous electrocardiographic monitoring (Siemens) was performed through out the experiment.

Animals received an iv bolus and had sc pumps implanted as in section 5.2.2. In all animals that received a 28d infusion, at 14d, another incision was made in the contralateral groin crease and a pocket created as before. 3 new pumps were inserted and the pocket closed. The original pocket was left alone with the pumps in situ.

Angiography was performed as in section 5.2.2 but instead of oversized balloon angioplasty, intracoronary stents were inserted. Pre-mounted BiodivYsio Penchant PC coated stents (Abbott Vascular Ltd) were deployed into both the LAD and the RCA. Quantified digitised angiography (the IDIS system) was used to determine the site of stent deployment such that the stent/artery ratio was 1.25:1 (a 3.5 mm stent in a 2.8 mm section of the artery and a 3.0 mm stent in a 2.4 mm section of artery). Balloon inflation was at 8atmospheres for 30 seconds. After stent deployment, the catheters were removed and the carotid artery ligated. Each animal received 150mg of oral aspirin for 5 days, starting the day before the procedure. An angiogram was

performed at the end of each procedure to document arterial patency. The animal was allowed to recover. No neurological deficit occurred because of collateral supply from the contralateral carotid artery and the Circle of Willis.

5.2.4 Artery extraction and tissue processing

At selected time intervals post-procedure, pigs were re-sedated with azaperone (12mg/kg, Janssen Animal Health) and a lethal intravenous overdose of pentobarbitone sodium (Animalcore Ltd, Dinnington, York, UK) administered. A median sternotomy was performed and the whole heart explanted and washed in 0.09% saline. For the angioplastied vessels, the whole heart was perfusion fixed in 10% (v/v) formalin at 100mmHg for 15 – 30 minutes. Pressure was maintained using a pressure bag. Following fixation, the angioplastied vessel was removed in its entirety, serially cross-sectioned from proximal to distal into blocks of tissue 2-3 mm long and immersion fixed in formalin for 24h before transferral into PBS. Once in PBS, segments were kept at 4°C pending embedding in paraffin wax for histology. For the stented vessels, no formalin fixation was performed; the 3.5 mm stents were identified and excised *in situ*. Each vessel was flushed through with 0.09% saline, and immersion fixed in formalin for 24h and then transferred into PBS and kept at 4°C pending embedding in methyl-methacrylate resin.

5.2.5 Histology

The angioplastied artery blocks for light microscopy were embedded in paraffin wax and a microtome used to cut 4 μ m thick cross-sections. These were stained with haematoxylin and eosin or Miller's elastin and van Gieson's stain (to reveal elastin and fibrous tissue) and viewed under conventional light microscopy. The sections of normal artery that had not undergone balloon angioplasty were identified and excluded from analysis. Angioplastied artery was identified by breaches in the elastic laminae of the vessel wall, indicating injury. The stented vessels were all embedded in methyl-methacrylate resin. Briefly, the whole explanted section of artery was dehydrated in acetone for 24h and then embedded into a methyl methacrylate resin (Technovik 8100, Taab laboratories, Berkshire, UK). Each artery was serially sectioned using a Buehler Isomet diamond edged saw. The section obtained was further ground and polished using a Metaserv 2000 grinder/polisher (Buehler) resulting in a section of artery, 20 – 30 μ m thick. This method leaves the stent *in situ* and the tissue undamaged, enabling accurate assessment of tissue morphology [113].

5.2.6 Histomorphometric analysis

Sections of artery were examined using a quantitative method of histomorphometric analysis. The system comprised a Nikon Eclipse E600 microscope and a Basler camera attachment with output to a computerised image analysis system (Lucia Image Analysis Software, Nikon, UK). After

suitable calibration, a hand-held mouse was used to trace round the arterial wall layers (see Figure 17 for the angioplastied sections and Figure 23 for the stented sections). The Lucia software calculated distances and areas. The cross-sectional areas (CSAs) of the lumen, neointimal, media, adventitia, stent and whole vessel were recorded and an injury score for each section determined (see 5.2.7). All injured sections that had undergone PTCA were analysed. For the PTCA group, sections that were incomplete, had branch distortion or tissue loss were rejected. For the stented vessels, using the technique described above, multiple sections were obtained from each artery. Alternate sections were analysed and sections were rejected on the grounds of an incomplete ring of struts or branch distortion. On average 4 – 6 sections were analysed per PTCA vessel and 6 – 10 per stented vessel.

5.2.7 Arterial injury score and corrections

The lengths of breaches in the external elastic lamina (EEL) and the internal elastic lamina (IEL) were recorded for the angioplastied sections. The lengths of breaches were converted to % total EEL or IEL circumference. This was used as a basic injury score for the angioplastied vessels. The ratio of intima/media area was calculated, allowing for larger vessels having greater dimensions. This ratio was further divided by the % IEL breach in an attempt to correct the amount of neointimal formation for the degree of trauma.

For the stented sections, each strut was assigned an injury score according to previously defined criteria. Two previously established scores were used, the Schwartz injury score [114] and the Modified Schwartz injury score [115].

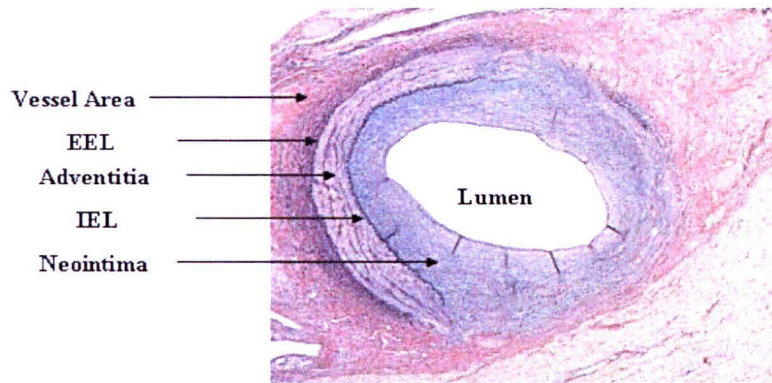


Figure 17 Measurements taken for histomorphometric analysis of PTCA sections

Each arterial layer is traced using a hand-held mouse and the cross-sectional area determined by the Lucia software

Briefly, the Schwartz score assesses whether the IEL, EEL and media have been ruptured or not. It assigns each strut a score from 0 – 3 according to the following criteria. 0, no rupture; 1, ruptured IEL; 2, ruptured media; and 3, complete EEL rupture. The modified Schwartz (Gunn) injury score utilises a score from 0 – 4 and differs from the Schwartz score in that it takes into account strut impaction and stretch. 0, no impression of metal upon media; 1, deformation of the IEL $<45^\circ$; 2, deformation of the IEL $>45^\circ$; 3, rupture of the IEL; 4, rupture of the EEL (that is, complete medial rupture). The score for each section was the mean of the individual strut scores. To account for vessel size, each parameter was divided by the total vessel area and then a further correction for injury was made by dividing the size corrected parameter by the mean injury score for each section.

5.4 RESULTS – PTCA section analysis

5.3.1 Histomorphometric analysis of PTCA sections

For all of the following results, there were 6 pigs in each treatment group yielding 12 vessels per group. Histological examination of all of these sections revealed a varying amount of injury (as determined by the degree of IEL breach) that ranged from no injury to extensive disruption. Of the vessels studied, 50 sections had injury and were suitable for analysis in the IL-1ra treated group and 51 sections in the vehicle treated group. All data are presented as mean \pm SEM and significance determined using an unpaired Students' t-test.

5.3.2 PTCA section analysis

The measurements taken for each PTCA section are shown in figure 17. All analyses were operator blinded and two independent observers measured all sections. There was no significant difference between the values obtained ($p > 0.85$ for all measurements with $< 10\%$ magnitude of difference between the two observers).

5.3.3 Total vessel cross-sectional area for PTCA sections

The cross-sectional area of the total vessel was calculated. As figure 18a shows, there is no significant difference between the vehicle and IL-1ra treated groups with respect to vessel size.

5.3.4 Injury score

The injury score for the PTCA sections was determined by the % breach of the internal elastic lamina (IEL). The lengths of breaches were converted to % total IEL circumference. This value was used as an injury score for the angioplastied vessels. Figure 18b shows the difference in %IEL breach between the IL-1ra and Vehicle treated groups. Although there is a trend for more injury in the vehicle treated animals, this does not reach significance.

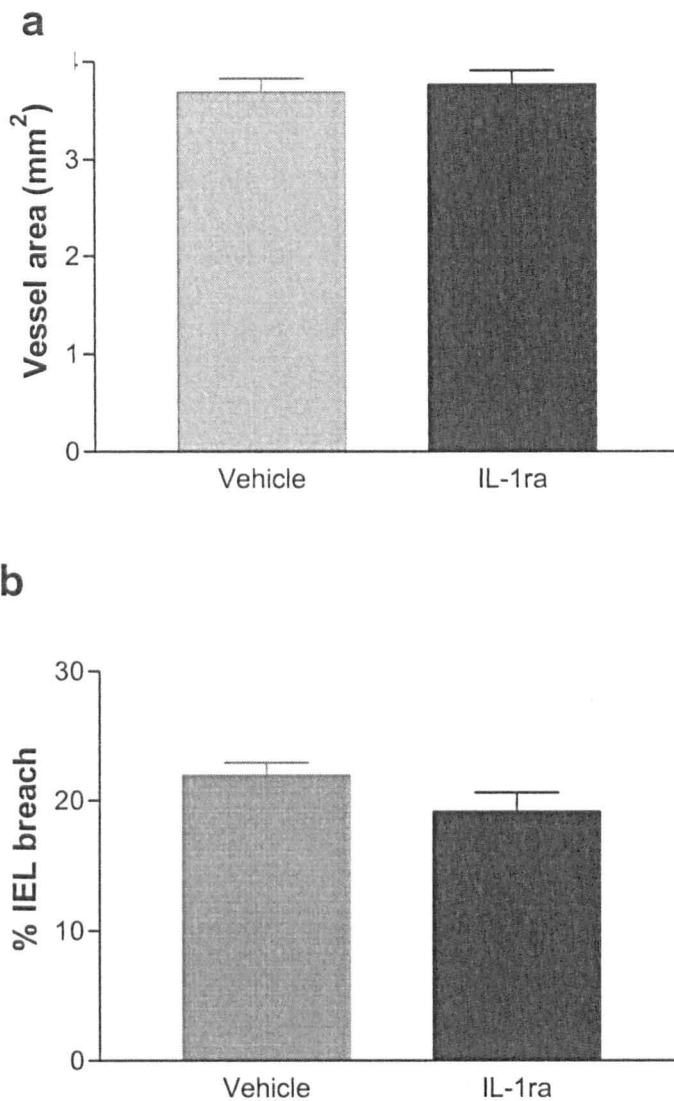


Figure 18 Modulation of PTCA Injury by IL-1ra: (a) Total Vessel Cross-sectional area (mm²) and (b) % IEL breach (injury score)

The data are expressed as mean (\pm SEM). (a): There is no significant difference between the two groups (n=6, p = 0.68). (b): There is no significant difference between the two treatment groups (n=6, p = 0.13), although there is a trend towards increased injury in the vehicle treated animals.

5.3.5 Neointimal area of the PTCA sections

The intimal thickening that occurs in response to injury is shown in this model by an increase in neointimal area (mm^2). Figure 19 demonstrates that when the animals receive an iv bolus of IL-1ra followed by a continuous subcutaneous infusion, there is a 23% decrease in neointima formation and the response to injury which is significant ($p < 0.04$).

5.3.6 Lumen area of the PTCA sections

The cross-sectional area of the lumen is shown in Figure 20. As expected, the animals that received IL-1ra and had a smaller amount of neointima have a larger lumen although the difference seen does not reach significance.

5.3.7 Intima: media ratio of the PTCA treated arteries

In order to correct for differences in vessel size between the animals, the neointima area is divided by the cross-sectional area of the media for each section. Figure 21a demonstrates that when vessel size is accounted for, there is a significant reduction in neointima area ($p = 0.01$). As previously discussed, each section has a differing amount of injury. In order to account for this, each intima: media ratio is further divided by the injury score for each section i.e. the % IEL breach. Figure 21b shows that even with this further correction, the effect of IL-1ra on reducing neointimal area is still significant ($p = 0.04$). Representative histological sections are shown in Figure 22.

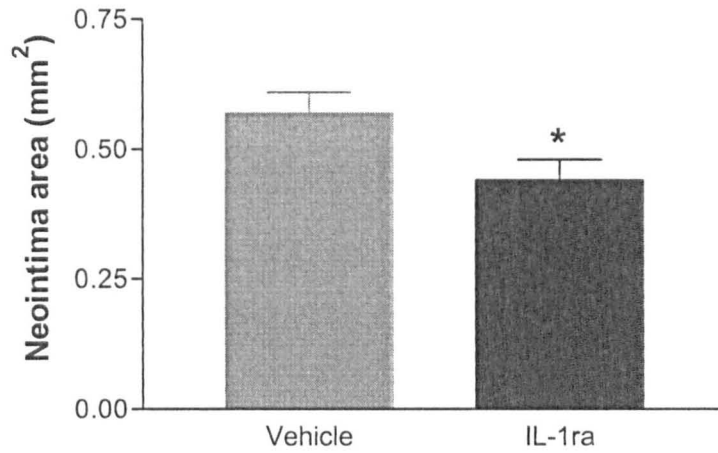


Figure 19 Modulation of PTCA Injury by IL-1ra: Neointimal cross-sectional area (mm²)

The data are presented as mean \pm SEM). There is a significant difference between the two groups (n=6, * p = 0.04), with less neointima formation in the IL-1ra treated animals.

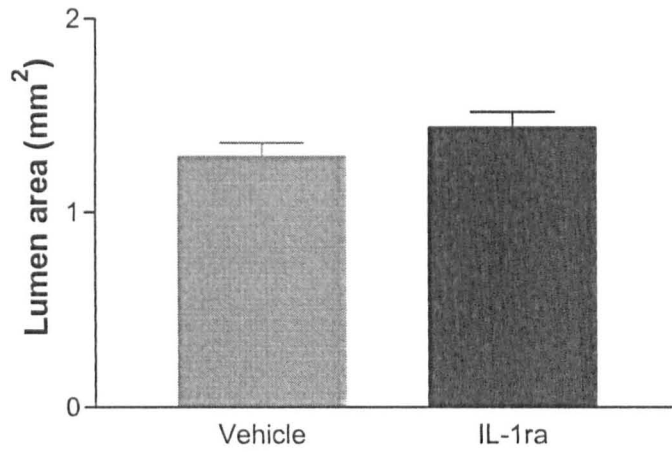
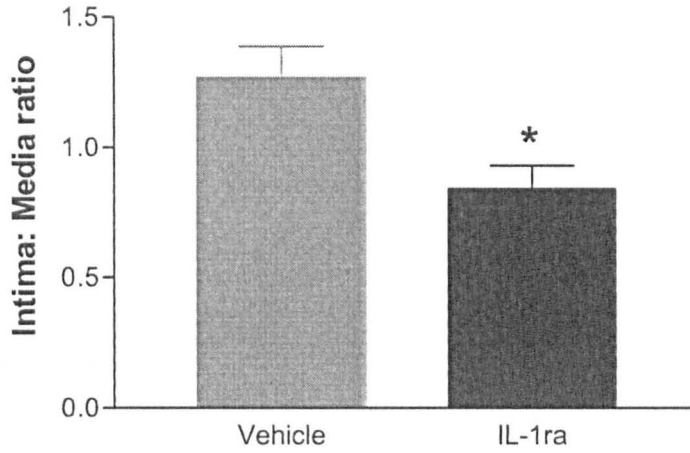


Figure 20 Modulation of PTCA Injury by IL-1ra: Cross-sectional area of the lumen (mm²)

The data are presented as mean \pm SEM. There is no significant difference between vehicle and IL-1ra treated vessels (n=6, p = 0.08), although there is a trend towards an increased lumen in the IL-1ra treated group.

a



b

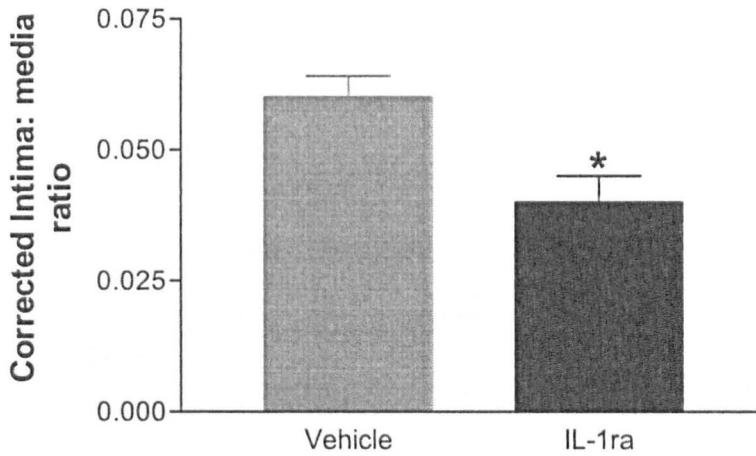


Figure 21 Modulation of PTCA Injury by IL-1ra corrected for vessel size and injury

The uncorrected (a) and corrected (b) intima: media ratio of PTCA treated arteries are shown above. In both cases, IL-1ra results in significantly less neointima formation, even with a correction for vessel size and injury (n=6, * p = 0.006; and p = 0.04).

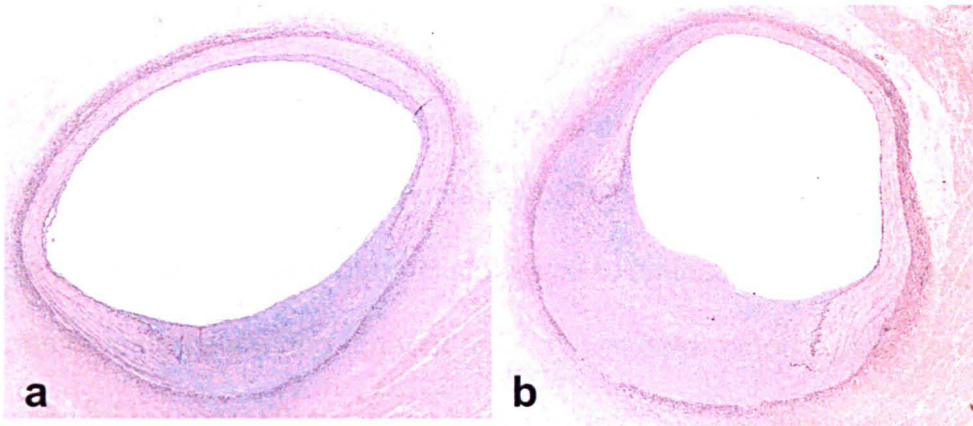


Figure 22 Tissue response to PTCA in porcine coronary arteries

Histological sections from pig coronary artery following PTCA are shown. IL-1ra infusion was for 14-days and analysis was at 28-days. (a) shows a section of coronary artery from an animal that received IL-1ra and (b) shows a corresponding section from a vehicle treated animal. Both sections have been stained with Miller's elastin and van Gieson's stain. Both show a 23% breach in the internal elastic lamina. There is clearly much less neointima in the IL-1ra treated vessel.

5.4 RESULTS – Intracoronary stenting

5.4.1 Histomorphometric analysis of stented sections

For all of the following results, there were 6 pigs in each treatment group, apart from the final 90 day time-point in which there were 4 animals. This yielded 8 -12 vessels per group. Histological examination of all of these sections revealed a varying amount of injury (as determined by the previously described injury score) that ranged from no injury to extensive disruption. The initial group of animals studied received a 14-day infusion and sacrifice was at 28-days. A 28-day time-point is traditionally studied with the porcine model as this has been shown previously to be approximately comparable with 6 months in the human (the time-point within which restenosis traditionally occurs) [116]. Shorter time-points give extra information as to the processes occurring following stenting. Sectioning each artery as described in 5.2.4 yields 15 – 20 sections per vessel. This gives 6 – 10 sections per vessel that are analysable. Figure 23 demonstrates the measurements taken for each section. Analysis was operator blinded and two independent observers measured all sections. There was no significant difference between the values obtained ($p > 0.05$ for all measurements with $< 10\%$ magnitude of difference between the two observers). All data are presented as mean \pm SEM and significance determined using an unpaired Students' t-test.

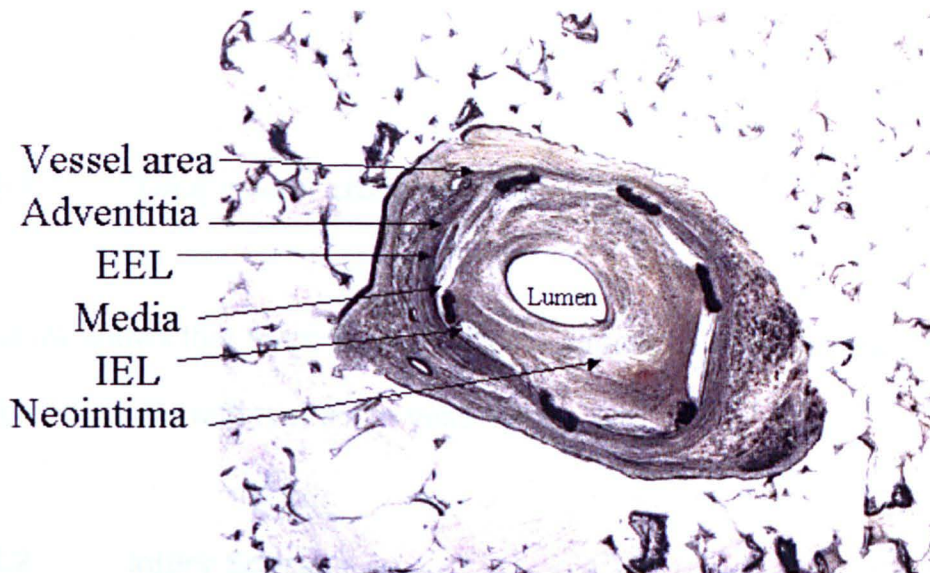


Figure 23 Measurements taken for histomorphometric analysis of stented sections

Histomorphometric measurements made

5.4.2.3 Neointima area

The data shown in Figure 26a is the raw neointima area. After a 14-day infusion of drug and a 28-day sacrifice, there is a significant increase in the neointima area in the IL-1ra treated animals ($p < 0.001$). The data shown in

5.4.2 Analysis: 14-day infusion, 28-day time-point

The following data are for animals which have received a 14-day infusion of either IL-1ra or vehicle and that have been killed at 28-days. 112 sections were suitable for analysis in the IL-1ra treated group and 98 sections in the vehicle treated group.

5.4.2.1 Total vessel cross-sectional area

Figure 24 shows that there is no significant difference between the two treatment groups with respect to vessel size.

5.4.2.2 Injury Score

The injury score shown is the Modified Schwartz (Gunn) injury score. Figure 25 shows that there is a trend for more injury in the vehicle group but this does not reach statistical significance ($p=0.06$). Although not shown, when the Schwartz injury score is calculated, there is also no significant difference between the two groups ($p = 0.50$).

5.4.2.3 Neointima area

The data shown in Figure 26a is the raw neointima area. After a 14-day infusion of drug and a 28-day sacrifice, there is a significant increase in the neointima area in the IL-1ra treated animals ($p < 0.001$). The data shown in

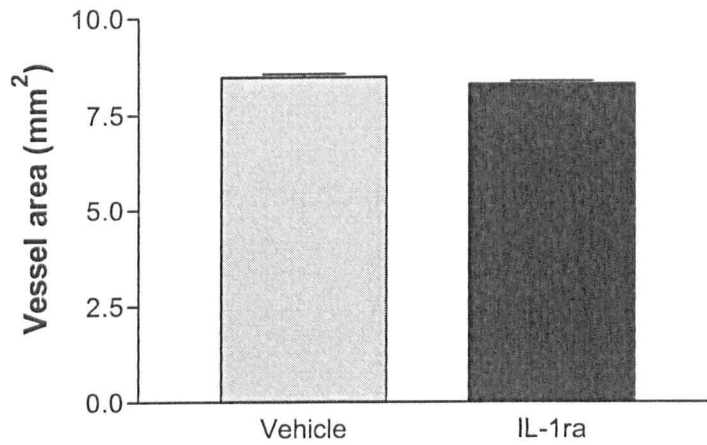


Figure 24 Modulation of intracoronary stenting by IL-1ra (14d infusion, 28d analysis): Cross sectional vessel area

Animals received a 14-day infusion of either IL-1ra or vehicle. Animals were killed at 28-days. There is no significant difference between the two groups (n=6, p = 0.08)

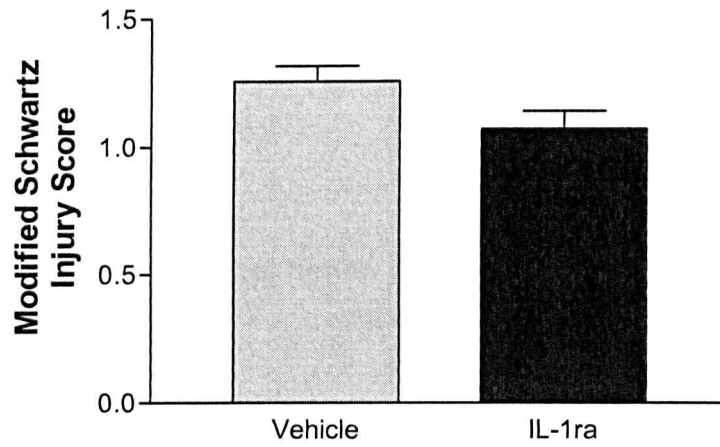


Figure 25 Modulation of intracoronary stenting by IL-1ra (14d infusion, 28d analysis): Injury score correction

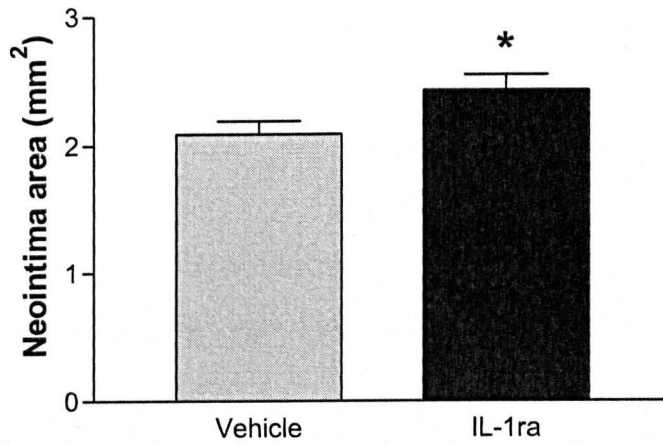
No significant difference between groups is seen (n=6, p = 0.06).

Figure 26b is the corrected neointima area, that is the neointima area corrected for both vessel size and injury. After a 14-day infusion of drug and a 28-day sacrifice, there is a significant increase in the corrected neointima area in the IL-1ra treated animals ($p < 0.001$). Representative histological sections are shown in Figure 27.

5.4.2.4 Cross-sectional lumen area

The lumen area was calculated for each section. When comparing the two treatment groups, it can be seen from Figure 28 that there is a significant difference between the two groups ($p = 0.02$).

a



b

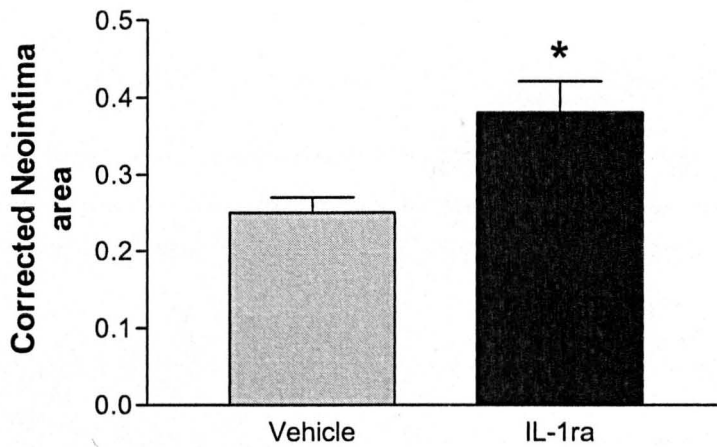


Figure 26 Modulation of intracoronary stenting by IL-1ra (14d infusion, 28d analysis): Neointima Area

Uncorrected (a) and corrected (b) neointima area of porcine coronary arteries following stenting and IL-1ra or vehicle infusion. In both cases, in contrast to PTCA treated arteries, IL-1ra causes a significant increase in neointima area (n=6, p< 0.001).

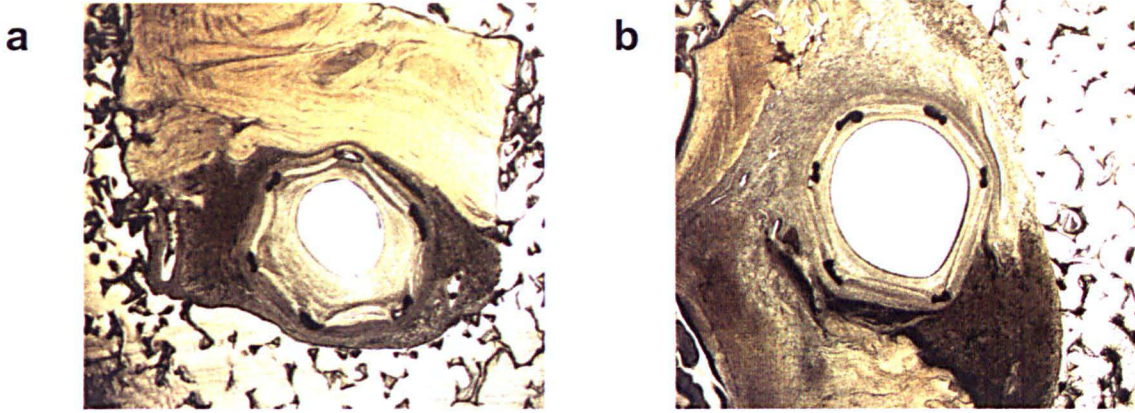


Figure 27 Tissue response to Intracoronary stenting (14 day infusion, 28 day analysis).

Both these histological sections are representative of the sections obtained from (a) IL-1ra treated animals and (b) placebo treated animals. For a similar degree of injury, there is more neointima in the IL-1ra treated group

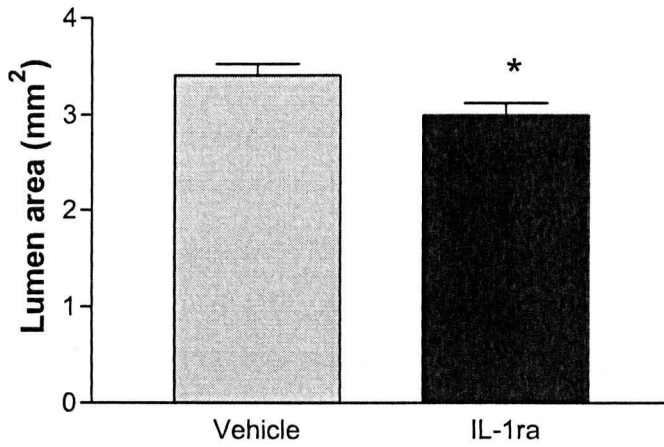


Figure 28 Modulation of intracoronary stenting by IL-1ra (14d infusion, 28d analysis): Lumen Area

There is a bigger lumen in the vehicle treated group (n=6, p = 0.02).

5.4.3 Analysis: 14-day infusion, 14-day time-point

The following data are for animals which have received a 14-day infusion of either IL-1ra or vehicle and that have been killed at 14-days. 83 sections were suitable for analysis in the IL-1ra treated group and 82 sections in the vehicle treated group.

5.4.3.1 Total vessel cross-sectional area

The cross-sectional area for each section was calculated. Data are presented as mean and standard error of the mean for each treatment group. Figure 29 shows that there is no significant difference between the two treatment groups.

5.4.3.2 Injury Score

The injury score shown is the Modified Schwartz (Gunn) injury score that takes into account stretch as well as fracture of the elastic laminae. Figure 30 shows that there is no significant difference between the two treatment groups ($p=0.44$). Although not shown, when the Schwartz injury score was calculated, there is also no difference between the two groups.

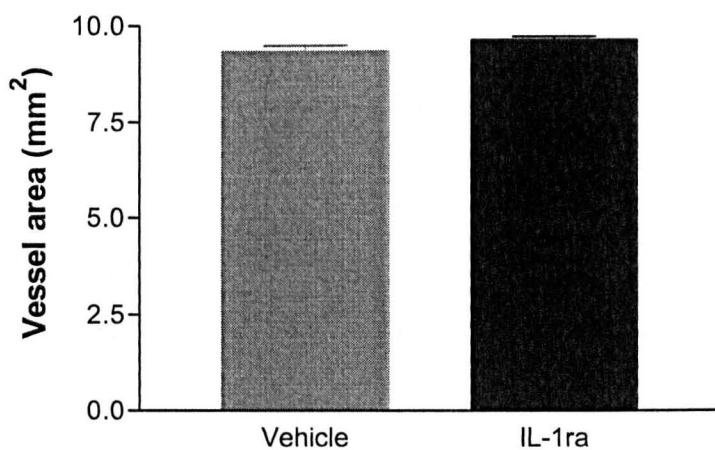


Figure 29 Modulation of intracoronary stenting by IL-1ra (14d infusion, 14d analysis): Total vessel cross-sectional area

There was no significant difference between the two treatment groups (n=6, p=0.11).

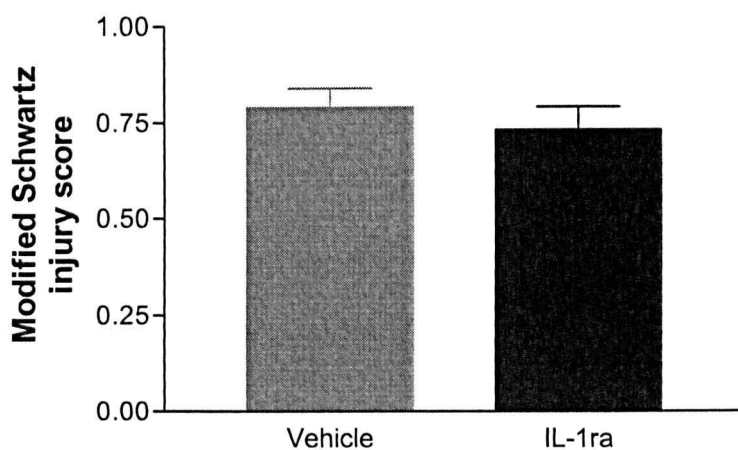


Figure 30 Modulation of intracoronary stenting by IL-1ra (14d infusion, 14d analysis): Injury score correction

After application of the Modified Schwartz (Gunn) injury score, there was no significant difference between the two treatment groups (n=6, p = 0.44).

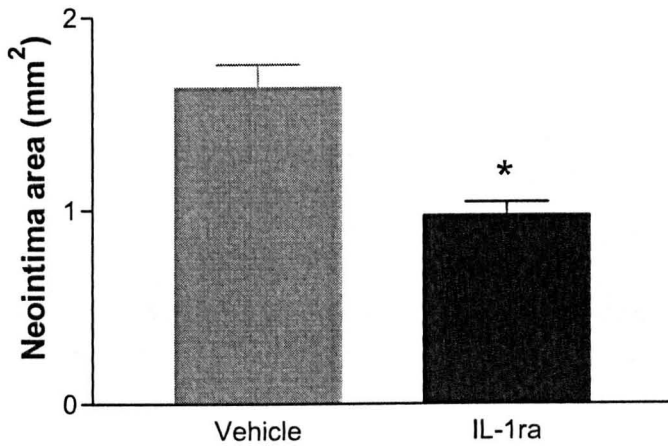
5.4.3.3 Neointimal area

Figure 31a shows the uncorrected neointima area after IL-1ra or vehicle treatment of stented porcine coronary arteries. There was a significant decrease in neointima area with IL-1ra treatment ($p < 0.001$). In order to take into account vessel size and the degree of injury for each section, the cross-sectional neointimal area for is section has been corrected by dividing the value obtained by the vessel size followed by a further correction for the mean injury score of that section. Figure 31b shows that when comparing the two treatment groups, IL-1ra significantly reduces the neointimal response to injury ($n=6$, $p < 0.0001$). Figure 32 shows representative histological sections from each treatment group.

5.4.3.4 Cross-sectional lumen area

The lumen area was calculated for each section. Given the reduced neointima in the IL-1ra treated group (see section 5.4.3.3), it follows that treatment with IL-1ra also results in a significantly larger lumen than treatment with vehicle ($n=6$, $p < 0.0001$, Figure 33).

a



b

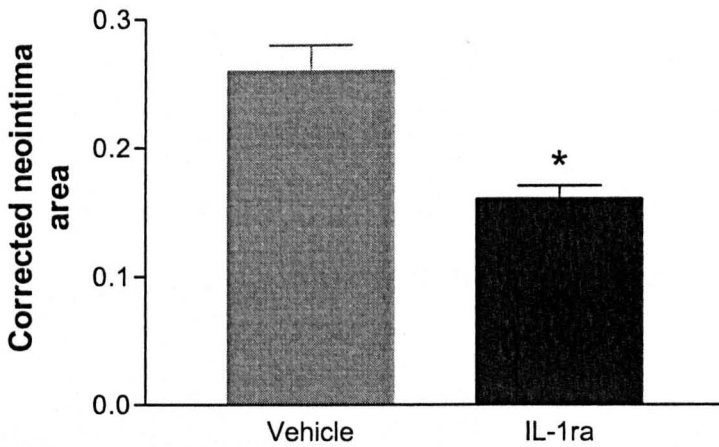


Figure 31 Modulation of intracoronary stenting by IL-1ra (14d infusion, 14d harvest): Neointima Area

Uncorrected (a) and corrected (b) neointima area of porcine coronary arteries following stenting and IL-1ra or vehicle infusion for the duration of the experiment (14-days). In both cases, as with PTCA treated arteries, IL-1ra causes a significant decrease in neointima area (n=6, p< 0.001).

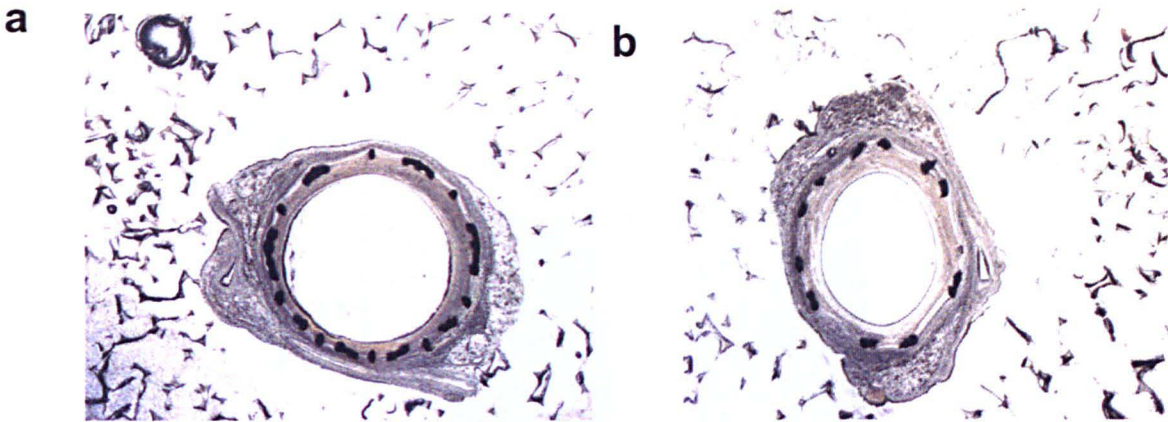


Figure 32 Tissue response to Intracoronary stenting (14 day infusion, 14 day analysis).

Infusion, 14 day analysis, Lumen Area

Both these histological sections are representative of the sections obtained from (a) IL-1ra treated animals and (b) placebo treated animals. For a similar degree of injury, there is less neointima in the IL-1ra treated group

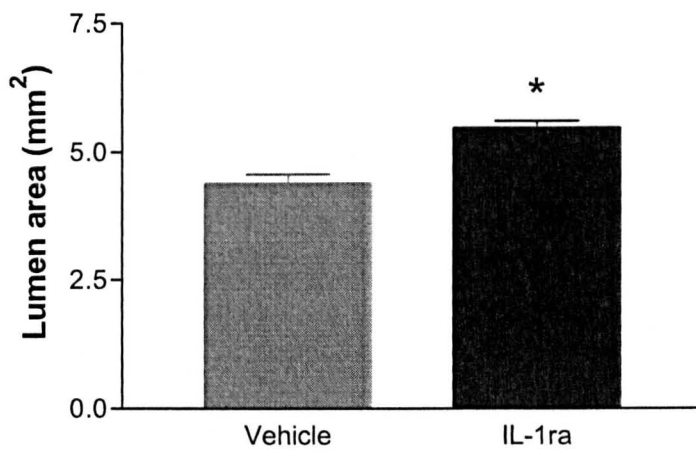


Figure 33 Modulation of intracoronary stenting by IL-1ra (14d infusion, 14d analysis): Lumen Area

Vessels were harvested at 14-days. There is a bigger lumen in the IL-1ra treated group (n=6, p < 0.0001).

5.4.4 Analysis: 28-day infusion, 28-day time-point

The following data are from animals which have received a 28-day infusion of either IL-1ra or vehicle and that have been killed at 28-days. 69 sections were suitable for analysis in the IL-1ra treated group and 64 sections in the vehicle treated group.

5.4.4.1 Total vessel cross-sectional area

The cross-sectional area for each section was calculated. Data are presented as mean and standard error of the mean for each treatment group. Figure 34 shows that there is no significant difference between the two treatment groups.

5.4.4.2 Injury Score

The injury score shown is the Modified Schwartz (Gunn) injury score. Figure 35 shows that there is a significant difference between the two treatment groups with more injury in the IL-1ra treated group ($n=6$, $p=0.001$). Although not shown, when the Schwartz injury score is calculated, there is no significant difference between the two groups. This highlights the difference between the two scores (see section 5.4.4.3).

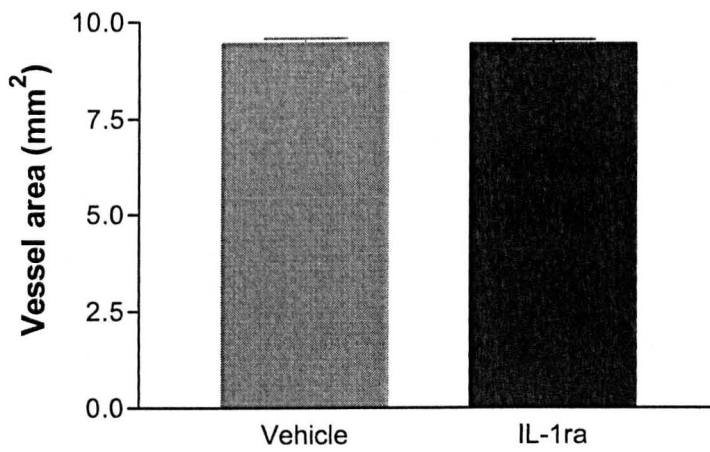


Figure 34 Modulation of porcine coronary artery response to stenting by IL-1ra (28d infusion, 28d analysis): Total vessel cross-sectional area (mm²)

There was no significant difference between the two treatment groups (n=6, p=0.90).

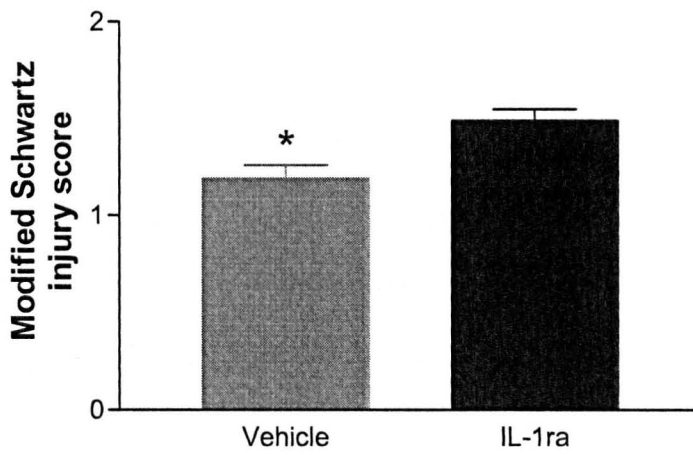


Figure 35 Modulation of porcine coronary artery response to stenting by IL-1ra (28d infusion, 28d analysis): Injury Score correction

There is a significant difference between the two treatment groups with far more injury in the IL-1ra treated animals (n=6, p = 0.001).

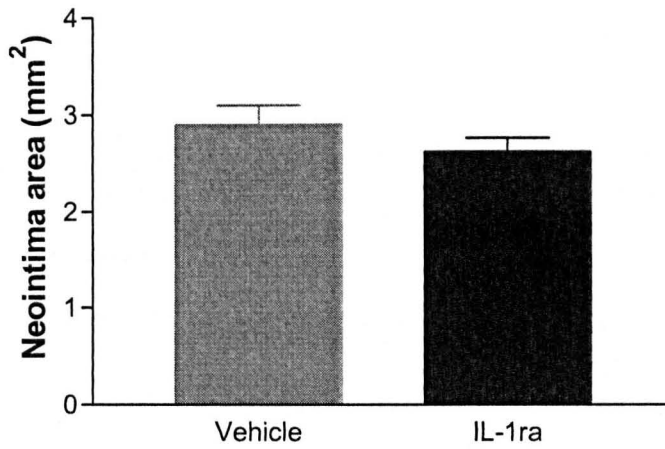
5.4.4.3 Neointima area

Figure 36 shows the uncorrected and corrected neointima area data following stenting in the 28 day infusion and 28 day analysis group. The importance of the correction for injury score is specifically highlighted by these data since in the uncorrected group of animals (i.e. when vessel size and injury score are not accounted for), there is no significant decrease in neointima area with IL-1ra treatment (Figure 36a) ($n=6$, $p = 0.33$). In order take into account vessel size and injury, the neointima area is corrected by dividing the value obtained by the vessel size followed by a further correction for the mean injury score of that section (Figure 36b). When the correction is applied, it reveals that when comparing the two treatment groups, IL-1ra significantly reduces the neointimal response to injury ($n=6$, $p < 0.0005$). This highlights the importance of the correction for injury, especially when the injury scores differ in the two groups as in this case. Again representative histological sections from each treatment group are shown (Figure 37).

5.4.4.4 Cross-sectional lumen area

The lumen area was calculated for each section. When treatment is continued for 28-days, there is no significant difference in lumen size with IL-1ra although there is a trend for a bigger lumen in the IL-1ra treated group ($n=6$, $p = 0.30$, Figure 38).

a



b

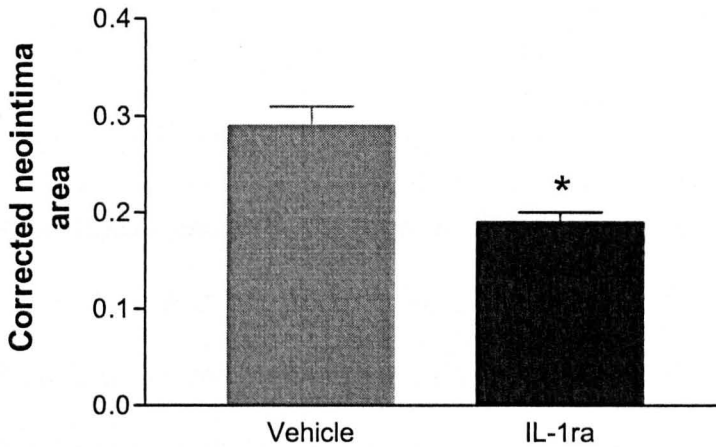


Figure 36 Modulation of porcine coronary artery response to stenting by IL-1ra (28d infusion, 28d analysis): Neointima Area

Uncorrected (a) and corrected (b) neointima area of porcine coronary arteries following stenting. With no correction (a), there is no significant difference between the two treatment groups (n=6, p = 0.33). When a correction for vessel size and injury is made, as with PTCA treated arteries (b), IL-1ra causes a significant decrease in neointima area (* n=6, p< 0.0005).

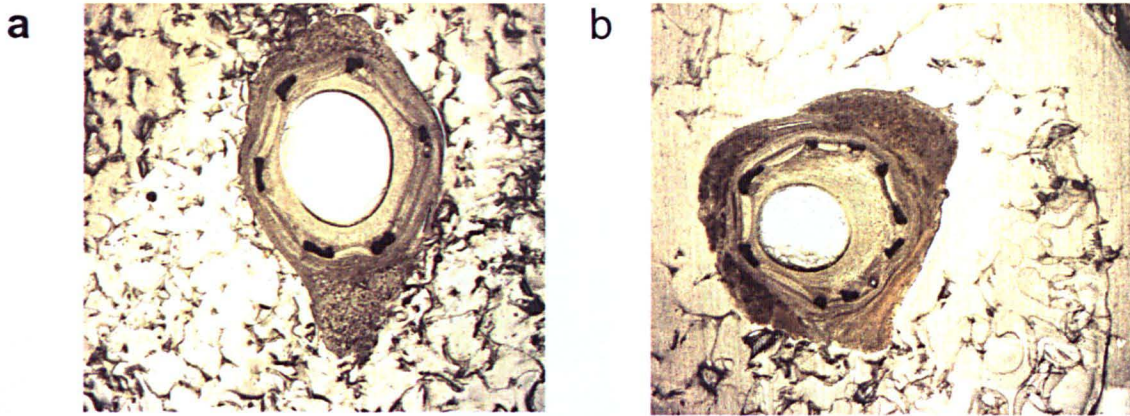


Figure 37 Tissue response to Intracoronary stenting (28 day infusion, 28 day analysis).

Both these histological sections are representative of the sections obtained from (a) IL-1ra treated animals and (b) placebo treated animals. As with the 14 day infusion and 14 day analysis animals, for a similar degree of injury, there is less neointima in the IL-1ra treated group

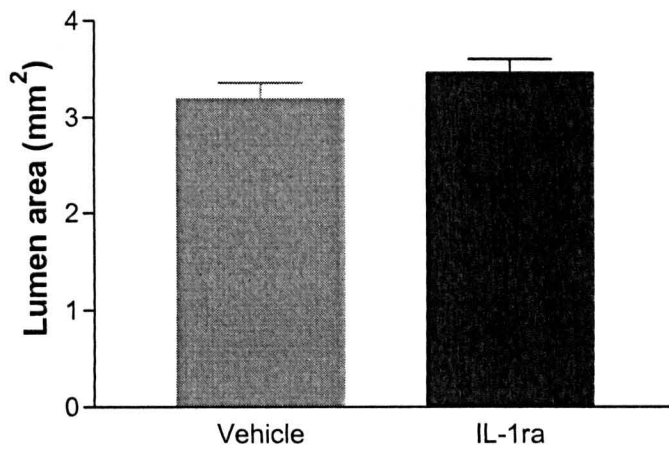


Figure 38 Modulation of porcine coronary artery response to stenting by IL-1ra (28d infusion, 28d harvest): Lumen area (mm²)

There is a bigger lumen in the IL-1ra treated group although this does not reach significance (n=6, p = 0.30).

5.4.5 Analysis: 28-day infusion, 90-day time-point

The following data are from animals which have received a 28-day infusion of either IL-1ra or vehicle and that have been killed at 90-days. There were 4 animals in each group. 50 sections were suitable for analysis in the IL-1ra treated group and 44 sections in the vehicle treated group.

5.4.5.1 Total vessel cross-sectional area

The cross-sectional area for each section was calculated. Data are presented as mean and standard error of the mean for each treatment group. Figure 39 shows that there is no significant difference in vessel area between the two treatment groups.

5.4.5.2 Injury Score

The injury score shown is the Modified Schwartz (Gunn) injury score. Figure 40 shows that there is no significant difference between the two treatment groups.

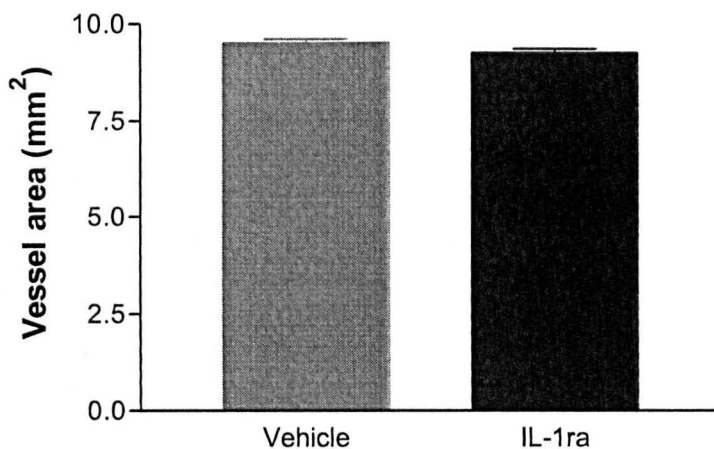


Figure 39 Modulation of porcine coronary artery response to stenting by IL-1ra (28d infusion, 90d analysis): Vessel area (mm²)

There was no significant difference between the two treatment groups (n=4, p=0.06).

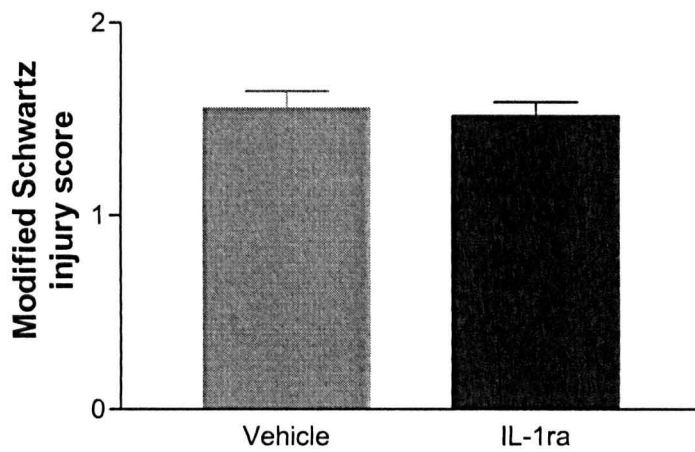


Figure 40 Modulation of porcine coronary artery response to stenting by IL-1ra (28d infusion, 90d analysis): Injury Score

There is no significant difference between the two treatment groups (n=4, p = 0.69).

5.4.5.3 Neointima area

Figure 41 shows the uncorrected and corrected neointima area data following stenting in the 28 day infusion and 90 day analysis group. The raw neointima area (Figure 41a) shows a significant difference between the two treatment groups with less neointima following IL-1ra therapy (n=4, $p < 0.0001$). When the data is corrected as described in 5.4.4.3, the significant difference between the two groups in favour of IL-1ra is maintained (Figure 41b) (n=4, $p < 0.000001$). Figure 42 shows histological sections from each group, highlighting the difference in neointima seen.

5.4.5.4 Cross-sectional lumen area

The lumen area was calculated for each section. When treatment is continued for 28-days, and the harvest performed at 90 days, there is a larger lumen size with IL-1ra treatment (n= 4, $p < 0.005$, Figure 43).

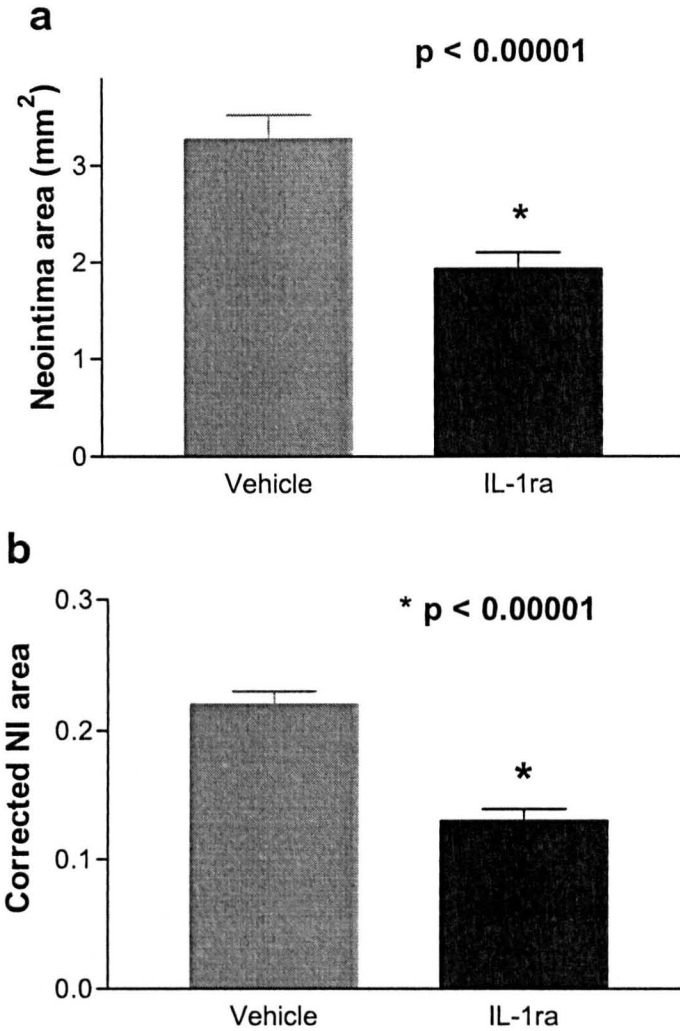


Figure 41 Modulation of porcine coronary artery response to stenting by IL-1ra (28d infusion, 90d analysis): Neointima Area

Uncorrected (a) and corrected (b) neointima area of porcine coronary arteries following stenting. With no correction (a), there is a significant difference between the two treatment groups (n=4, * $p < 0.0001$). When a correction for vessel size and injury is made (b), IL-1ra still causes a significant decrease in neointima area (* n=4, $p < 0.000001$).

a



b

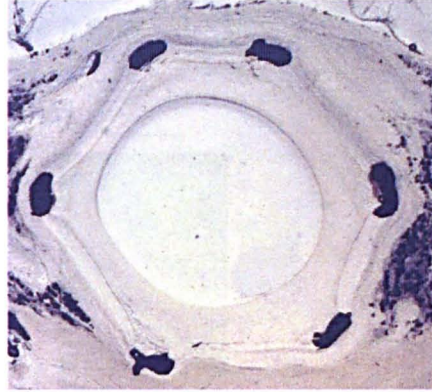


Figure 42 Tissue response to Intracoronary stenting (28 day infusion, 90 day analysis).

Both these histological sections are representative of the sections obtained from (a) IL-1ra treated animals and (b) placebo treated animals. For a similar degree of injury, there is 41% less neointima in the IL-1ra treated group

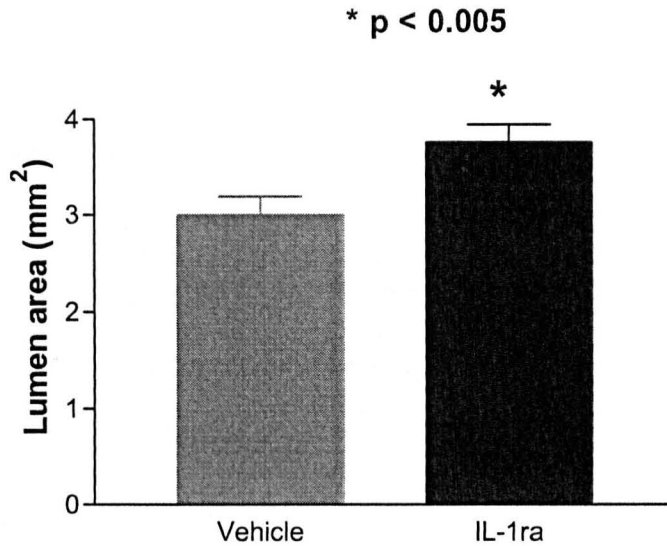


Figure 43 Modulation of porcine coronary artery response to stenting by IL-1ra (28d infusion, 90d analysis): Lumen area (mm²)

There is a bigger lumen in the IL-1ra treated group which reaches significance (n= 4, p < 0.005).

5.5 DISCUSSION

5.5.1 Summary of findings

The work in this chapter has shown that antagonism of IL-1 by IL-1ra inhibits neointima formation after coronary artery injury and stenting in a porcine model. In the case of PTCA, IL-1ra resulted in a 23% decrease in neointima area, independent of the length of IL-1ra therapy. In the case of stenting, IL-1ra inhibited neointima formation for the duration of the infusion, but after cessation of the infusion around 14 days, there was a 'catch-up' phenomenon, with a 34% larger neointima in IL-1ra treated arteries than vehicle. However, if the infusion is continued for 28 days and the vessels harvested at 90 days, again there is a 41% decrease in neointima area. It seems likely therefore that there is a critical length of infusion needed to suppress neointima formation and that the chronic inflammatory response caused by the stent struts needs prolonged (28 days) suppression for after implantation.

5.5.2 The effect of IL-1ra on the vessel response to balloon angioplasty

IL-1ra treatment results in significantly less neointima formation than in vehicle treated arteries. Although over 90% of procedures now involve placement of a stent, there are still instances when balloon angioplasty in isolation is used, e.g. in tortuous arteries when a stent cannot physically be placed into the vessel or in very small vessels where the use of stents remains controversial because the published data reveals disparate results

[117]. Injury following balloon angioplasty is different to injury following stenting. Balloon injury is analogous to acute fissuring of the vessel, with thrombus accumulation and healing taking place immediately following disruption. Stenting is a chronic stimulus that produces profound neointima formation. The inflammatory process following balloon angioplasty is therefore shorter than that post-stenting. The 14-day infusion of IL-1ra is long enough to cover the acute inflammatory process following PTCA and after that healing occurs so a prolonged infusion of IL-1ra is not necessary. The 23% reduction in neointima seen in this study is impressive following balloon only angioplasty. Early drug delivery strategies using a "leaky" balloon were cumbersome, dangerous, wasteful and ultimately unsuccessful. It follows that a systemic approach to therapy may be more appropriate following balloon angioplasty than a local drug delivery one. This aside, the fact remains that the majority of lesions are treated with intracoronary stent placement and balloon only angioplasty has a limited remit.

5.5.3 The effect of IL-1ra on the vessel response to intracoronary stenting.

Following intracoronary stent placement, there is a significant reduction in neointima formation following IL-1ra therapy for the duration of the experiment (38% following 14-days and 34% after 28-days of treatment). If the infusion is continued for 28 days and the vessels harvested at 90 days, the inhibition of neointima is maintained at 41%. However, if the infusion is stopped early, there is rebound neointima formation (with 34% more neointima in the IL-1ra

treated animals). When sirolimus and paclitaxel were given for 28 days in a porcine model of stenting, they caused a 50% and 39.5% respective reduction in neointima formation [118, 119], which is comparable to the results seen in this study. However when a 90 day time-point is considered, the results differ greatly. When pigs undergo intracoronary stenting with a Sirolimus eluting stent and the vessels are harvested at 90 days, there is no longer suppression of neointima formation and the amount of neointima seen in the Sirolimus-eluting stents equals that of the control bare metal stent [118]. Similarly, when Paclitaxel eluting stents are placed into rabbit arteries and the vessels harvested at 90 days, despite an initial impressive reduction in neointima formation at 30 days, at 90-days the effect is lost with no significant difference between the Paclitaxel eluting stents and the bare metal stents [119]. It seems likely therefore that for prolonged inhibition of neointima formation in the porcine model, an anti-inflammatory approach may give better suppression of neointima than an anti-proliferative one.

The increase in neointima formation seen when IL-1ra is discontinued between 14 and 18-days and analysis conducted at 28-days was a surprising finding. The reduction of neointima at 28-days when the IL-1ra was continued for the complete duration of the study indicates not only the importance of IL-1 in this process, but also indicates the duration of the IL-1 mediated response following stenting. Since neointima is also reduced at 90 days after IL-1ra treatment for 28 days, this indicates that the duration of the 'IL-1ra inhabitable' inflammatory response following stenting is between 14 and 28-days. This stenting response also contrasts with the PTCA response (balloon angioplasty

alone with 14-day IL-1ra and analysis at 28-days), when a reduction in neointima was induced. Since PTCA is a 'one-off' injury, it appears that a 14-day infusion of IL-1ra is sufficient to have inhibitory effects upon distant (28-day) responses. The stenting response to this regime of IL-1ra however suggests that the injury resulting from stent placement causes a more chronic inflammatory stimulus. This has to be presumed to arise from the vessel wall cells as inflammatory white cells and platelets are not a prominent feature at 14-days and beyond. We hypothesized that the IL-1ra infusion could not only be inhibiting IL-1 signalling but also inhibiting IL-1 production, and that discontinuation of the IL-1ra around 14-days was associated with a rebound production of IL-1.

5.5.4 Implications of findings

This work is the first to show that IL-1 is directly involved in the vessel wall response to injury and in neointima formation after intracoronary stenting. This work is also the first to use a purely anti-inflammatory agent to inhibit neointima formation. The agents in current clinical use for suppression of neointima such as sirolimus and paclitaxel are in the main, cytostatic [76] [120]. An anti inflammatory strategy, using IL-1ra is novel and, if these results translate to man may prove an effective alternative or additional treatment in coronary heart disease. It may be that certain patterns of coronary heart disease (e.g. acute coronary syndromes), which are associated with 'inflammatory' lesions, may be particularly suitable for an anti-inflammatory approach in the context of therapeutic PCI. When considering prolonged

suppression of neointima, these data show that unlike the cytostatic agents, IL-1ra causes prolonged suppression of neointima formation at 90 days post stent implantation. This is potentially important when considering the long-term effects of these agents.

5.6 Conclusions and future directions

Following balloon angioplasty, IL-1ra results in a significant reduction in neointima formation. The same is true following stenting but the reduction is only seen if the infusion of IL-1ra is continued for the length of the experiment. If it is stopped early, a 'catch up' in neointima is seen, with more neointima being formed in the IL-1ra treated animals. When a longer time point of 90 days is studied, suppression of neointima is maintained despite the IL-1ra only being given for the first 28 days. In order to determine the appropriate therapy length for IL-1ra treatment, it is important to determine the mechanism of the 'catch-up' phenomenon seen. We know from the literature that IL-1 β is present in the arterial wall up to 3 days following balloon angioplasty [31]. To test the hypothesis that the 'catch up' occurred because of a rebound in IL-1 production, Western blotting and Real-time quantitative PCR were used to assess IL-1 production in the vessel wall.

CHAPTER 6

MECHANISM OF ACTION OF IL-1ra IN THE VESSEL WALL AFTER STENTING

6.1 INTRODUCTION

The only known action of IL-1ra is to inhibit IL-1 by competitively binding to the Type 1 receptor. Therefore, the rebound increase in neointima formation seen following discontinuation of IL-1ra therapy must involve IL-1 in some way. The hypothesis behind the work presented in this chapter was that discontinuation of IL-1ra led to an increase in vessel wall production of IL-1. The work presented here attempted to determine whether, at both the protein and mRNA level, there was an increase in vessel wall IL-1.

6.1.1 Regulation of production of IL-1

The majority of microbial products induce IL-1 β via the Toll like receptor family of receptors. Depending on the stimulant, IL-1 β mRNA levels rise quickly but by 4 hours start to decline. This decline is thought to be due to the local production of a transcriptional repressor and/or a decrease in mRNA half-life [121]. IL-1 β can stimulate its own gene expression and when it does, mRNA levels are sustained for over 24 hours. IL-1 α also stimulates IL-1 β gene expression via a cyclic-AMP mediated process [122]. The primary sources of

IL-1 β protein are blood monocytes and macrophages. ATP results in the rapid release of mature IL-1 β and because of this observation, a receptor-mediated release event via an ion channel has been proposed although not yet fully proven.

6.1.2 Quantification of tissue levels of IL-1

When considering IL-1 biology and its regulation, it is often necessary to quantify the amount of IL-1 present at either an mRNA or a protein level. Protein levels may be detected using Western blotting however using this technique, quantification of actual amounts is difficult. The real time reverse transcription polymerase chain reaction (real time RT-PCR) is the most sensitive method for the detection and quantification of low abundance mRNA from tissue samples. RT-PCR can be used to compare different levels of mRNA in different sample populations. Both these techniques can be used to determine whether IL-1 production is up regulated following cessation of IL-1ra therapy.

6.1.3 Aims of this study

The aim of this final section of the thesis was to determine whether early cessation of IL-1ra therapy causes a rebound in IL-1 production, resulting in an exaggerated neointima response.

6.2 MATERIALS AND METHODS

6.2.1 Quantification of protein and mRNA levels from porcine coronary arteries

In order to determine the changes in levels of IL-1 induced by IL-1ra at a molecular level, porcine coronary arteries were snap frozen into liquid nitrogen immediately after removal of the stent. Protein and RNA were extracted from this tissue and Real-Time PCR and Western blotting used to determine the amount of IL-1 protein and mRNA present in each sample.

6.2.2 Sample collection

Two groups of animals underwent intracoronary stenting as described in section 5.2.3. One group received IL-1ra for 14 days and were killed at 17 days and the other group received IL-1ra for 17 days and were killed at 17 days. The time-point of 17 days was chosen in order to allow 5 drug half lives to pass and then to allow time for rebound IL-1 production to occur. The 3 days without IL-1ra was a best guess time-point. Animals that received a 14-day infusion of IL-1ra but that were culled at 17 days had their pumps removed at day 14. Those who received an infusion for the full 17-days had new pumps inserted as before (see section 5.2.3). Animals in both these groups had a second 3.0mm stent inserted into distal vessel (in both the LAD and RCA).

At 17-days, animals were killed as previously described (see section 5.2.4). The 3.0 mm stents were also explanted *in situ* but the stent was then removed from the artery and the tissue snap-frozen in vials of liquid nitrogen (for laboratory analysis such as real time PCR, see sections 6.2.2. and 6.2.13).

6.2.3 Protein extraction from porcine coronary arteries

Stored tissue was removed, weighed and ground to a fine powder under liquid nitrogen with a pestle and mortar. Powdered tissue was placed into a microfuge tube containing 3ml RIPA lysis buffer (see Appendix A.3) and 30 μ l of 10mg/ml phenylmethylsulfonyl fluoride (PMSF) per gram of tissue. This was incubated on ice for 30mins and then centrifuged at 10,000g for 10 mins at 4°C. The pellet was discarded and centrifugation repeated until a clear lysate obtained. A MicroBCATM protein assay (Pierce, Rockford, USA) was performed (see 2.10.2) to determine the protein concentration of each sample and samples were stored at -20°C until further use.

6.2.4 Pierce MicroBCATM protein assay

This assay was used to determine the concentration of protein in each coronary artery. This allowed equal loading of protein onto a western blot in order for meaningful comparisons to be made. The working reagent was made up according to manufacturers instructions, mixing 25 parts reagent MA, 24 parts reagent MB and 1 part reagent MC.

The assay was performed in a 96-well plate and each plate read at 540nm at room temperature, using Labsystems Genesis V3.05 software. To each of the required wells on a 96-well plate, 150 μ l of sample or standard and 150 μ l of working reagent were added in order. The plate was covered and incubated at 37°C for 2 hours and cooled to room temperature before being read. The unknowns were compared with a known concentration of bovine serum albumin (ranging from 0.5 - 200 μ g/ml).

6.2.5 Sodium Dodecyl Sulphate Polyacrylamide Gel Electrophoresis: SDS-PAGE

This technique is used to detect proteins that have been transferred to a solid support (in this case a nitrocellulose membrane) from a polyacrylamide gel after electrophoretic separation. Proteins can be identified by the use of specific antibodies against the protein of interest.

6.2.6 Acrylamide gel preparation

A 15% acrylamide resolving gel was prepared and poured into the 'mighty small dual gel chamber' (Hoefer Scientific, San Francisco, USA), which was assembled according to manufacturers instructions. The ammonium persulphate (APS, BDH) and N,N,N,N'-tetramethylethylenediamine (TEMED) were added last as these cause polymerisation of the gel. The resolving gel separated the proteins according to size. Proteins separate on size and not charge as the sodium dodecyl sulphate (SDS) present within the gel coats all

proteins, giving them the same charge. The gel was overlaid with water-saturated butanol and allowed to polymerise for 45 mins. Once set, a 4% acrylamide stacking gel was prepared and poured on top of the resolving gel, the comb inserted to form sample wells and the gel allowed to polymerise (20 mins). Details of gel preparation are shown in Appendix C.

6.2.7 Sample loading and electrophoresis

After the gel had polymerised, the comb was removed and the wells rinsed with distilled water. The plates were assembled in the 'mighty small II' running apparatus (Hoefer Scientific) and Tris-glycine-SDS buffer (25mM Tris/ 250mM glycine/ 0.1% SDS) was poured into the top and bottom reservoirs. Protein samples were thawed and an equal volume of 2X SDS protein sample loading buffer was added to each sample (see Appendix A.3). The protein sample-loading buffer contains beta-mercaptoethanol that keeps the proteins in a reduced state. For each blot, Rainbow markers (Amersham, UK) were used to enable correct protein size identification. All samples were heated at 100°C for 5 mins to separate the proteins and stop them binding to each other or forming homodimers. 50µg of protein was loaded per well. Positive controls were loaded onto each gel (200ng of carrier-free recombinant porcine-IL-1 alpha or beta, R&D Systems, UK). An Alpha tubulin Monoclonal antibody was used at the detection stage as a loading control (product size 50kDa). Each gel was run for 30-60 mins at 150 – 200V until the lowest marker had migrated to the bottom of the gel.

6.2.8 Semi-Dry Electro Blotting

After electrophoresis, the gel was removed from the running apparatus and the stacking gel cut away. Each gel was then covered with 1-5mls of Towbin transfer buffer (39mM glycine/48mM Tris/0.037% SDS/20% methanol) to allow it to equilibrate and prevent it drying out. Each gel was measured and a suitably sized piece of nitrocellulose membrane cut to exactly fit the gel. 6 pieces of Whatman 3 filter paper was also cut to size and these along with the nitrocellulose membrane were placed into Towbin transfer buffer to allow hydration. Transfer was carried out using the 'semi-phor' Hoefer Scientific semi dry blotter. The blot was assembled as follows: 3 pieces of Whatman 3 filter paper, the nitrocellulose membrane, the gel and then the remaining 3 pieces of filter paper. Each blot was transferred for 90 mins at 5V at room temperature. After 90 mins, the blot was dismantled and labelled.

6.2.9 Staining proteins

The efficiency of protein transfer was established using Coumassie brilliant blue R250 (BDH, Poole, UK) to stain the gel and Ponceau S stain (BDH, Poole, UK) to stain the membrane.

6.2.10 Immunological Detection of Bound Proteins - Blocking Non-Specific Binding Sites

Non-specific binding sites on the membrane were blocked by placing it overnight in 5% (w/v) non-fat dried milk (Marvel) in Tris buffered saline, pH 7.6 (TBS) at 4°C.

6.2.11 Immunological Detection of Bound Proteins - Primary Antibody Incubation

All primary antibodies were diluted in 10mls of blocking buffer containing 0.05% (v/v) Tween-20 (Sigma, UK). The antibodies used were as follows: For IL-1 β detection, anti-porcine IL-1 β affinity purified goat IgG antibody (RnD systems, Minneapolis, USA) at a concentration of 0.2 μ g/ml and for IL-1 α detection, anti-porcine IL-1 α affinity purified goat IgG antibody (RnD systems, Minneapolis, USA) at a concentration of 0.2 μ g/ml. Hybridisation was carried out for 1h on a rotating platform and each blot was then washed in 3X TBS/0.05%(v/v) Tween-20 for 5 mins.

6.2.12 Immunological Detection of Bound Proteins - Secondary Antibody Incubation

Secondary antibody incubation was carried out using anti-goat IgG directly conjugated to Horse Radish Peroxidase (HRP) at a dilution of 1:1000. Incubation was again for 1h, followed by 3 x 10min washes as above.

6.2.13 Immunological Detection of Bound Proteins - Visualisation of bound proteins

The use of HRP results in the deposition of a coloured substrate on the membrane at the reaction site. Enhanced Chemiluminescence (ECL) was used to reveal the substrate and detection and detection was carried out using X-ray film.

An ECL kit (Amersham Life Sciences) was used for the detection. 500 μ l of each detection reagent provided by the kit were mixed together. The excess TBS was drained from the membrane and it was placed between clean pieces of plastic wrap. The mixed detection reagent was poured over the membrane surface and incubated for 1 minute. Excess reagent was drained off and the membrane was then exposed to X-ray film. Exposure times varied from 10 minutes to 1 hour. Protein bands were then compared with the position of the markers to allow size determination.

6.2.14 Extraction of RNA from arterial tissue

RNA was extracted from porcine coronary arteries using an RNAeasy Mini Kit (Qiagen). It was vital that the RNA obtained was uncontaminated therefore; an extra DNAsin step was incorporated to ensure no genomic DNA contamination was present.

Stored porcine coronary artery (30mg, see section 6.2.2) was ground to a fine powder under liquid nitrogen with a pestle and mortar. The ground tissue was transferred into an RNase-free liquid nitrogen cooled, 2ml eppendorf. Any excess liquid nitrogen was allowed to evaporate and then 600 μ l of Buffer RLT added. The lysate was pipetted directly onto a QIAshredder spin column (Qiagen, UK) placed in a 2ml collection tube, and centrifuged for 2min at maximum speed. The lysate was removed and centrifuged for 3 min at maximum speed in a microcentrifuge. After centrifugation, the supernatant was transferred to a new microcentrifuge tube. 600 μ l of 70% ethanol was added to the cleared lysate and mixed immediately by pipetting. 700 μ l of this sample (including any precipitate that formed) was added to an RNeasy mini column placed in a 2ml collection tube. This was centrifuged for 15s at 10,000rpm. Any flow-through was discarded and successive aliquots loaded onto the column and centrifuged as above. 350 μ l buffer RW1 was added to the column and the column was centrifuged for 15s at 10,000rpm to wash the column. The flow-through and collection tube were then discarded. 10 μ l of DNase I stock solution was added to 70 μ l Buffer RDD and mixed by gentle inversion. The DNase I mix (80 μ l) was added directly onto the RNeasy silica-gel membrane, and placed on benchtop for 15min. 350 μ l of buffer RW1 was added to the column and the column centrifuged at room temperature for 15 s at 10,000rpm. The flow through was discarded. The column was transferred onto a new 2ml collection tube, 500 μ l buffer RPE added to the column and the column centrifuged for 15s at 10,000rpm. A further 500 μ l of buffer RPE was added to the column that was centrifuged for 2min at 10,000rpm to dry the RNeasy silica-gel membrane. To elute the RNA, the column was transferred

to a new 1.5ml collection tube and 50 μ l RNase free water pipetted directly onto the silica-gel membrane. This was centrifuged at rtp for 1 min at 10,000rpm to elute the RNA. The elution step was then repeated with 30 μ l RNase free water (see Appendix A.2). The amount of RNA present was determined using a spectrophotometer (see Appendix B).

6.2.15 Extraction of RNA from porcine vascular smooth muscle cells

This was done to obtain samples for use as a positive control. The method followed was as for 6.2.14 except that the media was removed from the flask of the cells and the cells washed with 10mls PBS. This was then removed and 600 μ l of buffer RLT was added directly to the flask. The cells were scraped from the bottom of the flask with a plastic scraper and the solution pipetted directly onto the QIAshredder spin column. The method then proceeded as described in 6.2.14.

6.2.16 Reverse transcription polymerase chain reaction (RT-PCR)

RT-PCR was used to prepare cDNA for subsequent analysis. The first stage of RT-PCR is the synthesis of cDNA from the mRNA template. Once the cDNA had been formed, newly synthesized cDNA was amplified using specific pairs of primers designed to flank areas of genes of interest.

6.2.16.1 Reverse Transcription

3 μ g total RNA was transcribed in a 20 μ l volume. The reaction was carried out in RNase-free disposable microfuge tubes and the reaction mixture contained, sterile water, 2 μ l; MgCl₂, 4 μ l; 10X buffer, 2 μ l; dNTPs (1mM each), 8 μ l; random hexanucleotide primers, 1 μ l; Rnasin, 0.5 μ l and avian myeloblastosis virus reverse transcriptase (AMV-RT), 1 μ l. All reagents were from Promega. 3 μ l of RNA was added to 17 μ l of sample mix. For the negative control, 3 μ l of sterile water was used. A positive control was also used, in the case of these experiments, RNA extracted from THP1 cells and porcine smooth muscle cells that had been stimulated with LPS (1ng/ml) were used. PCR was carried out on the PTC-200 Peltier Thermal Cycler (M J research). The PCR was carried out under the following conditions:

Step	Temperature (°C)	Time (min)
1	23	10
2	42	60
3	99	5
4	4	10
5	15	∞

6.2.16.2 Polymerase Chain Reaction (PCR)

Newly synthesized cDNA was amplified using specific primers for porcine IL-1 alpha, beta and IL-1 receptor antagonist. 5 μ l of cDNA was typically used for

each reaction. In all of these experiments, β -actin was used as a loading control as it is abundant in porcine tissue. All primers were designed and used as a 15 μ M stock solution. All samples to be used were defrosted. All RNA underwent RT-PCR (see 2.10.6.1) to obtain the cDNA. A negative control was performed for all experiments and sterile water was used. The sample mix buffer was made up as follows: Sterile water, 18.25 μ l; 10X buffer, 2.5 μ l; dNTPs, 2 μ l; primer 1, 0.5 μ l; primer 2, 0.5 μ l; Taq Polymerase, 0.25 μ l; and MgCl₂, 1 μ l. The annealing temperature used for the PCR depended upon the primer pairs used but an example of a typical PCR program is shown:

Step	Temperature (°C)	Time (min)
1	94	2 (initial cDNA:mRNA denaturation)
2	94	1 (denatures cDNA)
3	53-60	1 (annealing of primers)
4	72	1 (DNA extension)
5	return to step 2 for cycling (repeated 29 – 35 times)	
6	72	5 (final extension)
7	4	10
8	15	∞ (holding temperature)

6.2.17 PCR primer design

Primers for β -actin and porcine IL-1 β were available for use within the department. The sequences for the primers used to isolate porcine IL-1 α were taken from Spagnuolo-Weaver *et al* [123]: The sequence for porcine IL-

1ra is known and the computer program MacVector was used to design primer pairs for isolation of IL-1ra, thereby avoiding adverse structural properties such as 'hairpin loops'.

Primer Information:

Table 1 Primers constructed for PCR

Target	Accession Number	Primer sequence (5' – 3')	Product size (bp)
IL-1 α	X52731	F:ACAGAAGTGAAGATGGCCAAAGTC R:TCATGTTGCTCTGGAAGCTGTATG	385
IL-1 β	M86725	F: TCATCGTGGCAGTGGAGAAGC R: TCTGGGTATGGCTTTCCTTAG	619
IL-1ra	L38849	F: CTTTCCTCCTTTTCCTGTTCCAC R: TGGTGACCTTGACGGCTGC	471
β -actin	U07786	F: CTCGGTCAGGATCTTCATGAGG R: TTCTACAATGAGCTGCGTGTGG	324

Primers were constructed by Oswel/Eurogentec SA (Oswel, Hampshire, UK).

They were received in dry pellet form and resuspended in sterile water.

Purified primer concentration was calculated using a spectrophotometer at 260nm ($\text{RNA } \mu\text{g}/\mu\text{l} = A_{260} \times \text{dilution factor} \times 0.04$). Despite numerous attempts with different primer pairs (an example of one primer set tried is given above)

and different annealing temperatures, no successful amplification of porcine IL-1ra was achieved.

6.2.18 Agarose Gel Electrophoresis

Once complete, the products were run on a 2% agarose gel to confirm that amplification of the correct sized product had occurred. Powdered agarose (Promega) was melted in 1 x TAE buffer (0.04M Tris-acetate/0.001M EDTA) in a microwave for 2 mins. 10mg/ml ethidium bromide (Sigma) was added to the gel to give a final concentration of 0.5µg/ml. The liquid gel was poured into a gel tray and allowed to cool. 15µl of PCR product was used for electrophoresis along with DNA markers (Promega) of known molecular sizes to allow size determination. For these experiments, PhiX174 DNA HAE marker (Promega, UK) was used at a concentration of 1µg/µl for all gels. 5µl of loading dye (type IV loading dye – 40% (w/v) sucrose in sterile water with 10 µg bromophenol blue) was added to each sample. Electrophoresis was carried out in 1 x TAE buffer at 90V for 20 – 60 mins. The negatively charged DNA migrated towards to anode and was separated on the basis of size. Visualisation of PCR products was carried out under UV light.

6.2.19 TA Cloning into Plasmid Vectors

TA Cloning provides a means of inserting a PCR product into a plasmid vector. Taq polymerase has a nontemplate-dependent activity that adds a single deoxyadenosine (A) to the 3' end of amplified PCR products. The

vector contains single 3' T-overhangs at its insertion site and therefore, the 3' A-overhangs of the PCR produce can be inserted into the vector. Fresh PCR products were used for all ligation experiments.

6.2.20 Transformation of DNA into bacteria

TOP 10 competent cells (Promega), an E. Coli bacterial strain, were used for all transformations. Transformation was according to manufacturers protocol. Briefly, 200 μ l cells were mixed with 1-2 μ l plasmid DNA. The cells were incubated on ice for 30 minutes, heat shocked at 42°C for 40 seconds and then incubated on ice for a further 2 minutes. 900 μ l of Luria-Bertani (LB) medium was added to each vial of cells at they were incubated at 37°C for 60 minutes in a shaking incubator. 100 μ l of each mixture was plated onto LB agar plates and incubated in a shaking incubator at 37°C overnight. Transformants were selected by antibiotic selection. LB agar plates were prepared containing, 25 μ g/ml of Kanamycin.

Blue/white colour screening was used for selection. The plasmid vector will produce β -galactosidase by α -complementation when transformed into bacteria after exposure to IPTG (β -D-isopropyl-thiogalactopyranoside). α -complementation is a process by which a functional β -galactosidase (LacZ) gene is generated when LacZ α -peptide (provided by the vector) complements the ω fragment of LacZ (provided by the bacteria). In the presence of X-gal (5-bromo-4-chloro-3-indoyl- β -galactopyranoside), cells with a plasmid but no DNA insert exhibit a blue colour and those with a DNA insert

exhibit a white colour (the LacZ gene is interrupted and α -complementation prevented).

6.2.21 Cloning PCR products

The reaction was set up according to manufacturers instructions. Briefly, the ligation reaction was as follows: 5 μ l sterile water, 1 μ l 10 X reaction buffer, 2 μ l pCR $\text{\textcircled{R}}$ 2.1 vector, 1 or 2 μ l PCR product, 1 μ l T4 DNA ligase (The total volume of the reaction was 10 μ l so where 2 μ l of PCR product was used, the volume of sterile water was reduced to 4 μ l). The ligation reaction was incubated at 14 $^{\circ}$ C overnight. The ligated vector was transformed into TA cloning one-shot competent cells (TOP 10 E.Coli). One vial of cells was used per ligation reaction. For each reaction, 1,2 and 3 μ l of ligation reaction was mixed gently with the cells. The cells were incubated on ice for 30 minutes, heat shocked at 42 $^{\circ}$ C for 40 seconds and incubated on ice for 2 minutes. 900 μ l of SOC medium was added to each vial of cells and incubated at 37 $^{\circ}$ C for 60 minutes with agitation. During this time, 25 μ l of X-Gal was spread onto previously poured LB agar plates containing Kanamycin. After incubation, 100 μ l of transformed cells were spread over each agar plates (one plate per transformation) and incubated overnight at 37 $^{\circ}$ C. White colonies were then chosen for plasmid isolation as they contained the cloned PCR product.

6.2.22 Plasmid DNA Miniprep

Once appropriate clones had been chosen, single colonies were used to inoculate 5mls of LB medium containing Kanamycin. This was then incubated overnight in a 15ml tube in a shaking incubator at 37°C. The protocol used for the Miniprep was the QIAprep Spin Miniprep Kit.

6.2.22.1 The QIAprep Spin Miniprep Kit

The protocol was followed according to the manufacturers instructions. In brief, 1ml of each overnight bacterial culture was pelleted in a microfuge tube by centrifugation at 8000rpm for 5mins. The supernatant was removed and the pellet resuspended in 250µl Buffer P1. To this, 250µl Buffer P2 was added and the microfuge tube gently inverted 4 – 6 times to mix. 350µl Buffer N3 was added and the tube inverted immediately 4 – 6 times. This was then centrifuged at room temperature for 10min at 13,000rpm. The supernatants were transferred to the QIAprep column by decanting or pipetting. These were centrifuged for 60sec at 13,000rpm and the follow through discarded. The column was washed by adding 0.5ml Buffer PB and centrifuging for 60sec (13,000rpm). A further wash was then performed by adding 0.75ml Buffer PE and centrifuging for 60 sec (13,000rpm). The follow through was again discarded and residual wash buffer removed by a further 60 sec centrifugation (13,000rpm). The QIAprep column was placed into a clean 1.5ml microcentrifuge tube. To elute DNA, 50µl of Buffer EB (10mM Tris.HCl, pH8.5) was added to each column. The column allowed to stand for 1min and

then centrifuged for 1 min (13,000rpm). The DNA sample obtained was then digested and analysed by agarose gel electrophoresis. The DNA was then stored at -20°C until further use. Details of the buffers used are given in Appendix A.4.

6.2.22.2 Restriction Digest of Plasmid

This was performed to ensure that the plasmid had incorporated the gene of interest. For the pCR2.1 vector, the Eco RI restriction enzyme cleaves either side of the insert site and therefore this enzyme was used for all digests. The reaction was set up as follows: 5µl nuclease free water, 2µl multi-core restriction enzyme 10X buffer; 2µl Acetylated bovine serum albumin (1 mg/ml); 10µl DNA sample; 1µl restriction enzyme (Eco RI). The reaction mixture was incubated at 37°C for 4h at 37°C. Once complete, 5µl of loading dye was added to each sample and the samples electrophoresed on a 2% (w/v) agarose gel.

6.2.23 Plasmid DNA Maxipreps

Maxipreps are used to isolate large quantities of DNA. The sample that had the brightest band on the gel after restriction digest was used for the Maxiprep procedure. Many different kit and non-kit based methods are available, for this section of work the EndoFree Plasmid Maxi Protocol (Qiagen) was used.

6.2.23.1 EndoFree Plasmid Maxi Protocol

This Maxiprep kit allows the isolation of endotoxin free plasmid DNA by using a Qiagen resin packed into a Qiagen tip. It allows the binding of plasmid DNA to an anion exchange resin. Proteins and RNA are removed and the DNA is eluted and concentrated and purified by iso-propanol precipitation. The protocol was carried out according to the manufacturers instructions.

In brief, 200µl of sample was added to 200ml of LB broth (containing 25µg/ml Kanamycin) and placed in shaking incubator at 37°C overnight. The bacterial cells were harvested by centrifugation at 6000-x g for 15min at 4°C, the supernatant discarded and the pellet resuspended in 10ml Buffer P1. The mixture was transferred into a 50ml falcon tube. 10ml Buffer P2 was added and mixed gently and thoroughly by inverting 4 – 6 times. This was then incubated at room temperature for 5 mins. 10ml of chilled Buffer P3 was added to the lysate, and mixed immediately by inverting 4 – 6 times. The lysate was poured into the barrel of the QIAfilter Cartridge and incubated at room temperature for 10mins. The cap from the outer nozzle was removed and the plunger inserted. The lysate was filtered into a 50ml falcon tube. 2.5ml of Buffer ER was added to the filtered lysate and mixed by inverting the tube 10 times. This was incubated on ice for 30 min. A QIAGEN-tip 500 was equilibrated by applying 10 ml Buffer QBT and the column allowed to empty by gravity flow. The filtered lysate was added to the QIAGEN tip and allowed to enter the resin by gravity flow. The tip was washed with 2X 30ml Buffer QC. The DNA was then eluted with 15ml Buffer QN into a glass endotoxin-

free tube and precipitated by adding 10.5ml room temperature isopropanol, it was then mixed and centrifuged immediately at 15,000g for 30 min at 4°C. The supernatant was decanted and the DNA pellet washed with 5ml of endotoxin-free room temperature 70% ethanol and centrifuge at 15,000g for 10 min. The supernatant was the decanted taking care not to disturb the pellet. The pellet was then air-dried for 5-10 min and the DNA then re-dissolved in 250µl of endotoxin-free Buffer TE. Details of the buffers are given in Appendix A.4

The yield of DNA was determined by spectrophotometry and run on a 2% (w/v) agarose gel. A restriction digest (see 2.13.4) was set up to confirm presence of the insert.

6.2.24 Analysis of mRNA content of tissue using the Real-Time Quantitative reverse transcription polymerase chain reaction (RT-PCR)

Reverse transcription polymerase chain reaction is the most sensitive method available for the detection and quantification of low-abundance mRNA. This technique enables the detection of small differences in gene expression between tissues. In this work, it was used to determine whether differences in the level of IL-1 α and IL-1 β levels in the vessel wall following balloon angioplasty or stenting could be identified. Following RT-PCR, two quantification strategies, either absolute or relative can be employed. In absolute quantification, the absolute mRNA copy number per reaction is determined by comparison with external calibration curves. This allows

comparisons between reactions carried out on different days or with different reagents. The relative expression is based on the expression ratio of a target gene to a reference gene and enables investigation of physiological changes in gene expression levels. Relative expression explains trends but results will depend upon the reference gene and the normalization procedure used. One draw back of quantification using relative expression ratios is that it only allows comparison of one sample with the reference gene. A new software tool REST© (relative expression software tool), has been developed that allows for comparison of two sample groups, with up to 16 data points in the sample and control group, and tests the group differences for significance with a newly developed randomisation test [124].

Total RNA was extracted using the commercially available RNeasy mini kit (Qiagen) (see 6.2.14). In each case on column DNA digestion was carried out using the RNase-free DNase set (Qiagen) to prevent carryover of contaminating genomic DNA to the PCR reaction. Concentration of total RNA was determined by measuring the absorbance at 260nm in a spectrophotometer. For each sample, 500ng total RNA was reverse transcribed to cDNA using the commercially available Superscript III kit (Invitrogen) with random hexamers as primers according to the manufacturers instructions. For each sample, an 'RT minus' control reaction was carried out in parallel. cDNA / 'RT minus' samples were then diluted 1:10 with water and stored at -20 °C for later use. Primers were designed for the genes of interest and housekeeping genes using the commercially available molecular biology program MacVector (version 7.1.1). Primer parameters were as follows:

product size 75-150 base pairs; primer length 18-30 base pairs; primer GC content 30-70 % and primer Tm 55-80 ° C (Accession numbers: Pig IL-1 alpha, X52731; Pig IL-1 beta, M86725; Human 18SrRNA, K03432). There is only a partial sequence in the database for Pig 18SrRNA. However such is the homology between 18SrRNA sequences across species that primers designed to the human 18SrRNA sequence were found to work well on Pig total RNA.

Primer sequences:

Table 2 Primers used for Real-Time PCR

Target	Accession number	Primer sequence (5' – 3')	Product size (bp)
Pig IL-1 α	X52731	F:CCTCTAAGACATCCAGGCTAACTTC R: CTTCCAGGTCGTCATCGGTG	385
Pig IL-1 β	M86725	F: TGAAGAATCCCTCCTCCCAGG R: GGCATCACAGACAAAGTCATCATTG	617
Human 18SrRNA	K03432	F:ACACGGACAGGATTGACAGATTGATAG R: ATGCCAGAGTCTCGTTCGTTATCG	122

Primers were synthesized and HPLC purified commercially (Sigma-Genosys). All PCR reactions were carried out in an iCycler (Bio-Rad) using SYBR Green I (Molecular Probes) as the fluorescent dye. Triplicate 20 μ l reactions were

carried out for each sample using the commercially available iQ Supermix (Bio-Rad). Thermal cycling parameters were as follows:

Step	Temperature (°C)	Time (sec)
1	95°C	180 (Hotstart)
2	95 °C	30 (Denaturation)
3	repeat step 2 for 40 cycles	
4	60 °C	30 (Annealing/Extension)
5	95°C	30 (Melt curve analysis)
6	50 °C	30
7	50 °C	10
8	repeat step 7 90 cycles and add 0.5 °C every 10 seconds	

In order to validate primer sets for amplification efficiency and specificity prior to use on biological samples, genes of interest were subcloned into a plasmid vector according to standard molecular biological techniques; pCR 2.1 (Invitrogen) for Pig IL-1 alpha and beta (see 6.2.20) and pGEM-T Easy (Promega) for Human 18SrRNA. Restriction digests and direct sequencing in each case confirmed successful subcloning. Plasmids were linearised by the use of a single cutting restriction enzyme ensuring the single site was outside the subcloned region. Linearised plasmids were purified using the commercially available PCR purification kit (Qiagen) and a ten fold dilution series was generated. The specific primer sets were tested against the ten fold dilution series of the corresponding plasmid and by plotting the threshold cycle (Ct) against the log of the initial starting concentration a standard curve

was generated whose slope gives the amplification efficiency by the equation:

$$E (\%) = (10^{(-1/\text{slope})} - 1) \times 100.$$

All 3 primer sets gave a single peak on melt curve analysis implying that only one product was being amplified and thereby confirming the specificity of the reaction. Amplification efficiencies were as follows: Pig IL-1 alpha E = 93.1% (correlation coefficient = 0.998); Pig IL-1 beta E = 101.7% (correlation coefficient = 0.998); Human 18SrRNA E = 95.0% (correlation coefficient = 1.000). Having validated the specific primer sets on plasmid cDNA they were then used on tissue cDNA samples to generate data. Each run contained an RT minus control for each sample and a no template control for each primer set. Data was collected as the mean of the cycle threshold (Ct) for triplicate reactions on each sample +/- S.E.M.

6.2.25 Quantitative Real time polymerase chain reaction

These experiments were performed to see if changes in IL-1 mRNA levels could explain the 'catch-up' phenomenon seen following cessation of the IL-1ra treatment. Tissue was obtained following stenting; RNA extracted and off IL-1 α and IL-1 β levels in the vessel wall determined using quantitative RT-PCR. IL-1ra treatment was compared with vehicle treatment following 14-day and 28-day infusions and also a further two groups of animals were compared, one group that received IL-1ra for 14-days and was sacrificed at 17 days and the other that received IL-1ra for the full 17-days. Quantification was carried out relative to an untreated control sample and normalized to

18SrRNA levels as previously described using the equation: $2^{-\Delta\Delta Ct}$ where $\Delta Ct = Ct(\text{target gene}) - Ct(\text{housekeeping gene})$ and $\Delta\Delta Ct = \Delta Ct(\text{treated sample}) - \Delta Ct(\text{untreated sample})$. Statistical analysis was performed using REST© software.

6.3 RESULTS

6.3.1 Protein assay

The first approach to quantify IL-1 levels in the vessel wall after stenting used Western Blotting. A protein assay was performed to ensure that equal concentrations of protein were loaded into each well for each Western blot. This enabled meaningful comparisons to be made between samples. Figure 44 shows an example of a Bovine serum albumin standard curve obtained. The total concentration of protein in each sample was then determined from the standard curve and a known amount of protein loaded into each well for the Western blot.

6.3.2 Detection of protein levels – Western blots

Western blotting was performed to see if a difference in protein levels between the animals that received IL-1ra for 14-days and were killed at 17-days and those that received an IL-1ra infusion for the full 17-days could be detected. Figure 45a (blot for IL-1 β) is an example of a blot obtained. As it can be seen, no IL-1 β protein was detected in any of the samples analysed. In all cases, the positive control alpha tubulin was present (see Figure 45b). Blots were performed, using the protein samples extracted from all the animals studied, unfortunately, despite good protein yields, and loading of 50 μ g total protein on the gel, no IL-1 was detected.

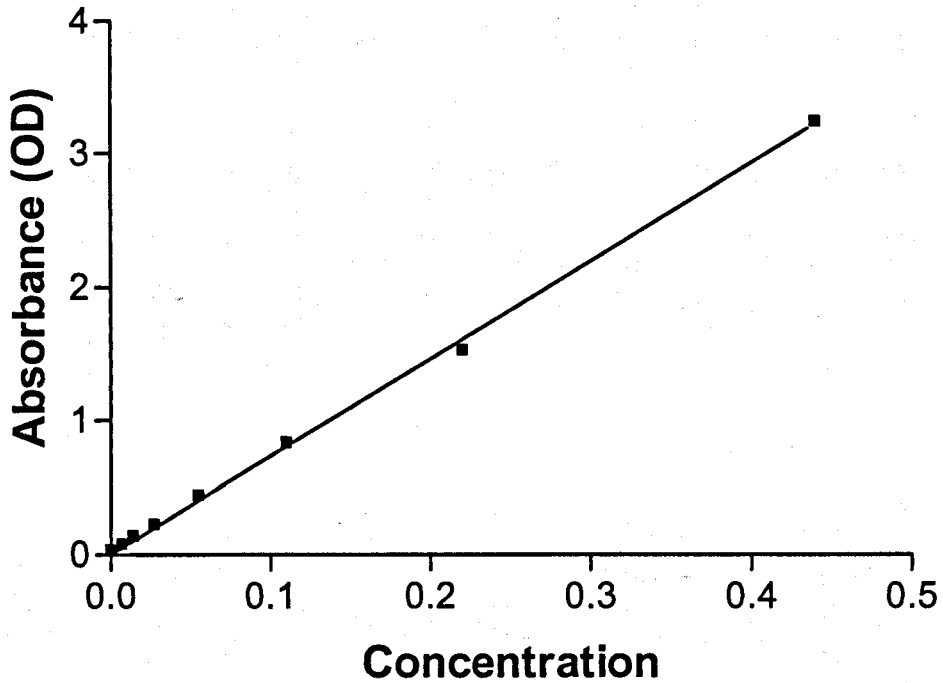
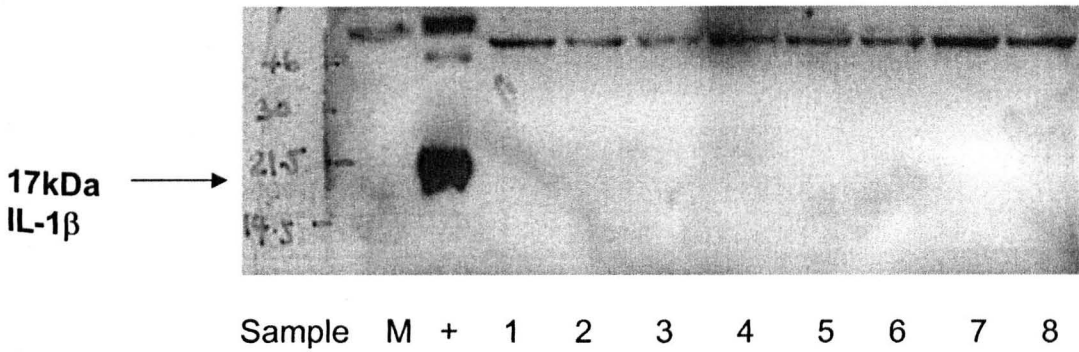


Figure 44 An example of a standard curve obtained using the Pierce MicroBCA™ protein assay

Protein standards were bovine serum albumin.

a



b

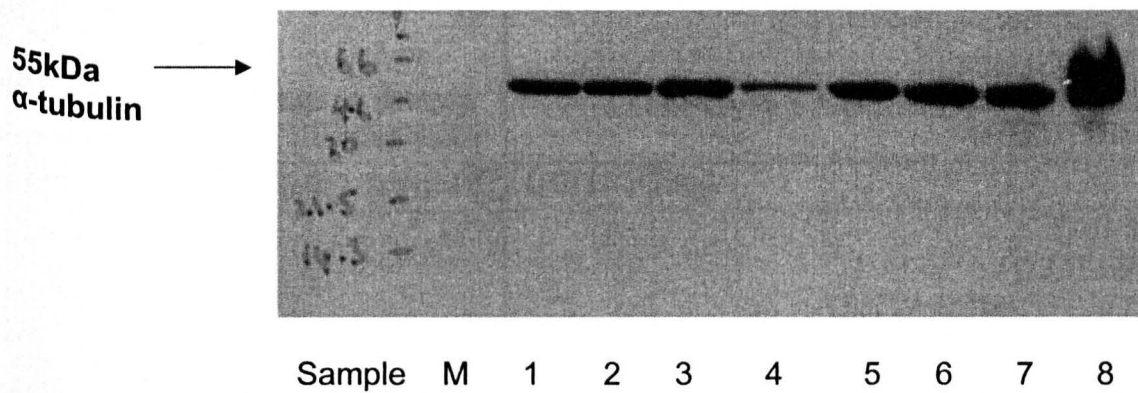


Figure 45 Independent Western blots for (a) IL-1 β , 17kDa and (b) loading control α -tubulin, 55kDa (each blot is representative of n=3)

M represents molecular weight markers not clearly visible after reproduction but marked on the left hand side of the blot. In (a) lane + is porcine recombinant IL-1 β (100ng/ml), lanes 1 – 7 are samples (JG767 LAD, JG767 RCA, JG768 LAD, JG 768 RCA, JG769 LAD, JG769 RCA, JG770 LAD). In (b) Lane 8 is the positive control, lanes 1 – 7 are samples (JG767 LAD,

JG767 RCA, JG768 LAD, JG 768 RCA, JG769 LAD, JG769 RCA, JG770 LAD), where JG767 and JG769 were 14d infusion, 17d harvest and JG768 and 770 were 17d infusion, 17d harvest).

6.3.3 RT-PCR, cDNA amplification and TA cloning of porcine IL-1alpha

In order to validate primer sets for amplification efficiency and specificity prior to use on biological samples, segments of the genes of interest were subcloned into a plasmid vector according to standard molecular biological techniques; pCR 2.1 (Invitrogen) for Pig IL-1 alpha and beta (see 6.2.21) and pGEM-T Easy (Promega) for Human 18SrRNA. Restriction digests and direct sequencing in each case confirmed successful subcloning. Plasmids were linearised by the use of a single cutting restriction enzyme ensuring the single site was outside the subcloned region. Porcine IL-1 β had previously been subcloned and was available for use within the department. Figure 46 shows the amplification of porcine IL-1 α mRNA from porcine vascular smooth muscle cells. Once the cDNA had been isolated, a miniprep was used to amplify the gene (Figure 47a). The gene of interest was then sent for sequencing. Once this had confirmed successful cloning, a maxiprep was performed to obtain large amounts of the gene of interest for use in the Real-Time PCR experiments (Figure 47b).

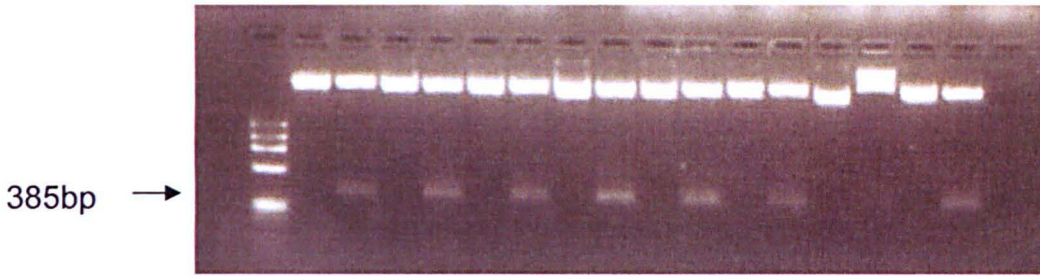


Figure 46 Amplification of porcine IL-1 α from porcine vascular smooth muscle cells (VSMC)

Lane 1 shows the marker. Lanes 2,3 and 5 show the loading controls (in this case β -actin, product size 324bp) extracted from porcine coronary artery (lanes 2 and 3) and porcine VSMC (lane 5). The negative controls are shown in lanes 4 and 7. When specific IL-1 α primers are used, IL-1 α is successfully isolated from porcine unstimulated VSMC (lane 10, product size 385bp) but not from porcine coronary arteries (Lanes 8 and 9). Lane 6 was left blank.

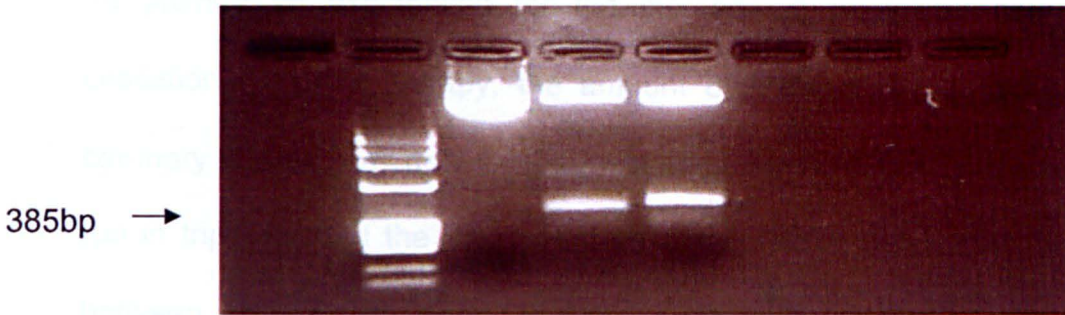
maxiprep culture. (b) Restriction digest of the maxiprep with EcoRI. Lane 1, no digest, lanes 2 and 3 show EcoRI restriction and an insert at 385bp.

a



Sample M 1 2 3 4 5 6 7 8 9 10 11 12 13 14 15 16

b



Sample M 1 2 3

Figure 47 Minipreps of IL-1 α cDNA from porcine VSMCs

(a) Amplification of IL-1 α cDNA is shown in even lanes and control amplifications in odd lanes. There is good amplification from all cultures apart from lane 14. From these, the 2 brightest bands were chosen, in this case from lanes 8 and 10 and these clones were then used for inoculation of the maxiprep culture. (b) Restriction digest of the maxiprep with EcoR1. Lane 1, no digest, lanes 2 and 3 show EcoR1 restriction and an insert at 385bp.

6.3.4 Extraction of RNA from porcine coronary arteries

RNA was extracted from each piece of coronary artery as described in 6.2.13. Concentration of total RNA was determined by measuring the absorbance at 260nm in a spectrophotometer. Values obtained ranged from 4 – 300µg/ml. Once extracted, the RNA was stored at -20°C until further use.

6.3.5 Real-time PCR

To provide an explanation for the increase in neointima seen following cessation of IL-1ra therapy, the amount of IL-1 α and β mRNA in porcine coronary vessels was determined by quantitative RT-PCR. Each sample was run in triplicate and the mean of the values obtained used for comparisons between groups. Comparison was made using REST[®]. 18srRNA was chosen as the housekeeping gene. As SyBr green is a non-specific fluorescent dye, i.e. binds to all DNA, specificity of the primers was confirmed by melt-curve analysis (Figure 48). Having confirmed that for all primers, a single product was obtained, the samples were then analysed. Using this technique, no difference in the IL-1 α or IL-1 β levels could be detected between animals implying that at the time-point studied, early cessation of IL-1ra therapy had no significant effect on the total levels of IL-1 α and IL-1 β (mean expression ratios 1.966 and 1.307, $p = 0.41$ and $p = 0.67$ respectively, see Figure 49).

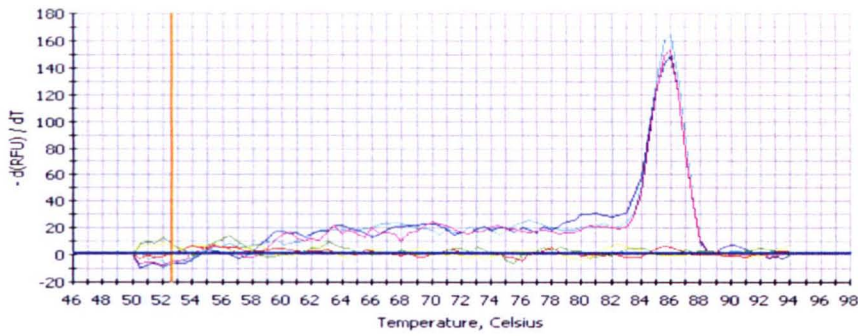
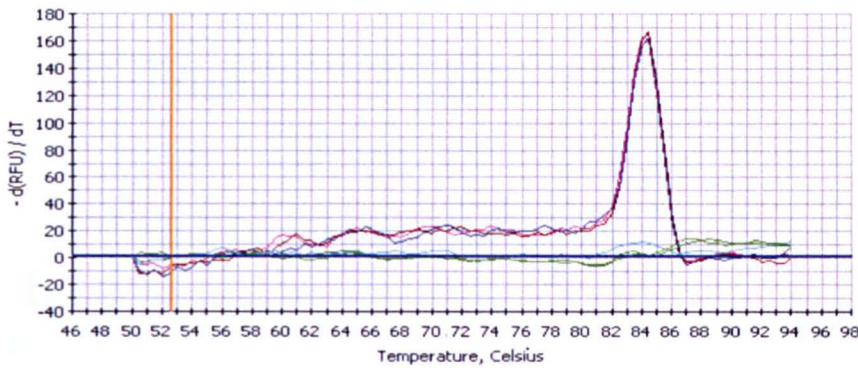
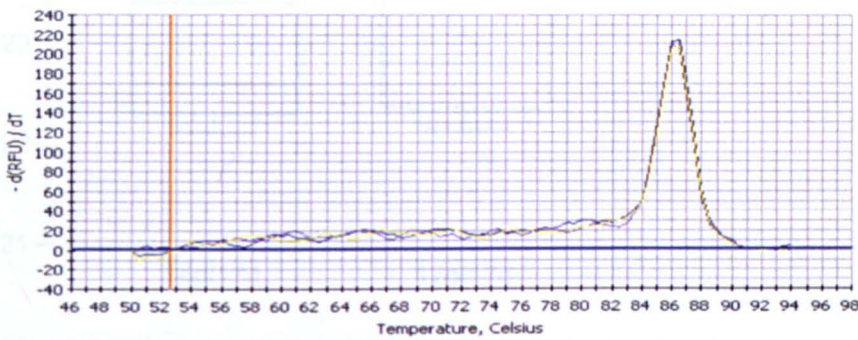
a**b****c**

Figure 48 Melt curves generated during qRT-PCR

(a) pIL-1 α , (b) pIL-1 β , (c) h18srRNA. Note: one single PCR species (ie 1 peak) in each case.

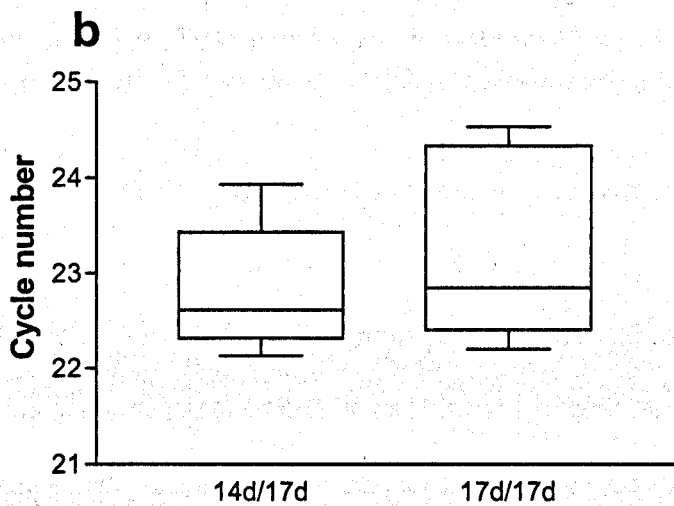
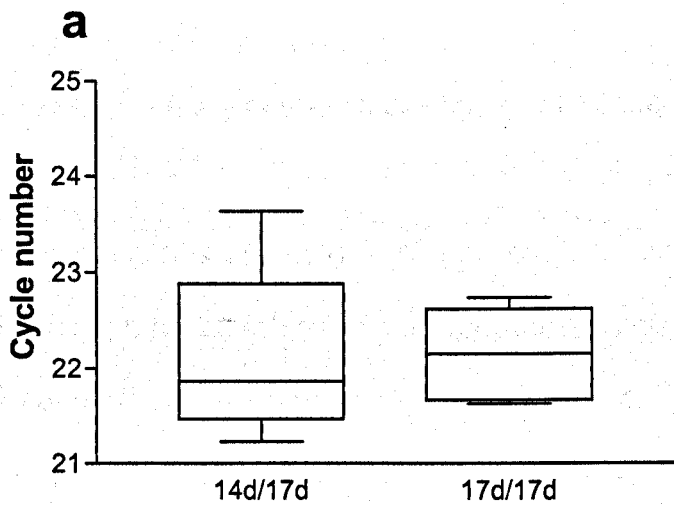


Figure 49 Box and whisker plots showing the effect of IL-1ra therapy on vessel wall (a) IL-1 α mRNA and (b) IL-1 β mRNA levels

Total IL-1 levels in the vessel wall were determined by quantitative RT-PCR and plotted as cycle number (minus 18SrRNA (housekeeping gene)).

6.4 DISCUSSION

6.4.1 Summary of findings

When IL-1ra therapy was discontinued at 14 days, there was a rebound in neointima formation following stenting. In order to try and explain this, it was hypothesised that the IL-1ra infusion could be not only inhibiting IL-1 signalling but also inhibiting IL-1 production, and that discontinuation of the IL-1ra around 14-days was associated with a rebound production of IL-1.

Analysis of protein expression and mRNA levels for IL-1 α and β 3 days after IL-1ra discontinuation at 14-days (in this case by removal of the pumps) did not indicate any such increased levels. The cause of the rebound production in the neointima is still under investigation.

6.4.2 Detection of protein levels – Western Blotting

No increase in IL-1 at the protein level was detected by Western blotting. There are several possible explanations for this. First, IL-1 expression in the vessel wall is likely to be constitutively low. Levels within the vessel wall may be below the lowest level of detection even when up-regulated. Second, following death, it takes an unavoidable amount of time (at least 10 mins) to explant the heart and remove the vessel and stent. Due to this, protein degradation before snap freezing has to be considered as a potential source of sample loss. Third, IL-1 release and/or altered processing mechanisms

may result in cytokine loss into the circulation or alterations in protein structure that the current analysis systems fail to detect.

6.4.3 Detection of mRNA

The time-point of three days post cessation of IL-1ra therapy was chosen to allow five drug half-lives to pass and then to allow 24 hours for rebound production of IL-1 to occur. No differences in levels of either IL-1 α or IL-1 β mRNA at the time-points studied were detected. IL-1 mRNA is known to be unstable and it is likely that due to sample processing, some IL-1 mRNA degraded hence any differences in levels could not be detected. It is also worth considering that the wrong time-point may have been studied and that either an earlier or later time-point should have been considered.

Unfortunately, this model does not easily allow for sampling at different time-points. Another reason for failure to detect a difference in mRNAs is that perhaps the focus should be on other cytokine or processing molecules e.g. Caspase-1. In addition, molecules further downstream in the signalling cascade such as IL-6 or IL-8 may be up-regulated along with up-stream molecules such as PDGF.

6.4.4 REST© software analysis

Relative expression is used in the analysis of results obtained in real-time PCR. The expression of the target gene is standardised by a non-regulated reference gene. The relative expression software tool (REST©) is novel in

that it allows a comparison of two groups, with up to 16 samples in both the sample and control group and up to four target genes. The mathematical model used is based upon the PCR efficiencies (E) and the mean crossing point deviation between the sample and control group (ΔCP). The expression ratio obtained is then tested for significance by a randomisation test.

6.5 Conclusions and future directions

The data presented so far does not support the hypothesis that the increase in neointima formation following cessation of IL-1ra therapy is caused by a rebound increase in IL-1 production. Unfortunately the porcine model does not allow for the sampling of multiple time-points in multiple animals and therefore, the possibility that IL-1 mRNA would have been altered at earlier or later times following IL-1ra discontinuation cannot be excluded. Further work is needed to determine the molecular basis of the catch-up seen.

Unfortunately, real-time PCR is the most sensitive technique available to detect changes in mRNA levels. If the sample degradation is the cause of our inability to see significant changes in IL-1 mRNA levels then studying different time-points using the same technique are unlikely to be successful. An earlier (18h) or later time-point of 48-hours will be studied and we shall also look for the up-regulation of other molecules such as IL-1 signalling intermediates IL-6 or PDGF to see if any difference in expression can be detected.

CHAPTER 7

CONCLUSIONS AND FUTURE WORK

This work has shown that antagonism of IL-1 by IL-1ra inhibits neointima formation after coronary artery injury and stenting in a porcine model. In the case of PTCA, IL-1ra resulted in a 23% decrease in neointima area, independent of the length of IL-1ra therapy. In the case of stenting, IL-1ra inhibited neointima formation for the duration of the infusion, but after cessation of the infusion around 14 days, there was a 'catch-up' phenomenon, with a 34% larger neointima in IL-1ra treated arteries than vehicle. The mechanism for this difference in effect of IL-1ra has yet to be explained.

IL-1ra is a large protein with inhibitory properties upon the Type 1 IL-1 receptor. Agonistic IL-1 cytokines signal inflammatory events via this receptor, which is blocked by IL-1ra. In general terms, IL-1ra blocks new IL-1 signalling events over the Type 1 receptor, rather than acting by competitive displacement binding. Blockade of the Type 1 IL-1 receptor is the only known anti-inflammatory property of IL-1ra [125]. Thus, the data presented here, which show a powerful modulatory effect upon the neointimal response to injury, are conclusive evidence that IL-1 has a critical role in this process.

IL-1, together with TNF and complement, in a variety of complex inflammatory models, processes and diseases are viewed as having an apical position in

the signalling cascade that produce the multiplicity of effects seen in these situations. This apical position indicates not only the relative importance of these agents (i.e. lack of redundancy) but is also proven when they are antagonised. A notable example would be the inhibition of TNF α and IL-1 in rheumatoid arthritis [126]. The results reported here suggest that IL-1 may have a crucial position in the arterial response to injury.

There are multiple potential sources of IL-1 at the time of arterial injury. Adherent platelets may produce IL-1, as well as the recruited inflammatory cells. In addition endothelial cells, which re-grow and cover the site of injury may also produce IL-1. IL-1 has many inflammatory effects upon endothelial cells and vascular smooth muscle cells, plausibly associated with neointima formation and notable amongst these is the autocrine induction of PDGF by vascular smooth muscle cells [3].

As already discussed, the pig is a commonly used model for studies such as these however; a recurring criticism of such studies concerns the validity of animal models. Animal models contribute significantly to the assessment of safety of a stent/drug combination, but efficacy is more contentious. These models lack atherosclerosis, and rely upon *de novo* growth of neointima arising from intervention in an undiseased artery. In their favour, microscopic examination of this neointima is reassuring – it is histologically indistinguishable from that seen in human restenotic tissue obtained at necropsy or atherectomy. Another disadvantage with animal models is that they employ juvenile subjects which grow significantly during the course of the

experiment under the influence of a growth hormone milieu which is likely to be significantly different from that seen in a middle aged human subject. Finally, of course, are the inevitable genetic differences. Here, the pig model scores highly because of the well-known similarities between the pig genetic constitution and man. A useful paradigm is rapamycin. When rapamycin-loaded stents were tested in a porcine coronary artery model, the effect upon in-stent neointima formation was not as dramatic as the results from the first human studies where restenosis was reduced to 0%. The magnitude of inhibition of neointima response found in our studies is in keeping with that study and therefore may indicate an important and potentially useful clinical effect.

In the clinical setting, it is not realistic to administer IL-1ra by continuous subcutaneous infusion. This would necessitate long inpatient hospital stays and would be uncomfortable and difficult for patients to manage. In the animal study performed, the IL-1ra was delivered using mini-osmotic pumps. Complications attributed to subcutaneous administration of other fluids, include tissue necrosis at the infusion site, cellulitis, abscess formation and even gas gangrene. Although these complications are rare nowadays (because of improved aseptic techniques), they remain a potential problem with prolonged infusion. In reality, the administration of continued IL-1ra for treatment of in-stent restenosis will require the development of a stent-based delivery system. The intravenous bolus of IL-1ra administered at the start of all of the experiments performed in this work could still be administered to a patient with an acute coronary syndrome on arrival to hospital, either

immediately before transfer or on arrival to the catheter laboratory. However, before IL-1ra on a stent can be considered we need to look carefully at mechanism of any rebound effect. It may be that the timing is such that IL-1ra is required for months.

The strength of using a coated stent as the carrier for an anti-restenosis agent is the ability to achieve a high local concentration of potent therapeutic, exactly where it is required, whilst using a tiny total quantity of drug, thereby avoiding any systemic side effects. When designing a drug-eluting stent, the polymer to which the drug is attached is of paramount importance. In order to achieve local delivery, a drug must be loaded onto a delivery platform that allows its controlled release. The polymer must, amongst other properties, have the capacity to allow drug uptake and release, be inert to prevent an adverse reaction and be able to withstand the rigours of sterilisation and stent deployment. Several different agents have already been shown to fulfil these and other criteria, including, phosphorylcholine (used for dexamethasone elution) and chondroitin sulfate and gelatin (used for paclitaxel elution).

The therapeutic implications of these results are at least two fold. First, there can be little doubt that IL-1ra is a potential therapeutic agent for the treatment of proliferative vascular responses. The potential application of such an anti-inflammatory treatment is clearly of some excitement in the context of coronary artery disease, which is now viewed as an inflammatory process both in terms of atherogenesis and mechanisms of disease presentation. Secondly, these results suggest that examination of the duration of such

therapy will be crucial for its success. The duration of the healing response and neointima following stent implantation is still imprecisely understood but clinical studies as well as experience suggest that the process may continue up to 9 months [69]. We can only speculate upon what the duration of IL-1ra would need to be for clinical utility, but by analogy with cytostatic stent based delivery, many weeks may be needed.

To use IL-1ra as a treatment strategy for humans, further work must be performed to determine the mechanism of catch up seen following cessation of therapy. Unlike TNF- α or other pro-inflammatory cytokines, the IL-1 signalling pathway is complex and regulated at many levels. Pro-IL-1 β is released from vascular cells via an as yet largely unknown, possibly P2X7 dependent mechanism. On its release it is cleaved by Caspase-1 into mature IL-1 β and then signals via the type-1 receptor. Signalling via the receptor leads to up-regulation of other pro-inflammatory cytokines. This work has only investigated up-regulation of IL-1 α and IL-1 β in the vessel wall. As no difference has been seen, further work will focus on other RNAs, for example, endogenous porcine IL-1ra or other IL-1 signalling intermediaries such as soluble IL-1 R-associated kinase-4 (IRAK-4) or PDGF. The work presented failed to detect any IL-1 protein in the vessel wall after stenting. This seems unlikely, as following angioplasty IL-1 protein levels are detectable. A failure to detect any IL-1 protein in this case is likely to be secondary to processing difficulties and more work is needed to refine this technique. Better antibodies for IL-1 detection may also be required.

It is not surprising that the action of IL-1 and hence the mode of delivery of IL-1ra may need to be different in the case of PTCA and stent. There is a major physical difference between the two interventions in that following stent insertion, the metal is left in situ. Compare this to balloon angioplasty where the balloon is inflated and then deflated, removing the inflammatory stimulus. Chronic stretch itself may be driving the prolonged inflammatory stimulus. The effect of stretch on up-regulation of inflammatory cytokines in the context of coronary stenting also needs further work.

The long time point studied in this work with 28 days of IL-1ra therapy and vessel harvesting at 90 days shows that suppression of neointima is maintained. It therefore seems likely that in the pig model, 28 days of drug is enough to inhibit the chronic inflammation induced by the stent struts and to prevent the rebound effect previously seen with cessation of IL-1ra therapy.

Questions exist as to the comparability between human and animal studies. The stages of healing in the two are very similar however they differ in the temporal response, which is prolonged in humans. The life span of a human is more than 70 years, compared with a pig lifespan of 16 years. Differential rates of healing may be proportional to longevity [127]. Caution must therefore still exist as the negative results seen in the pig with Sirolimus and Paclitaxel at 90 days mean that long term follow up in the human is imperative as it may take years for any catch up to be seen.

Further work is also planned to determine whether IL-1ra can be delivered from a stent platform. IL-1ra differs from the cytostatic agents in use in that it is a protein and therefore susceptible to alterations in both structure and activity by changes in conditions such as temperature. The combination of such a molecule with a polymer may reduce its biological activity or render it inert. Initial experiments will focus on combining IL-1ra with a polymer and then demonstrating that in combination, IL-1ra will still bind to IL-1R1. In order to do this, a combination of IL-1ra and a drug-delivery polymer will be attached to a BIAcore sensor chip and then IL-1R1 flowed over the chip to determine whether binding still occurs.

If the IL-1ra can be combined with a polymer and still bind to the IL-1R1 then the next step will be to determine whether it has maintained its inhibitory activity. To do this, a skin bioassay will be used. A stent will be coated in IL-1ra and polymer and then small sections of that stent placed under the skin of a pig. Intradermal injections of IL-1 β will be performed on top of the stent and neutrophil recruitment assessed.

Delivery of agents from a stent-based system can be manipulated by altering the properties of the polymer to achieve a slow or fast release of drug. Stents can be 'top-coated' to delay drug delivery. Making the polymer more hydrophobic prolongs the time over which a drug is eluted. As IL-1ra is highly water soluble, it is almost certain that some form of topcoat will be necessary.

If IL-1ra can be successfully bound to a polymer and maintain its inhibitory activity, subsequent experiments will involve using the porcine model to determine whether stent-based delivery of IL-1ra is as potent an inhibitor of restenosis as systemic delivery. A consensus group has recently produced guidelines for the evaluation of drug-eluting stent in preclinical studies [128]. Suggested requirements from the document include, *in vitro* and *in vivo* pharmacokinetics of drug delivery, dose justification and then the use of animal models to determine efficacy. The use of either a pig model or a rabbit iliac artery model is suggested with appropriate controls to include bare-metal stents and coating only. The effect of overlapping stents must be evaluated and stent efficacy assessed by absent thrombosis and neointimal reduction. Time points to be assessed include an early one, i.e. 3 or 7 days, 28-days and a late time-point at 3 or 6 months. Necropsy evaluation must be performed and all unexpected and premature deaths studied. Arteries should be perfusion fixed and details of the detailed histopathologic and histomorphometric analyses required are given. Although intended only as a guide, it is likely that all the information requested will be necessary to fully evaluate any new drug-eluting stent.

In conclusion, IL-1ra has beneficial effects upon the coronary artery response to injury. Following PTCA, it results in 23% less neointima formation and following stenting, results in > 35% less neointima for the duration of the infusion. If the infusion is continued for 28 days and the vessels harvested at 90 days then unlike the cytostatic agents studied, neointima formation remains suppressed. The results obtained indicate that the duration of such

therapy needs to be for 28 days. The work presented here, shows for the first time that a purely anti-inflammatory agent can be used to modulate the porcine coronary artery response to injury. This agent causes prolonged inhibition of neointima formation at 90 days, unlike Sirolimus and Paclitaxel. Potential therapeutic use of this agent to modify vascular proliferative responses in the human, specifically to prevent restenosis following intracoronary stenting looks promising and further work is underway to determine whether this work (using a porcine model) translates into an effective treatment for man.

REFERENCES

1. Gresham, *Atherosclerosis: controversial aspects*. Hospital update, 1986: p. 765-768.
2. Timmis AD, N.A., *Essentials of Cardiology*. 1993: Blackwell, Oxford.
3. Ross, R., *Atherosclerosis--an inflammatory disease*. N Engl J Med, 1999. **340**(2): p. 115-26.
4. Glass, C.K. and J.L. Witztum, *Atherosclerosis. the road ahead*. Cell, 2001. **104**(4): p. 503-16.
5. Ross, R., *The pathogenesis of atherosclerosis: a perspective for the 1990s*. Nature, 1993. **362**(6423): p. 801-9.
6. Glagov, S., et al., *Compensatory enlargement of human atherosclerotic coronary arteries*. N Engl J Med, 1987. **316**(22): p. 1371-5.
7. Diaz, M.N., et al., *Antioxidants and atherosclerotic heart disease*. N Engl J Med, 1997. **337**(6): p. 408-16.
8. Zhang, S., I. Day, and S. Ye, *Nicotine induced changes in gene expression by human coronary artery endothelial cells*. Atherosclerosis, 2001. **154**(2): p. 277-83.
9. Calles-Escandon, J. and M. Cipolla, *Diabetes and endothelial dysfunction: a clinical perspective*. Endocr Rev, 2001. **22**(1): p. 36-52.
10. Libby, P., D. Egan, and S. Skarlatos, *Roles of infectious agents in atherosclerosis and restenosis: an assessment of the evidence and need for future research*. Circulation, 1997. **96**(11): p. 4095-103.
11. Falk, E. and A. Fernandez-Ortiz, *Role of thrombosis in atherosclerosis and its complications*. Am J Cardiol, 1995. **75**(6): p. 3B-11B.

12. Vilcek, *The Cytokines: An Overview*. The Cytokine Handbook, ed. D. CA. Vol. 3. 1998: Academic Press Limited. 1-20.
13. Aarden, L.A., Brunner, T.K., Cerottini, J.-C., Dayer, J.-M., de Weck, A.L., Dinarello, C.A., Di Sabato, G., Farrar, J.J., Gery, I., Gillis, S., Handschumacher, R.E., Henney, C.S., Hoffmann, M.K., Koopman, W.J., Krane, S.M., Lachman, L.B., Lefkowitz, I., Mishell, R.I., Mizel, S.B. and Oppenheim, J.J., *Revised nomenclature for antigen-nonspecific T cell proliferation and helper factors*. J. Immunol., 1979. **123**: p. 2928-2929.
14. Dinarello, *Chapter 3, Interleukin-1*. 3rd ed. The Cytokine Handbook, ed. T. A. 1998: Academic Press Limited.
15. Stevenson, F.T., et al., *Interleukin 1: the patterns of translation and intracellular distribution support alternative secretory mechanisms*. J Cell Physiol, 1992. **152**(2): p. 223-31.
16. Black, R.A., et al., *Generation of biologically active interleukin-1 beta by proteolytic cleavage of the inactive precursor*. J Biol Chem, 1988. **263**(19): p. 9437-42.
17. Ghezzi, P., et al., *Hypoxia increases production of interleukin-1 and tumor necrosis factor by human mononuclear cells*. Cytokine, 1991. **3**(3): p. 189-94.
18. Schindler, R., J.A. Gelfand, and C.A. Dinarello, *Recombinant C5a stimulates transcription rather than translation of interleukin-1 (IL-1) and tumor necrosis factor: translational signal provided by lipopolysaccharide or IL-1 itself*. Blood, 1990. **76**(8): p. 1631-8.

19. MacKenzie, A., et al., *Rapid secretion of interleukin-1beta by microvesicle shedding*. *Immunity*, 2001. **15**(5): p. 825-35.
20. Gabay, C., et al., *Interleukin 1 receptor antagonist (IL-1Ra) is an acute-phase protein*. *J Clin Invest*, 1997. **99**(12): p. 2930-40.
21. Wilson, H.L., et al., *Secretion of intracellular IL-1 receptor antagonist (type 1) is dependent on P2X7 receptor activation*. *J Immunol*, 2004. **173**(2): p. 1202-8.
22. Sims, J.E., S.L. Painter, and I.R. Gow, *Genomic organization of the type I and type II IL-1 receptors*. *Cytokine*, 1995. **7**(6): p. 483-90.
23. Stylianou, E., et al., *Interleukin 1 induces NF-kappa B through its type I but not its type II receptor in lymphocytes*. *J Biol Chem*, 1992. **267**(22): p. 15836-41.
24. Wesche, H., et al., *The interleukin-1 receptor accessory protein (IL-1RAcP) is essential for IL-1-induced activation of interleukin-1 receptor-associated kinase (IRAK) and stress-activated protein kinases (SAP kinases)*. *J Biol Chem*, 1997. **272**(12): p. 7727-31.
25. Greenfeder, S.A., et al., *Molecular cloning and characterization of a second subunit of the interleukin 1 receptor complex*. *J Biol Chem*, 1995. **270**(23): p. 13757-65.
26. Colotta, F., et al., *Interleukin-1 type II receptor: a decoy target for IL-1 that is regulated by IL-4*. *Science*, 1993. **261**(5120): p. 472-5.
27. Gallis, B., et al., *IL-1 induces rapid phosphorylation of the IL-1 receptor*. *J Immunol*, 1989. **143**(10): p. 3235-40.

28. Wang, A.M., M.V. Doyle, and D.F. Mark, *Quantitation of mRNA by the polymerase chain reaction*. Proc Natl Acad Sci U S A, 1989. **86**(24): p. 9717-21.
29. Shimokawa, H., et al., *Chronic treatment with interleukin-1 beta induces coronary intimal lesions and vasospastic responses in pigs in vivo. The role of platelet-derived growth factor*. J Clin Invest, 1996. **97**(3): p. 769-76.
30. Galea, J., et al., *Interleukin-1 beta in coronary arteries of patients with ischemic heart disease*. Arterioscler Thromb Vasc Biol, 1996. **16**(8): p. 1000-6.
31. Chamberlain, J., et al., *Temporal and spatial distribution of interleukin-1 beta in balloon injured porcine coronary arteries*. Cardiovasc Res, 1999. **44**(1): p. 156-65.
32. Recktenwald JE, M.L., Huber TS,, *Direct evidence for cytokine involvement in neointimal hyperplasia*. Circulation, 2000. **102**: p. 1697-1702.
33. Laughlin, M.J., et al., *Hematopoietic recovery following high-dose combined alkylating-agent chemotherapy and autologous bone marrow support in patients in phase-I clinical trials of colony-stimulating factors: G-CSF, GM-CSF, IL-1, IL-2, M-CSF*. Ann Hematol, 1993. **67**(6): p. 267-76.
34. Smith, J.W., 2nd, et al., *The toxic and hematologic effects of interleukin-1 alpha administered in a phase I trial to patients with advanced malignancies*. J Clin Oncol, 1992. **10**(7): p. 1141-52.

35. Elhage, R., et al., *Differential effects of interleukin-1 receptor antagonist and tumor necrosis factor binding protein on fatty-streak formation in apolipoprotein E-deficient mice*. *Circulation*, 1998. **97**(3): p. 242-4.
36. Nicklin, M.J., et al., *Arterial inflammation in mice lacking the interleukin 1 receptor antagonist gene*. *J Exp Med*, 2000. **191**(2): p. 303-12.
37. Fiotti, N., et al., *Atherosclerosis and inflammation. Patterns of cytokine regulation in patients with peripheral arterial disease*. *Atherosclerosis*, 1999. **145**(1): p. 51-60.
38. Shibata M, E.S., Inada K, *Elevated plasma levels of interleukin-1 receptor antagonist and interleukin-10 in patients with acute myocardial infarction*. *J. Interferon Cytokine Res*, 1997. **17**: p. 145-150.
39. Bresnihan, B., *Treatment of rheumatoid arthritis with interleukin 1 receptor antagonist*. *Ann Rheum Dis*, 1999. **58 Suppl 1**: p. 196-8.
40. Campion, G.V., et al., *Dose-range and dose-frequency study of recombinant human interleukin-1 receptor antagonist in patients with rheumatoid arthritis. The IL-1Ra Arthritis Study Group*. *Arthritis Rheum*, 1996. **39**(7): p. 1092-101.
41. Porat, R., et al., *Interleukin-1 (IL-1) receptor blockade reduces endotoxin and Borrelia burgdorferi-stimulated IL-8 synthesis in human mononuclear cells*. *Faseb J*, 1992. **6**(7): p. 2482-6.
42. Antin, J.H., et al., *Recombinant human interleukin-1 receptor antagonist in the treatment of steroid-resistant graft-versus-host disease*. *Blood*, 1994. **84**(4): p. 1342-8.

43. Granowitz, E.V., et al., *Pharmacokinetics, safety and immunomodulatory effects of human recombinant interleukin-1 receptor antagonist in healthy humans*. *Cytokine*, 1992. **4**(5): p. 353-60.
44. Fye, *Atherosclerosis and coronary heart disease*, ed. R.R. Fuster V, Topol EJ. 1996: Lippencott-Raven.
45. Mann JM, D.M., *Epidemiology and pathophysiology of coronary artery disease*. *Practical interventional cardiology*, ed. R.D. Grech ED. 1997, London: Martin Dunitz. 1 - 10.
46. Davies, *The pathophysiology and investigation of chronic stable angina*. *Diseases of the heart*, ed. C.A. Julian DG, Fox KM, Hall RJC, Poole-Wilson PA. 1989, London: Balliere Tindall. 1103 - 1125.
47. Braunwald, E., *Unstable angina. A classification*. *Circulation*, 1989. **80**(2): p. 410-4.
48. Wheatley, *Surgery in ischaemic heart disease*. *Diseases of the heart*, ed. C.A. Julian DG, Fox KM, Hall RJC, Poole-Wilson PA. 1989, London: Balliere Tindall. 1203 - 1226.
49. Kurbaan AS, B.T., Rickards AF, *Pills, balloon or knife: a review of the trials*. *Heart*, 1997. **78**((Supp)): p. 2-5.
50. Ridker, P.M., et al., *Inflammation, aspirin, and the risk of cardiovascular disease in apparently healthy men*. *N Engl J Med*, 1997. **336**(14): p. 973-9.
51. *Randomised trial of cholesterol lowering in 4444 patients with coronary heart disease: the Scandinavian Simvastatin Survival Study (4S)*. *Lancet*, 1994. **344**(8934): p. 1383-9.

52. Bustos, C., et al., *HMG-CoA reductase inhibition by atorvastatin reduces neointimal inflammation in a rabbit model of atherosclerosis*. J Am Coll Cardiol, 1998. **32**(7): p. 2057-64.
53. Williams, J.K., et al., *Pravastatin has cholesterol-lowering independent effects on the artery wall of atherosclerotic monkeys*. J Am Coll Cardiol, 1998. **31**(3): p. 684-91.
54. Gruntzig, A., *Transluminal dilatation of coronary-artery stenosis*. Lancet, 1978. **1**(8058): p. 263.
55. Waller, *Pathology of coronary balloon angioplasty and related topics*. Textbook of interventional cardiology, ed. T. EJ. 1990, Philadelphia: WB Saunders. 395 - 451.
56. Lincoff AM, T.E., *Interventional catheterisation techniques*. Heart disease: a textbook of cardiovascular medicine, ed. B. E. 1997, Philadelphia: WB Saunders. 1366 - 1391.
57. Savage, M.P., et al., *Efficacy of coronary stenting versus balloon angioplasty in small coronary arteries. Stent Restenosis Study (STRESS) Investigators*. J Am Coll Cardiol, 1998. **31**(2): p. 307-11.
58. Fischman, D.L., et al., *A randomized comparison of coronary-stent placement and balloon angioplasty in the treatment of coronary artery disease. Stent Restenosis Study Investigators*. N Engl J Med, 1994. **331**(8): p. 496-501.
59. Feuerstein, G., *Coronary Restenosis: From genetics to therapeutics*. 1997: Marcel Dekker \inc.

60. Leimgruber, P.P., et al., *Influence of intimal dissection on restenosis after successful coronary angioplasty*. *Circulation*, 1985. **72**(3): p. 530-5.
61. Holmes, D.R., Jr., et al., *Restenosis after percutaneous transluminal coronary angioplasty (PTCA): a report from the PTCA Registry of the National Heart, Lung, and Blood Institute*. *Am J Cardiol*, 1984. **53**(12): p. 77C-81C.
62. Foley DP, S.P., *Post-angioplasty restenosis: definition, diagnosis and management*. *Difficult concepts in cardiology*, ed. J. G. 1994, London: Martin Dunitz. 19 - 42.
63. Nobuyoshi, M., et al., *Restenosis after successful percutaneous transluminal coronary angioplasty: serial angiographic follow-up of 229 patients*. *J Am Coll Cardiol*, 1988. **12**(3): p. 616-23.
64. Serruys, P.W., et al., *Incidence of restenosis after successful coronary angioplasty: a time-related phenomenon. A quantitative angiographic study in 342 consecutive patients at 1, 2, 3, and 4 months*. *Circulation*, 1988. **77**(2): p. 361-71.
65. Rosing, D.R., et al., *Three year anatomic, functional and clinical follow-up after successful percutaneous transluminal coronary angioplasty*. *J Am Coll Cardiol*, 1987. **9**(1): p. 1-7.
66. Uchida, Y., et al., *Angioscopic observation of the coronary luminal changes induced by percutaneous transluminal coronary angioplasty*. *Am Heart J*, 1989. **117**(4): p. 769-76.
67. Chesebro JH, B.J., Badimon L, Fuster V, *Arterial angioplasty: injury, mural thrombus and restenosis*. *The practice of interventional*

- cardiology, ed. K.S. Vogel JHK. 1993, St Louis: Mosby Year Book. 509 - 520.
68. Wilensky, R.L., et al., *Vascular injury, repair, and restenosis after percutaneous transluminal angioplasty in the atherosclerotic rabbit*. *Circulation*, 1995. **92**(10): p. 2995-3005.
 69. Farb, A., et al., *Pathology of acute and chronic coronary stenting in humans*. *Circulation*, 1999. **99**(1): p. 44-52.
 70. Kornowski, R., et al., *In-stent restenosis: contributions of inflammatory responses and arterial injury to neointimal hyperplasia*. *J Am Coll Cardiol*, 1998. **31**(1): p. 224-30.
 71. Koch, W., et al., *Association of a CD18 gene polymorphism with a reduced risk of restenosis after coronary stenting*. *Am J Cardiol*, 2001. **88**(10): p. 1120-4.
 72. Danenberg, H.D., et al., *Systemic inflammation induced by lipopolysaccharide increases neointimal formation after balloon and stent injury in rabbits*. *Circulation*, 2002. **105**(24): p. 2917-22.
 73. Schillinger, M., et al., *Vascular inflammation and percutaneous transluminal angioplasty of the femoropopliteal artery: association with restenosis*. *Radiology*, 2002. **225**(1): p. 21-6.
 74. Feldman, L.J., et al., *Interleukin-10 inhibits intimal hyperplasia after angioplasty or stent implantation in hypercholesterolemic rabbits*. *Circulation*, 2000. **101**(8): p. 908-16.
 75. Wang, K., et al., *Prevention of intimal hyperplasia with recombinant soluble P-selectin glycoprotein ligand-immunoglobulin in the porcine*

- coronary artery balloon injury model*. J Am Coll Cardiol, 2001. **38**(2): p. 577-82.
76. Sousa, J.E., et al., *Sustained suppression of neointimal proliferation by sirolimus-eluting stents: one-year angiographic and intravascular ultrasound follow-up*. Circulation, 2001. **104**(17): p. 2007-11.
77. Marx, S.O. and A.R. Marks, *Bench to bedside: the development of rapamycin and its application to stent restenosis*. Circulation, 2001. **104**(8): p. 852-5.
78. Stone, G.W., et al., *A polymer-based, paclitaxel-eluting stent in patients with coronary artery disease*. N Engl J Med, 2004. **350**(3): p. 221-31.
79. Liu, X., et al., *Study of antirestenosis with the BiodivYsio dexamethasone-eluting stent (STRIDE): a first-in-human multicenter pilot trial*. Catheter Cardiovasc Interv, 2003. **60**(2): p. 172-8; discussion 179.
80. Mody VH, D.A., Mehra AO, *Pharmacological approaches to prevent restenosis*. Restenosis: A guide to Therapy, ed. F. DP. 2001, London, UK: Martin Durnitz. 97-112.
81. Holmes, D.R., Jr., et al., *Results of Prevention of REStenosis with Tranilast and its Outcomes (PRESTO) trial*. Circulation, 2002. **106**(10): p. 1243-50.
82. Farb, A., et al., *Oral everolimus inhibits in-stent neointimal growth*. Circulation, 2002. **106**(18): p. 2379-84.
83. Versaci, F., et al., *Immunosuppressive Therapy for the Prevention of Restenosis after Coronary Artery Stent Implantation (IMPRESS Study)*. J Am Coll Cardiol, 2002. **40**(11): p. 1935-42.

84. Dower, S.K., et al., *Interleukin-1 antagonists*. *Ther Immunol*, 1994. **1**(2): p. 113-22.
85. Jacobs, C.A., et al., *Experimental autoimmune encephalomyelitis is exacerbated by IL-1 alpha and suppressed by soluble IL-1 receptor*. *J Immunol*, 1991. **146**(9): p. 2983-9.
86. Bernstein, S.H., et al., *A phase I study of recombinant human soluble interleukin-1 receptor (rhu IL-1R) in patients with relapsed and refractory acute myeloid leukemia*. *Cancer Chemother Pharmacol*, 1999. **43**(2): p. 141-4.
87. Drevlow, B.E., et al., *Recombinant human interleukin-1 receptor type I in the treatment of patients with active rheumatoid arthritis*. *Arthritis Rheum*, 1996. **39**(2): p. 257-65.
88. Preas, H.L., 2nd, et al., *Effects of recombinant soluble type I interleukin-1 receptor on human inflammatory responses to endotoxin*. *Blood*, 1996. **88**(7): p. 2465-72.
89. Arend, W.P., et al., *Binding of IL-1 alpha, IL-1 beta, and IL-1 receptor antagonist by soluble IL-1 receptors and levels of soluble IL-1 receptors in synovial fluids*. *J Immunol*, 1994. **153**(10): p. 4766-74.
90. Lang, D., Knop, J., Wesche, H., *The type II IL-1 receptor interacts with the IL-1 receptor accessory protein: a novel mechanism of regulation of IL-1 responsiveness*. *J. Immunol*, 1998. **161**: p. 6871 - 6877.
91. Wilson, W.D., *Tech.Sight. Analyzing biomolecular interactions*. *Science*, 2002. **295**(5562): p. 2103-5.
92. *BIAtechnology Handbook*. 1998, Uppsala, Sweden.

93. Huether, M.J., et al., *Cloning, sequencing and regulation of an mRNA encoding porcine interleukin-1 beta*. *Gene*, 1993. **129**(2): p. 285-9.
94. Bendele, A., et al., *Efficacy of sustained blood levels of interleukin-1 receptor antagonist in animal models of arthritis: comparison of efficacy in animal models with human clinical data*. *Arthritis Rheum*, 1999. **42**(3): p. 498-506.
95. Braddock, M. and A. Quinn, *Targeting IL-1 in inflammatory disease: new opportunities for therapeutic intervention*. *Nat Rev Drug Discov*, 2004. **3**(4): p. 330-40.
96. Horai, R., et al., *Development of chronic inflammatory arthropathy resembling rheumatoid arthritis in interleukin 1 receptor antagonist-deficient mice*. *J Exp Med*, 2000. **191**(2): p. 313-20.
97. Rogy, M.A., et al., *Persistently elevated soluble tumor necrosis factor receptor and interleukin-1 receptor antagonist levels in critically ill patients*. *J Am Coll Surg*, 1994. **178**(2): p. 132-8.
98. Dinarello, C.A., *Interleukin-1, interleukin-1 receptors and interleukin-1 receptor antagonist*. *Int Rev Immunol*, 1998. **16**(5-6): p. 457-99.
99. Lavker, R.M., et al., *Hairless micropig skin. A novel model for studies of cutaneous biology*. *Am J Pathol*, 1991. **138**(3): p. 687-97.
100. Binns, R.M., et al., *In vivo E-selectin upregulation correlates early with infiltration of PMN, later with PBL entry: MAbs block both*. *Am J Physiol*, 1996. **270**(1 Pt 2): p. H183-93.
101. A.J.Rees, C.S.a., *Role of neutrophils in vasculitis*. *The Handbook of Immunopharmacology*, ed. P.G.H.a.T.J. Williams. 1994: Academic Press.

102. Mullane, K.M., R. Kraemer, and B. Smith, *Myeloperoxidase activity as a quantitative assessment of neutrophil infiltration into ischemic myocardium*. J Pharmacol Methods, 1985. **14**(3): p. 157-67.
103. Ridger, V.C., et al., *Effect of the inducible nitric oxide synthase inhibitors aminoguanidine and L-N6-(1-iminoethyl)lysine on zymosan-induced plasma extravasation in rat skin*. J Immunol, 1997. **159**(1): p. 383-90.
104. Kuebler WM, A.C., Schuerer L, Goetz AE, *Measurement of neutrophil content in brain and lung tissue by a modified myeloperoxidase assay*. International Journal of Microcirculation, 1996. **16**(2): p. 89-97.
105. Blank, J.A., et al., *Procedure for assessing myeloperoxidase and inflammatory mediator responses in hairless mouse skin*. J Appl Toxicol, 2000. **20**(S1): p. S137-S139.
106. Liu, M.W., et al., *Trapidil in preventing restenosis after balloon angioplasty in the atherosclerotic rabbit*. Circulation, 1990. **81**(3): p. 1089-93.
107. Currier, J.W., et al., *Low molecular weight heparin (enoxaparin) reduces restenosis after iliac angioplasty in the hypercholesterolemic rabbit*. J Am Coll Cardiol, 1991. **17**(6 Suppl B): p. 118B-125B.
108. Lee, *Swine as animal models in cardiovascular research*. Swine in Biomedical Research. Vol. 3. 1986. 1481-1496.
109. Hughes, H.C., *Swine in cardiovascular research*. Lab Anim Sci, 1986. **36**(4): p. 348-50.
110. Kantor, B., et al., *The experimental animal models for assessing treatment of restenosis*. Cardiovasc Radiat Med, 1999. **1**(1): p. 48-54.

111. Schwartz, R.S., et al., *Restenosis after balloon angioplasty. A practical proliferative model in porcine coronary arteries*. *Circulation*, 1990. **82**(6): p. 2190-200.
112. Malik, N., et al., *Phosphorylcholine-coated stents in porcine coronary arteries: in vivo assessment of biocompatibility*. *J Invasive Cardiol*, 2001. **13**(3): p. 193-201.
113. Malik, N., et al., *Intravascular stents: a new technique for tissue processing for histology, immunohistochemistry, and transmission electron microscopy*. *Heart*, 1998. **80**(5): p. 509-16.
114. Schwartz, R., Holmes DR, *Pigs, dogs, baboons and man: lessons for stenting from animal studies*. *J Intervent Cardiology*, 1994. **7**: p. 355 - 368.
115. Gunn, J., et al., *Coronary artery stretch versus deep injury in the development of in-stent neointima*. *Heart*, 2002. **88**(4): p. 401-5.
116. Schwartz, R.S., *Neointima and arterial injury: dogs, rats, pigs, and more*. *Lab Invest*, 1994. **71**(6): p. 789-91.
117. Morton AC, P.T., Wales C, Bowes R, Campbell S, Oakley D, Wheeldon N, Newman C, Crossman D, Cumberland D and Gunn J, *'Real World' Small Vessel Coronary Artery Stenting: an Analysis*. *Br J Cardiol (Acute Interv Cardiol)*, 2003. **10**(1): p. AIC 28 - AIC 32.
118. Suzuki, T., et al., *Stent-based delivery of sirolimus reduces neointimal formation in a porcine coronary model*. *Circulation*, 2001. **104**(10): p. 1188-93.
119. Farb, A., et al., *Pathological analysis of local delivery of paclitaxel via a polymer-coated stent*. *Circulation*, 2001. **104**(4): p. 473-9.

120. Stone, G., *TAXUS-IV: angiographic and IVUS results of the pivotal prospective, multicentre, randomized trial of polymer-based paclitaxel-eluting stents in patients with de novo lesions*. 2003.
121. Fenton, M.J., et al., *Transcriptional regulation of the human prointerleukin 1 beta gene*. *J Immunol*, 1987. **138**(11): p. 3972-9.
122. Vannier, E. and C.A. Dinarello, *Histamine enhances interleukin (IL)-1-induced IL-1 gene expression and protein synthesis via H2 receptors in peripheral blood mononuclear cells. Comparison with IL-1 receptor antagonist*. *J Clin Invest*, 1993. **92**(1): p. 281-7.
123. Spagnuolo-Weaver, M., et al., *A fluorimeter-based RT-PCR method for the detection and quantitation of porcine cytokines*. *J Immunol Methods*, 1999. **230**(1-2): p. 19-27.
124. Pfaffl, M.W., G.W. Horgan, and L. Dempfle, *Relative expression software tool (REST) for group-wise comparison and statistical analysis of relative expression results in real-time PCR*. *Nucleic Acids Res*, 2002. **30**(9): p. e36.
125. Dinarello, C.A., *Interleukin-1 Family [IL-1F1,F2]*. 4 ed. *The Cytokine Handbook*, ed. A.W.T.M.T. Lotze. 2003, London: Elsevier Science Ltd. 643 - 708.
126. Arend, W.P., *The balance between IL-1 and IL-1Ra in disease*. *Cytokine Growth Factor Rev*, 2002. **13**(4-5): p. 323-40.
127. Virmani, R., et al., *Drug eluting stents: are human and animal studies comparable?* *Heart*, 2003. **89**(2): p. 133-8.

128. Schwartz, R.S., et al., *Drug-eluting stents in preclinical studies: recommended evaluation from a consensus group*. *Circulation*, 2002. **106(14)**: p. 1867-73.

TECHNICAL APPENDIX

A. REAGENTS AND STOCK SOLUTIONS

A.1 BIAcore Reagents and Stock Solutions

BUFFER	PREPARATION
Immobilization buffer	10mM sodium acetate, pH to 5.0
Running buffer	015M HEPES buffered saline, 3.4mM EDTA, 0.05% Tween 20, pH to 7.4

A.2 RNA Reagents and Stock solutions

All RNA was extracted using the RNAeasy kit from Qiagen. The manufacturers give no details of the buffers.

A.3 Protein Stock Reagents and Buffers

SOLUTION	PREPARATION
2X SDS protein sample loading buffer	1ml glycerol, 0.5ml beta-mercaptoethanol, 3ml 10% SDS 1.25ml 1M Tris-HCl pH 6.7 1-2mg bromophenol blue. Store frozen in 200µl aliquots.
RIPA lysis buffer (1% NP-40/0.5% sodium deoxycholate/0.1% SDS)	1ml NP-40, 0.5g sodium deoxycholate, 0.5ml 20% SDS. Add PBS to 100ml Store at 4°C
NP-40 lysis buffer (150mM NaCl/1% NP-40/50mM tris-Cl, pH8.0)	0.88g NaCl, 1ml NP-40 (BDH), 0.604g Tris. Add water to 80 mls pH to 8.0 and adjust final volume to 100ml. Store at 4°C
1M Tris-HCl pH 6.8	121.1g Tris in 800mls water pH to 6.8 with concentrated HCL Adjust final vol to 1 litre
1.5M Tris-HCl pH 8.8	181.5g Tris in 800mls water pH to 8.8 with concentrated HCL Adjust final vol to 1 litre
10X Tris-glycine-SDS running buffer	30.3g Tris, 190g glycine, 100mls 10%

(250mM Tris/250mM glycine/10% SDS)	SDS, water to 1 litre. Dilute to 1X running buffer before use.
Towbin transfer buffer (39mM glycine/48mM Tris/0.037% SDS/20% methanol)	1.45g glycine, 2.9g Tris, 0.185g SDS, water to 400mls. Just before use add methanol (BDH) to a final volume of 20%. Store at room temperature
10% APS (ammonium persulphate)	0.1g APS, 1ml water. Store in 20µl aliquots at -20°C
Coomassie blue solution	1g Coomassie blue R250 (BDH), 450mls methanol, 450 mls water, 100mls glacial acetic acid
Destain solution	450mls methanol, 450 mls water, 100mls glacial acetic acid
Blocking buffer	20g Marvel, 500mls PBS
0.1M phenylmethylsulfonylfluoride (PMSF)	0.1742g PMSF (Sigma), 10mls isopropanol (BDH). Store at -70°C in 500µl aliquots

A.4 Plasmid Reagents and Stock Solutions

BUFFER	COMPOSITION
P1	50mM Tris-Cl, pH8.0; 10mM EDTA; 100µg/ml Rnase A

P2	200mM NaOH, 1% SDS (w/v)
P3	3.0M potassium acetate, pH5.5
QBT	750mM NaCl; 50mM MOPS, pH7.0; 15% isopropanolol (v/v); 0.15% Triton X-100 (v/v)
QC	1.0M NaCl; 50mM MOPS, pH7.0; 15% isopropanolol (v/v)
QF	1.25M NaCl; 50mM Tris-Cl, pH8.5; 15% isopropanolol (v/v)
QN	1.6M NaCl; 50mM MOPS, pH7.0; 15% isopropanolol (v/v)
TE	10mM Tris-Cl, pH8.0; 1mM EDTA
STE	100mM NaCl; 10mM Tris-Cl, pH8.0; 1mM EDTA
FWB2 (wash buffer)	1M potassium acetate pH5.0

B. DNA / RNA CONCENTRATION CALCULATIONS

B.1 RNA Concentration Calculation

$A_{260}/A_{280} = 1.8 - 2.0$ for a pure RNA preparation

$A_{260} 1.0 = 40\mu\text{g RNA per 1 ml}$

$[\text{RNA}] \mu\text{g}/\mu\text{l} = A_{260} \times \text{dilution factor} \times 0.04$

B.2 Oligonucleotide Concentration Calculation

$A_{260} 1 = 33\mu\text{g single stranded DNA per ml}$

$[\text{DNA oligo}] \mu\text{g}/\mu\text{l} = A_{260} \times \text{dilution factor} \times 0.033$

B.3 Molar concentration calculation

$\text{Moles} = [\text{g/l}] / \text{molecular weight of oligo}$

B.4 DNA Concentration calculation

$A_{260}/A_{280} = 1.8$ for a pure DNA preparation

$A_{260} 1.0 = 50\mu\text{g double stranded DNA per ml}$

$[\text{DNA}] \mu\text{g}/\mu\text{l} = A_{260} \times \text{dilution factor} \times 0.05$

C. PROTEIN ELECTROPHORESIS

C.1 Resolving Gel Preparation

Sterile water	3.4ml
30% stock acrylamide*	7.5ml
1.5M Tris pH 8.8	3.8ml
10% SDS	150 μ l
10% APS**	150 μ l
TEMED***	6 μ l

*Bio-Rad, molar ratio of bisacrylamide:acrylamide is 1:29.

**Ammonium persulphate, (BDH).

***N,N,N, N'-tetramethylethylenediamine, (Sigma).

C.2 Stacking Gel Preparation

Sterile water	3.4ml
30% stock acrylamide	830 μ l
1.5M Tris-Cl pH 6.8	630 μ l
10% SDS	50 μ l
10% APS	50 μ l
TEMED	5 μ l

D MEETING ABSTRACTS

1. Interleukin-1 receptor antagonist (IL-1ra) modulates the porcine coronary arterial response to oversized balloon angioplasty and stenting. **Morton AC**, Francis SE, Dower S, Arnold ND, Gunn J and Crossman DC. Cardiovascular Pathology 2004;13 3S (Suppl): S93.

2. Interleukin-1 receptor antagonist (IL-1ra) modulates the porcine coronary arterial response to oversized balloon angioplasty and stenting. **Morton AC**, Varcoe R, Francis SE, Dower S, Arnold ND, Gunn J and Crossman DC. Presented at the Young Research Workers competition at the British Cardiac Society. Heart 2004;90(Suppl.2):A1

3. Interleukin-1 receptor antagonist (IL-1ra) modulates the porcine coronary arterial response to oversized balloon angioplasty and stenting. **Morton AC**, Varcoe R, Francis SE, Dower S, Arnold ND, Gunn J and Crossman DC. Presented in the Young Research Workers competition at the British Atherosclerosis Society. Atherosclerosis 2004;174: S4

4. Interleukin-1 receptor antagonist (IL-1ra) modulates the porcine coronary arterial response to oversized balloon angioplasty and stenting. **Morton AC**, Francis SE, Dower S, Arnold ND, Gunn J and Crossman DC. Given in the plenary talk session at the Medical Research Society Annual meeting in November 2003.

5. Interleukin-1 receptor antagonist (IL-1ra) alters the arterial response to oversized balloon angioplasty and stenting in the porcine coronary artery.

Morton AC, Francis SE, Dower S, Arnold ND, Gunn J and Crossman DC.

Circulation 2003;108;17 (Suppl): IV-195